

**ISTANBUL TECHNICAL UNIVERSITY ★ GRADUATE SCHOOL OF SCIENCE**  
**ENGINEERING AND TECHNOLOGY**

**HYGRO\_RESPONSIVE STRUCTURE**  
**HUMIDITY RESPONSIVE MATERIAL SYSTEM DESIGN**



**M.Sc. THESIS**

**Gülce KIRDAR**

**Informatics Department**

**Architectural Design Computing Graduate Program**

**JUNE 2017**



**ISTANBUL TECHNICAL UNIVERSITY ★ GRADUATE SCHOOL OF SCIENCE**  
**ENGINEERING AND TECHNOLOGY**

**HYGRO\_RESPONSIVE STRUCTURE**  
**HUMIDITY RESPONSIVE MATERIAL SYSTEM DESIGN**



**M.Sc. THESIS**

**Gülce KIRDAR**

**(523141007)**

**Informatics Department**

**Architectural Design Computing Graduate Program**

**Thesis Advisor: Prof. Dr. Birgül ÇOLAKOĞLU**

**JUNE 2017**



**İSTANBUL TEKNİK ÜNİVERSİTESİ ★ FEN BİLİMLERİ ENSTİTÜSÜ**

**HİGRO\_TEPKİLİ STRÜKTÜR  
NEME DUYARLI MALZEME SİSTEMİ TASARIMI**

**YÜKSEK LİSANS TEZİ**

**Gülce KIRDAR  
(523141007)**

**Bilişim Anabilim Dalı**

**Mimari Tasarımda Bilişim Yüksek Lisans Programı**

**Tez Danışmanı: Prof. Dr. Birgül ÇOLAKOĞLU**

**HAZİRAN 2017**



**Gölce Kırdar**, a **M.Sc.** student of ITU **Graduate School of Science Engineering and Technology** student ID **523141007**, successfully defended the thesis/dissertation entitled “**HYGRO\_RESPONSIVE STRUCTURE HUMIDITY RESPONSIVE MATERIAL SYSTEM DESIGN**”, which she prepared after fulfilling the requirements specified in the associated legislations, before the jury whose signatures are below.

**Thesis Advisor :** **Prof. Dr. Birgül Çolakođlu** .....  
İstanbul Technical University

**Jury Members :** **Assoc. Prof. Dr.Leman Figen GÜL** .....  
İstanbul Technical University

**Assoc. Prof. Dr. Tuđrul YAZAR** .....  
İstanbulBilgi University

**Date of Submission : 4 May 2017**

**Date of Defense : 6 June 2017**







*To my family,*



## FOREWORD

First of all, I would like to thank my thesis advisor Prof. Dr. Birgöl Çolkođlu for her guidance and encouragement to enlarge my insight throughout the study. She allowed this paper to be my own work, but directme with her advices whenever she thought I needed it.

I would also like to thank my colleague of this study Zeynel Güler, material scientist. He was involved in the experimental study and made precious contributions to my study by sharing his knowledge about material properties. Furthermore, he developed a simple humidifier system forthe experiments. Without his participation, the material experiments could not have been successfully executed. I would also like to acknowledge Pınar Kırdar and Zeynel Güler, as the second readers of this thesis. I am indebted to them for their valuable comments on this thesis.

The thesis study is dedicated to my family in response to their unfailing care and love. I am grateful to my family Gülay Kırdar, Cemal Kırdar and Emre Kırdar, as my roommate, for providing me continuous encouragement and understanding throughout the exhausting study process. This thesis could not have been accomplished without their moral and material supports. I am indebted to my dear friends Cansu Uyar,Selin Öztürk and long list of all my dear friends, for their supports. They are always with me at all times and encourage me to work on the thesis. I would like to thank to my colleagues from Kemerburgaz University Merve Aşçıođlu, Meltem Çetinel, Büşra Başkurt and Aygün Aşık. Working for hours becomes enjoyable with them. Finally, I owe my students in Kemerburgaz University a debt of gratitude; they motivate me during my thesis study period. Lastly, I would like to thank the instructors in the university, especially the chair of the department Derya Yorgancıođlu, for supporting and sharing their experiences with me. Thank you.



## TABLE OF CONTENT

	<u>Page</u>
<b>FOREWORD</b> .....	<b>ix</b>
<b>TABLE OF CONTENT</b> .....	<b>xi</b>
<b>ABBREVIATION</b> .....	<b>xiii</b>
<b>SYMBOLS</b> .....	<b>xv</b>
<b>LIST OF TABLES</b> .....	<b>xvii</b>
<b>LIST OF FIGURES</b> .....	<b>xix</b>
<b>SUMMARY</b> .....	<b>xxiii</b>
<b>ÖZET</b> .....	<b>xxv</b>
<b>1. INTRODUCTION</b> .....	<b>1</b>
1.1. Purpose of the Thesis .....	1
1.2. Structure of the Thesis .....	2
<b>2. MATERIAL BASED RESPONSIVE SYSTEM DESIGN</b> .....	<b>5</b>
2.1. Responsive System Design .....	5
2.2. The Classification in Responsive Systems.....	12
2.3. Material Based Responsive System .....	15
2.4. Material Computation .....	16
2.5. Examples of Responsive Material System.....	18
<b>3. WOOD AS A MATERIAL SYSTEM</b> .....	<b>23</b>
3.1. Explorations at Embedded Material Properties.....	23
3.1.1. Hygroscope (Humidity transition) .....	24
3.1.2. Anisotropy (Grain directionality).....	26
3.2. Humidity Responsive Systems Using Wood .....	30
3.4. Examples of Humidity Responsive Composite.....	34
<b>4. RESPONSIVE COMPOSITE MATERIAL DEVELOPMENT</b> .....	<b>37</b>
4.1. Material Selection for Responsive Composite Material .....	38
4.2. Production of the Responsive Composite .....	40
4.3. Material Experiments .....	42
4.3. Evaluation on Material Experiments.....	59
<b>5. RESPONSIVE SYSTEM STRUCTURE</b> .....	<b>61</b>
5.1. Design Process of Responsive System Structure .....	62
5.2. Construction Process of the Responsive System Structure.....	68
<b>6. CONCLUSION</b> .....	<b>75</b>
<b>REFERENCES</b> .....	<b>79</b>
<b>APPENDICES</b> .....	<b>85</b>
<b>CURRICULUM VITAE</b> .....	<b>108</b>



## **ABBREVIATION**

**AI:** Artificial Intelligence  
**2D:** Two Dimensional  
**3D:** Three dimensional  
**CNC:** Computer Numeric Control  
**EAP:** Electro active polymer  
**EMC:** Equilibrium Moisture Content  
**FSP:** Fiber Saturation Point  
**GFRP:** Glass Fibre-Reinforce Composites  
**long:** longitudinal  
**MC:** Moisture Content  
**MEMs:** Micro-Electro-Mechanical Systems  
**NURBS:** Non-Uniform Rotational Basis Spline  
**PC:** Polycarbonate  
**PET:** Polyethylene Terephthalate  
**PETG:** Polyethylene terephthalate glycol-modified  
**PVC:** Polyvinyl Chloride  
**rad:** radial  
**SMA:** Shape Memory Alloy  
**tan:** tangential





## SYMBOLS

$\alpha_a$	:Hygroexpansion(shrinkage) coefficient of active layer
$\alpha_p$	:Hygroexpansion (shrinkage) coefficient of passive layer
$\Delta\alpha$	:Hygroexpansion difference of active and passive layers
$e_a$	: Elastic modulus (stiffness) of active layer
$e_p$	: Elastic modulus (stiffness) of passive layer
$f(m,n)$	: Curvature change coefficient
$K$	:Curvature of the element
$m$	: Thickness ratio
$\Delta MC$	:Moisture content change
$n$	: Elasticity (stiffness) ratio
$R$	:Radius of curvature of the element
$1/R_0$	:The initial curvature of the element
$t$	: Time
$t_a$	: Thickness of active layer
$t_p$	: Thickness of passive layer
$t_{total}$	: Total thickness of the composite



## LIST OF TABLES

	<u>Page</u>
<b>Table 2.1</b> :The developments in responsive design (by the author).....	<b>8</b>
<b>Table 2.2</b> :The key principles of the responsive design (By the author).....	<b>10</b>
<b>Table 2.3</b> :Comparison of the responsive systems types.....	<b>12</b>
<b>Table 3.1</b> : The shrinkage table according to wood types.....	<b>34</b>
<b>Table 4.1</b> : The stages of the responsive material development..	<b>43</b>
<b>Table 4.2</b> : The shrinkage table in selected wood types (Adapted from FPL, 2010).	<b>44</b>
<b>Table 4.3</b> : Table of the selected material... ..	<b>46</b>
<b>Table 4.4</b> : The experiment phases according to the parameters... ..	<b>50</b>
<b>Table 4.5</b> : Thickness and elasticity values of used polymer types and wood.....	<b>54</b>
<b>Table 4.6</b> : The experiment phases according to the parameters... ..	<b>55</b>
<b>Table 4.7</b> : Thickness and elasticity values of used wood types and poylmer.....	<b>58</b>
<b>Table 4.8</b> : Curvature change coefficient P1, P2 and P3 with elasticity and thickness proportions.....	<b>58</b>
<b>Table 5.1</b> : The classification of the used computational tools. ....	<b>69</b>
<b>Table 5.2</b> : The joint detail alternatives.....	<b>82</b>



## LIST OF FIGURES

	<u>Page</u>
<b>Figure 1.1:</b> The design progress of responsive material system. ....	4
<b>Figure 2.1:</b> The Colloquy of Mobiles Installation (a) and Generator interface (b) (Dunn, 2012). ....	6
<b>Figure 2.2:</b> Fun Palace illustration plan and interior perspective (Url-3). ....	6
<b>Figure 2.3:</b> SEEK exhibition images (Url-2). ....	7
<b>Figure 2.4:</b> Light responsive façade system (Url-4). ....	8
<b>Figure 2.5:</b> The sensor and actuator parts (a) and controllers (b) for the responsive system (Fox, 2009). ....	9
<b>Figure 2.6:</b> The analysis of non- functional responsive façade of Arab Institute (Meagher, 2015). ....	11
<b>Figure 2.7:</b> The parts of the complex responsive unit (Fortmayer & Linn, 2014). ....	12
<b>Figure 2.8:</b> Smart material samples (Url-10, Url-11, Url-12). ....	13
<b>Figure 2.9:</b> The shape memory effect of Nitinol wire (By the author). ....	14
<b>Figure 2.10:</b> Reef installation (Url-14). ....	15
<b>Figure 2.11:</b> EAP material structure (Url-16). ....	15
<b>Figure 2.12:</b> The humidity analysis of the wood veneer in CFD (Computer Fluid Analysis Program) (Url-17). ....	17
<b>Figure 2.13:</b> The processed wood veneer (Url-18). ....	18
<b>Figure 2.14:</b> Bloom installation and design process (Url-20, Url-21). ....	19
<b>Figure 2.15:</b> The conceptual drawings of Tracheolis (Url-22). ....	20
<b>Figure 2.16:</b> Responsive Surface physical model (Url-17). ....	21
<b>Figure 2.17:</b> Responsive Surface design development (Url-17). ....	21
<b>Figure 2.18:</b> Hygroscope installation in humidity controlled glass case (Url-19). ...	21
<b>Figure 2.19:</b> Responsive behavior of hygroscopic wood composites (Url-19). ....	22
<b>Figure 2.20:</b> The simulation and working mechanism of Hygroscope units (Menges et al., 2014). ....	22
<b>Figure 3.1:</b> Hygroscopic movement of oak wood. ....	26
<b>Figure 3.2:</b> Projection of maximum shrinkage percentage in each of grain direction in wood batle (Winandy, 1994) and wood trunk (Holstov et al., 2015). ....	27
<b>Figure 3.3:</b> Microscopic photographs of maple (Menges and Reichert, 2012). ....	27

<b>Figure 3.4:</b> The graph showing the shrinkage amount in different grain axis (Mengeset et al., 2014).....	28
<b>Figure 3.5:</b> Distortions of wood due to swelling and shrinking (Url-23).....	28
<b>Figure 3.6:</b> The experiment to test the anisotropic character of wood (By the author).	29
<b>Figure 3.7:</b> The difference in the hardwood and softwood species (FPL, 2010). ....	29
<b>Figure 3.8:</b> Traditional wood latticework, mashrabiya (Url-24).....	31
<b>Figure 3.9:</b> Wooden paneling of boathouses in Nordmore, Norway (Larsen and Marstein, 2000). ....	31
<b>Figure 3.10:</b> An experiment to observe the humidity reaction of the pinecone scales (By the author). ....	32
<b>Figure 3.11:</b> The hygroscope analysis of the cone scales (Kremsa et al., 2009).....	33
<b>Figure 3.12:</b> The bilayer structure of the pinecone (Burgert and Fratzl, 2009). ....	33
<b>Figure 3.13:</b> The humidity response process of the composite (a) and the controllable blooming and wilting of the petals (b), (Reyssat and Mahadevan, 2009).....	34
<b>Figure 3.14:</b> The experiments to analyze the material behavior (Correa, Reichert and Menges, 2014). ....	35
<b>Figure 4.1:</b> Different wood veneer cutting methods (Url-26). ....	38
<b>Figure 4.2:</b> Selected wood veneers as active layer.....	39
<b>Figure 4.3:</b> Selected polymer sheets as passive layer. ....	40
<b>Figure 4.4:</b> The comparison of the response principle of the composite and wood..	41
<b>Figure 4.5:</b> The layers of the bilayer composite. ....	41
<b>Figure 4.6:</b> The application process of the adhesive solution with brush. ....	42
<b>Figure 4.7:</b> The simplified humidity chamber.....	43
<b>Figure 4.8:</b> The diagram for the experiment setup.....	43
<b>Figure 4.9:</b> The arranged composite samples for material experiments. ....	44
<b>Figure 4.10:</b> The defined curve of the composite materials and the response graph.	45
<b>Figure 4.11:</b> The composite samples with different polymer types. ....	47
<b>Figure 4.12:</b> The defined curvature of composite in one caption (in $t_{15}$ and $t_{16}$ ). ....	47
<b>Figure 4.13:</b> The response graph of the samples in Experiment 1 ( $P_1, P_2, P_3$ ). ....	48
<b>Figure 4.14:</b> The curvature change coefficient graph of polymer types. ....	49
<b>Figure 4.15:</b> The composite samples with different wood types. ....	50

<b>Figure 4.16:</b> The defined curvature of composite in one caption (in $t_{15}$ and $t_{16}$ ). .....	50
<b>Figure 4.17:</b> The response graph of the samples in Experiment 2 ( $1P_2$ , $2P_2$ , $3P_2$ , $4P_2$ ).51	
<b>Figure 4.18:</b> The curvature change coefficient graph of the used wood types. ....	53
<b>Figure 4.19:</b> The cutting direction of the samples. ....	53
<b>Figure 4.20:</b> The shape transformation of composite samples from different views.54	
<b>Figure 4.21:</b> The shape transformation of composite samples due to anisotropy. ....	55
<b>Figure 4.22:</b> The distance between the grains in $3G_3$ , $3G_2$ and $3G_1$ . ....	56
<b>Figure 4.23:</b> The fibered composite samples. ....	56
<b>Figure 4.24:</b> The response graph of the samples in Experiment 4 ( $3G_1$ , $3G_2$ and $3G_3$ ).57	
<b>Figure 4.25:</b> The response graphic to compare the thickness of the polymer.....	58
<b>Figure 4.26:</b> Simulation of curvature of the composite material. ....	60
<b>Figure 5.1:</b> Sun radiation (a) Sunlight (b) analysis graphic on the geometry. ....	63
<b>Figure 5.2:</b> The form finding process of the surface regarding to analysis. ....	64
<b>Figure 5.3:</b> The sunlight analysis of the surface without (a) and within (b) the context.....	64
<b>Figure 5.4:</b> The extracted area according to sunlight analysis. ....	65
<b>Figure 5.5:</b> The extracted surfaces (a) and the attractor points located in centers of the surfaces (b). ....	65
<b>Figure 5.6:</b> The relation between the scaling parameter and the attractor point.....	66
<b>Figure 5.7:</b> The final model of the structure according to attractor points (from the top view and perspective).....	67
<b>Figure 5.8:</b> Algorithm of the formal operations.....	67
<b>Figure 5.9:</b> Overlapped sunlight analysis simulation and resultant form.....	68
<b>Figure 5.10:</b> The modules of the structure and the parts the modules.....	69
<b>Figure 5.11:</b> The design progress of puzzle joint and finger joint detail.....	69
<b>Figure 5.12:</b> The fabrication layout that arranged for balsa wood sheet.....	70
<b>Figure 5.13:</b> Partial physical model of the structure. ....	71
<b>Figure 5.14:</b> The section drawing of the structure. ....	71
<b>Figure 5.15:</b> The used material of the structure and responsive panels. ....	72
<b>Figure 5.16:</b> The relation between the openings' scale and panels' response.....	73
<b>Figure 5.17:</b> The light penetration in the structure.....	73





**HYGRO\_ RESPONSIVE STRUCTURE**  
**HUMIDITY RESPONSIVE MATERIAL SYSTEM DESIGN**  
**SUMMARY**

Responsive system is a method that is used to enhance buildings' environmental performance and ensure user comfort by enabling the buildings to adjust to changeable environmental circumstances. The system detects environmental changes via specific sensors, determines the action to be taken against current conditions via its control mechanism and responds to environmental changes through its actuators by changing the physical form of system components. In current use, responsive systems utilize energy-activated mechanical components such as sensors, actuators and microcontrollers; the dependency to which births the need for continuous energy supply and periodical maintenance.

Motivated from the problems that are probable to be encountered at the use of mechanical responsive systems, this thesis researches how responsiveness can be achieved without the utilization of mechanical components. In nature, responsiveness is acquired in material level without any energy consumption. Wood for instance, a natural material, responds to humidity alterations without any mechanical support. The design of mechanical systems however, tends not to take the potential of natural material into consideration. Thus, this thesis study focuses on ways through which responsiveness can be achieved via a material based design. Material based responsive design employs material-inherent properties in ensuring system responsiveness and eliminates the utilization of mechanical components.

Concentrating on wood as a natural material, this thesis study aims to explore the material based responsive system design through examining the inherent properties of wood material. Wood transforms its shape in response to humidity changes: It swells or shrinks in grain direction. Hygroscopicity and Anisotropy are the keywords in this scope; these terms represent the inherent material properties that provide responsiveness. Therefore, towards taking advantage of material properties in ensuring responsiveness, this study develops a specific composite material that possesses the hygroscopic properties of wood. The composite material employs wood as the active layer and polymer as the passive layer. The active wood layer responds to humidity and elongates due to its hygroscopic-derived characteristics. The passive polymer on the other hand does not respond to humidity and remains stable. The polymer layer provides a constraint for the hygroscopic elongation of the wood layer and results the wood to bend.

In this thesis study, the responsive behavior of the composite material is examined in a controlled environment through material experiments. The main objective of these experiments is to evaluate the humidity-driven behavior of the material and to improve the material performance through calibration of specific parameters such as wood types, polymer types, grain direction, fiber frequency in polymer and layer thickness. Conducted experiments are analyzed through empirical (observational)

and numerical (quantitative) analysis methods. The empirical method observes the curvature change of the composite material and conducts a responsiveness comparison through a response graph. The numerical method on the other hand, enables the observational analysis results to be justified through calculations. The material experiments are carried out in a collaborative work. The collaboration of the two methods ensures the development of simplified humidity box, the production of composite material and the numerical evaluation of material experiments.

The material based responsive system, introduced as the “Hygro\_Responsive Structure” integrates responsive material with ‘parametric structure’. The parametric structure is included in the approach considering the sunlight as a specific parameter, since sunlight has influence on relative humidity. The parametric design and the construction process of the structure are achieved through computational design tools. The sunlight analysis is conducted via Ladybug and the form development, which actually is based on sunlight analysis, is carried out via Grasshopper. The responsive material design experiments both the form of the system and the material itself; on the basis of environmental parameters. Humidity is the response driver for the material and sunlight is the design driver for the system’s parametric form generation. The composite material, the main actor of the structure, is utilized in form of humidity-responsive panels. The responsive panels adapt to alterations in humidity by changing shape.

The composite material utilize hygroscope in the wood material to achieve responsiveness, thus the responsive material system needs neither energy nor mechanical components to work. As a result, the material based responsive system developed in this thesis study can be introduced as an energy-efficient system. The main objective of this study is to employ material behavior in responsive architecture. Material based responsive systems can consist of an alternative to mechanically responsive systems in scope of design strategies.

# HİGRO\_ TEPKİMELİ STRÜKTÜR

## NEME TEPKİ VEREN MALZEME SİSTEMİ TASARIMI

### ÖZET

Endüstrileşme ve teknolojinin gelişmesiyle birlikte değişen yaşam koşulları, makine teknolojisi ve yapıları çevre enerji tüketimini zaman içerisinde hızla arttırmıştır. Kaynaklardan edinilen bilgiye göre, enerji tüketiminin yaklaşık yüzde ellisini binaların yapım ve işleyiş (havalandırma- ısıtma-soğutma sistemleri) sürecinde harcanan enerji oluşturmaktadır. Bu durum sonucunda mimarlar yapı elemanlarına entegre edilebilen, çevresel değişikliklere tepki verebilecek **tepkisel sistemleri** tasarlamaya yönelirler. Tepkimeli (tepkisel) sistemler; çevresel değişiklikleri algılayıcılar (sensörler) ile algılayabilen, sayısal tasarım araçları ile kontrol edilebilen, robotik hareketlendirici sistemler (motorlar) ile tepki verebilen sistemlerdir. Tepkimeli mimari sistemlerin temel amacı, çevresel koşullara göre hareket ederek, yapıların çevresel performansını geliştirmek ve kullanıcı konfor koşullarına cevap vermektir.

Yaygın olarak kullanılan mekanik tepkimeli sistemler mekanik bileşenlerin kullanımı, enerji tüketimine sebep olmaktadır. Doğada ise tepkisellik malzeme ölçeğinde, enerji harcanmadan gerçekleşir. Yürütülen tez çalışması, tepkisel sistem tasarımını ve farklı tepkisel tasarım yöntemlerini inceler. Çalışmada, tepkimeli sistemler enerji kullanımına ve malzemenin sisteme etkisine göre inceleyerek üç grupta sınıflandırılır. Mekanik tabanlı tepkisel sistemler aktif, akıllı malzemelerin mekanik sistemler ile birlikte kullanıldığı tepkisel sistemler hibrid, malzeme tabanlı tepkisel sistemler pasif tepkimeli sistemler olarak sınıflandırılır.

Malzemenin yapısal özelliklerinden yararlanarak geliştirilen malzeme tabanlı tepkisel tasarım sistemleri, tepkisel sistemlerde mekanik bileşenlerin kullanımını ve bu sebeple meydana gelen enerji tüketimini ortadan kaldırmayı hedefler. Malzeme tabanlı tepkisel sistemler de çevreye cevap verebilen sistem tasarlarken malzeme üzerine ek bir mekanik sistem kurmak yerine, doğal malzemenin tepkisini ortaya çıkaran ya da malzemeden öğrenerek yeni malzeme sistemleri sunar. Malzeme tabanlı tepkimeli sistemlerde malzemenin yapısal özellikleri ve dış etkilere tepkisi tasarımın ana parametreleri kabul edilir ve sistem bu parametrelere en uygun cevap verebilecek şekilde tasarlanır. Çalışmada, malzeme tabanlı tepkisel sistem tasarım üzerine odaklanarak, tepkimeli malzeme sistem tasarımı örneklerine yer vermiştir. Malzeme tabanlı tepkisel sistem örneklerinin incelenmesi sonucu, tez çalışması ahşap malzemenin özünde var olan özelliklerini kullanarak tepkisel malzeme sistemi tasarlamayı hedefler.

Bu amaçla, tez kapsamında ahşap malzemenin yapısal özellikleri ve dış etkilere tepkisi araştırılır. Ahşap malzeme doğal ve yaşayan bir canlı olan ağacın işlenmesiyle elde edildiği için malzeme tabanlı tepkisel sistemlerde kullanılır. Ahşap, nem çekebilme (higroskopik) özelliği ile liflerinin yönelimine bağlı olarak (anizotropik) kendiliğinden şekil değiştirebilir. Higroskopik özelliğinden dolayı bulunduğu ortam ile nem alışverişinde bulunur: Havadaki nem oranı arttığında nemi çekerek şişer, nem oranı azaldığında ise malzemedeki nemi dışarı vererek büzülür. Kozalaklar, ortamdaki nem oranına göre biçim değiştirebilmesinden dolayı neme

duyarlı doğal tepkimeli sisteme örnektir. Ahşap anizotropik (yönelime bağlılık) özelliğinden dolayı, ortamdaki nem ile alışverişinde liflerinin dağılımına göre kıvrılır. Bu özellikler, ahşabı tepkisel bir malzeme haline getirir. Ahşap malzeme bu özelliklerinden dolayı kırılma, çatlama gibi sonuçlar doğuracağı için kurutulmaktadır. Çalışmada önerilen tepkisel malzeme sisteminde ise ahşap malzemenin bu özellikleri sistemin tepkiselliğini sağlamak için kullanılmaktadır.

Çalışma kapsamında neme tepkili kompozit malzeme tasarlanır. Çift katmanlı malzeme aktif ahşap katman ve pasif polimer katmanından oluşmaktadır. Bu katmanlar epoksi bazlı yapıştırıcı ile yapıştırılırlar. Ahşap nemli ortamlarda nemi alarak şişer ve uzar. Polimer ise nem değişiminden etkilenmez ve şekil değişikliği göstermez. Geliştirilen kompozitte aktif ahşap katmanı nem alarak uzamak isterken, pasif polimer katmanı uzamasını engeller. Bu durum sonucunda ahşap polimer yönünde kıvrılır. Böylece, kompozit malzeme nem değişikliği karşısında kıvrılarak nem koşullarına tepki verir.

Üretilen kompozit malzemenin tepkisel davranışı, geliştirilen nem kabiniinde gerçekleştirilen deneyler ile analiz edilir. Nem kabininin bağıl nem oranı  $80 \pm 5\%$  olarak belirlenmiştir. Kaynaklara göre bu nem oranı, termal konfor koşullarının en üst nem oranı olarak kabul edilmektedir ve aynı zamanda İstanbul’da görülen en yüksek nem oranıdır. Polimer ve ahşap çeşidi, ahşap fiberlerinin yönelimi ve katmanların kalınlıkları malzeme tepkiselliğine etkileyen parametreler olarak kabul edilir. Malzeme deneyleri ile kompozit malzemenin farklı parametrelere göre değişen tepkisel davranışı incelenir. Bu deneylere ek olarak, kompozit malzemenin kıvrılmasını kolaylaştırmak için polimerler fiberli hale getirilerek malzemenin tepkisel davranışına etkisi test edilmiştir. Yapılan deneyler gözleme dayalı ve hesaba dayalı analiz yöntemleri ile değerlendirilir. Gözleme dayalı analiz yöntemlerinde test edilen kompozit malzemelerin kıvrılma değişimini analiz edilerek, bir tepki grafiği çizilir ve bu grafik ile malzemelerin kıvrılma değişimleri karşılaştırılır. Hesaba dayalı analiz yönteminde ise gözleme sonucu elde edilen sonuçlar, hesaplamalar ile doğrulanır. Kompozit malzemelerin neme tepkisi sonucu kıvrılma miktarı hesaplanır. Bu analiz yöntemleri ile elde edilen sonuçlar karşılaştırılır ve en uygun tepki veren malzeme parametreleri saptanır.

Malzeme deneyleri, malzeme bilimci ve tasarımcının bir arada çalışması ile gerçekleştirilmiştir. İşbirlikçi çalışma ile deney ortamında kullanılan nem kabini tasarlanmış, kompozit malzeme üretilmiş ve deneyler hem gözlem hem de hesaplamalı yöntemler kullanılarak değerlendirilmiştir. Farklı disiplinler arasındaki işbirliği, tasarım yaklaşımının, sayılabilir yöntemlerle değerlendirilmesini sağlamıştır.

Çalışma, neme duyarlı kompozit malzemeleri parametrik strüktür tasarımı ile birlikte kullanarak tepkisel malzeme sistemi tasarlamayı amaçlar. Strüktür tasarımında hesaplamalı tasarım araçları kullanılmıştır. Güneş ışığı nemi etkileyen önemli faktörlerden olması sebebiyle, strüktürün form tasarımının tasarım parametresi olarak kabul edilir. Güneş ışığı analizi Grasshopper programının çevresel analiz eklentisi olan Ladybug programı kullanılarak gerçekleştirilir. Elde edilen güneş ışığı analizi verilerine göre, ilk biçim denemeleri Rhino programında yapılır. Biçim denemelerinde amaç daha fazla güneş ışığı alacak yüzeyler elde etmektir. Üretilen form, Grasshopper ile geliştirilir. Geliştirilen formda daha fazla güneş ışığı alan

yüzeylerdeki birimler daha geniş aralıklara sahipken, daha az güneş ışığı alan yüzeylerdeki birimler daha dar aralıklara sahiptir. Bu aralıklara tepkisel paneller yerleştirilir. Tasarlanan neme duyarlı kompozit malzeme sistemde tepkisel paneller olarak kullanılır.

Strüktürün yapım süreci de çalışmaya dahil edilmiş, birimlerin birleşme detayları hesaplamalı tasarım araçları kullanılarak tasarlanmıştır. Kullanılan birleşme detayları ile strüktürün birimlerinin herhangi ek malzeme kullanılmadan birleştirilmesi amaçlanır. Böylece strüktür sökülebilir, taşınabilir ve yeniden inşa edilebilir. Birimlerin lazer kesim ile üretilerek birleştirilmesiyle, strüktür inşa edilir.

Geliştirilen tepkisel malzeme sistemi, çevredeki değişen nem koşullarına uyum sağlamayı amaçlar. Tepkisel paneller nem oranı düştüğünde dışarı doğru (ahşap katmanın yönünde), nem oranı yükseldiğinde ise içeri doğru (polimer katmanı yönünde) kıvrılırlar. Böylece strüktürdeki hava akışı, neme duyarlı panellerin hareketiyle gerçekleşir. Mekâna süzülen ışık, panellerin neme bağlı hareketine göre gün içerisinde değişerek kullanıcıya neme göre farklı mekan deneyimi sunar. Değişen nem koşullarına tepki sırasında mekanik birleşen ve enerji kullanımına ihtiyaç duyulmadığından, geliştirilen tepkisel sistem enerji etkin (pasif) tepkisel sistem olarak tanımlanabilir.

Çalışmanın ilerleyen aşamalarında deneyler sonucu ile elde edilen veriler ile belirlenen malzemenin tepkisel davranışı, bilgisayar ortamında simule edilebilir. Kompozit malzemenin tepkisel davranışı sayısal ortamdaki analizlere dayanarak ilerleyen aşamalarda geliştirilebilir. Tepkisel malzeme sistemleri, tepkisel mimarlık alanında yaygınlaşırken, yürütülen tez çalışması malzemenin davranışının tepkisel sistemde nasıl kullanılacağını incelemiştir. Geliştirilen tepkisel malzeme sisteminin amacı, tepkisel sistem tasarımında malzeme davranışını kullanmaya teşvik ederek, mekanik tabanlı tepkisel sistemlere alternatif bir tasarım önerisi sunmaktır.



# **1. INTRODUCTION**

## **1.1. Purpose of the Thesis**

The study presented in this thesis questions how material behavior can be utilized in developing a responsive system. The aimed material based responsive system uses material behavior as an instrument for responsiveness. Hence, the responsiveness of the system is accomplished via responsive composite material.

Inspired by pinecone scales, the responsive material is obtained from a bilayer composite, which employs the hygroscopic behavior of wood and responds to humidity. The responsiveness is acquired by the inherent material behavior rather than by mechanical components that are subsequently added into the system. The humidity response of the composite is observed through material experiments. A series of experiments is conducted in order to examine the effect of material parameters (type, thickness, dimensions...) on the responsive behavior of the composite.

The developed responsive composite material is utilized by designing a parametric structure. Computational tools were utilized to develop the parametric structure, which introduces a simulative background of changeable environmental conditions. The responsive material system, the core inquiry of the thesis, is ultimately designed by integrating the responsive material with the designed parametric structure. The parametric structure and responsive material altogether found a 'Responsive Material System' in the presented thesis and named as "Hygro\_Responsive Structure".

## **1.2. Structure of the Thesis**

The thesis can be read in two main parts. The first part, comprising of Chapters 2 and 3, covers a comprehensive literature review of the thesis' context. Chapter 2, in specific, gives a definition-based overview of responsive system design. Based upon literature-extracted knowledge, the thesis sets forth three main responsive system types, which are classified according to the use of energy and material: Active Responsive Systems, Hybrid Responsive Systems and Passive Responsive Systems. The first of the three benefits from mechanical components and control mechanisms, both of which are dependent on energy supply. The second type integrates mechanical responsive systems with 'smart material' concept. The third category emphasizes the essence of material-inherent behavior for responsiveness and eliminates the use of energy-requiring mechanical systems. This thesis study puts its focus on the third type, which is referred to as Passive Responsive Systems. The study also introduces a definition of 'Material based Responsive Design Approach' towards constructing a perceptible framework of responsive material systems. Also, material computation, which can be described as the utilization of responsive material behavior in computational design, is explained in detail. A literature review as well is included and presented, along with examples from case studies conducted on responsive material systems.

Chapter 3 pursues an exploration of wood as a material; and in specific, of its behavior. This chapter inspects the inherent properties of wood that enable it to be utilized as an instrument for responsiveness. Subsequent to material examination, samples of previous studies are analyzed in means of selected materials, design and production methods. On ground of the analyzed example studies, a hygromorphic composite, as responsive material, is developed through integrating pinecone actuation principle with hygroscope and anisotropy properties of wood.

The second part, comprising of Chapters 4 and 5, includes a design proposal for a responsive material system. Chapter 4 provides details of the suggested responsive composite material and presents the methodology of material experiments. Chapter 5 describes the design process of the responsive system structure, in which computational design tools are utilized.

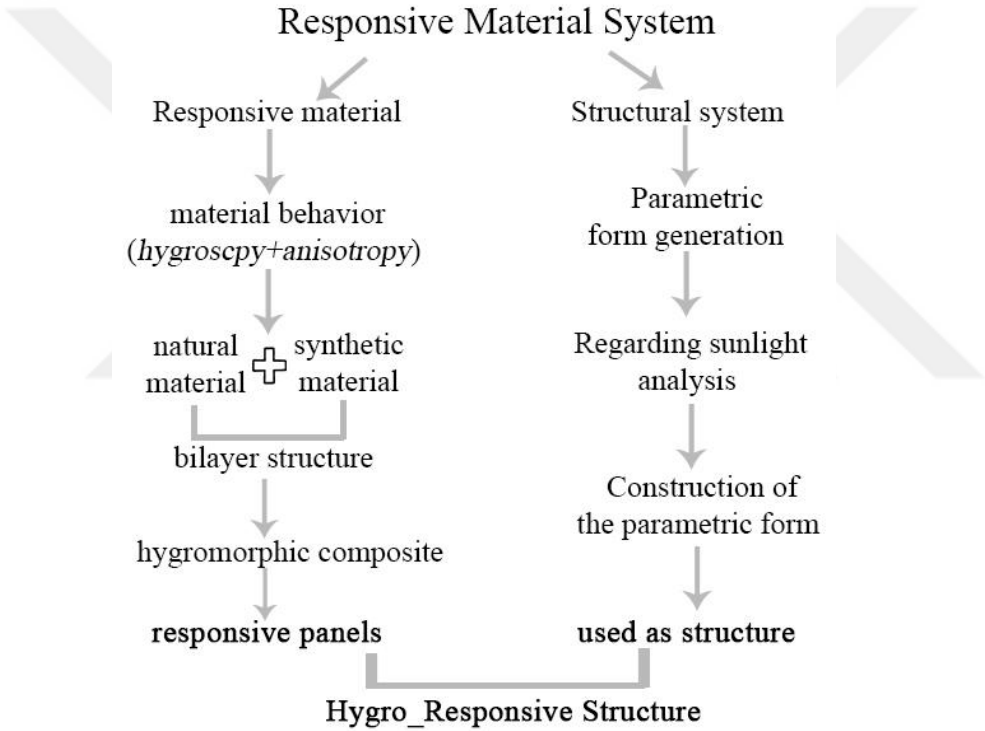


Chapter 4 demonstrates that previous studies and material examination constitute the foundation on which the described composite material of the responsive system is developed. The composite material comprises of two layers, the natural one; i.e. wood, being the active, and the synthetic one; i.e. polymer, being the passive. The hygroscopic property of wood procures responsiveness to the composite whereas the synthetic material facilitates responsiveness. The design process of the material based system relies on learning through experiment. A series of experiments is carried out to perceive responsive material behavior. The affective material parameters of the composite are evaluated through conducted experiments. The evaluation of material experiments relies on empirical (observational) and quantitative (numerical) analysis methods. In the empirical method, the responsive behavior of the tested composite samples is observed. A response graph is drawn to demonstrate the curvature change of composite materials and make a comparison of their responsiveness. In the numerical analysis, calculation is used to justify the observational analysis results: The above-mentioned curvature change of composite samples is calculated and responsiveness statuses are compared. On the ground of the experiment results, the optimum material parameters are determined in purpose of enhancing the responsive behavior of the composite.

Elaborating the design process of the responsive system structure, Chapter 5 includes (1) design; and (2) construction process of the structure. The design of the structure is conducted with computational methodologies that take environmental parameters as basis. Due to its influence on relative humidity, sunlight was picked as the design parameter for the structure's form generation. Ladybug (the environmental analysis plug-in of Grasshopper) is employed to model the sunlight simulation in this study. Form generation is carried out in Rhino and the generated form parameters regarding the sunlight simulation are modified through Grasshopper. The construction process involves (1) the joint design of the structure modules, (2) the fabrication and assembly processes of the structure. The connection between the modules (puzzle and finger joint) is obtained and optimized through digital tools. Two hundred (200) unique modules of the structure are put in order for digital fabrication through which a laser cutter is used. The fabricated components are assembled through joint

connections. The ultimate responsive composite is utilized as the developed structure's responsive panel pieces.

Chapter 6, the final chapter, conducts an overall review on responsive material system design, presenting a summary of the study with concluding remarks. The chapter furthermore points on the collaborative work conducted in this experimental study. The influence of collaborative design thinking on the experimental study is presented. Finally, further research and practices that can be presented to develop the study context of this thesis are discussed.



**Figure 1.1:** The design progress of responsive material system.

## 2. MATERIAL BASED RESPONSIVE SYSTEM DESIGN

The continuous increase of population, industrialization and hence, of the use of machinery, inevitably brought about incremental volumes of energy consumption. Machine-manufactured construction and maintenance of artificial building systems altogether constitute almost 50 percent of the total energy consumption (Armstrong, 2011). Energy consumption volumes in buildings lead architects to give a deeper regard to environmental awareness. In process of materializing their design of environmentally sustainable buildings, architects collaborate with engineers and other specialists and adjust energy consumption solutions into building systems (Durmisevic, 2015). Building components are designed to self-reconfigure to adapt to environmental changes and user behavior patterns through *responsive systems*. Responsive systems mechanically shift themselves in form to adapt to environmental conditions, serving to the ultimate purpose of increasing building performance and ensuring the highest possible level of comfort to users. Responsive systems convert buildings from energy consumers into energy adapters (Linn, 2014).

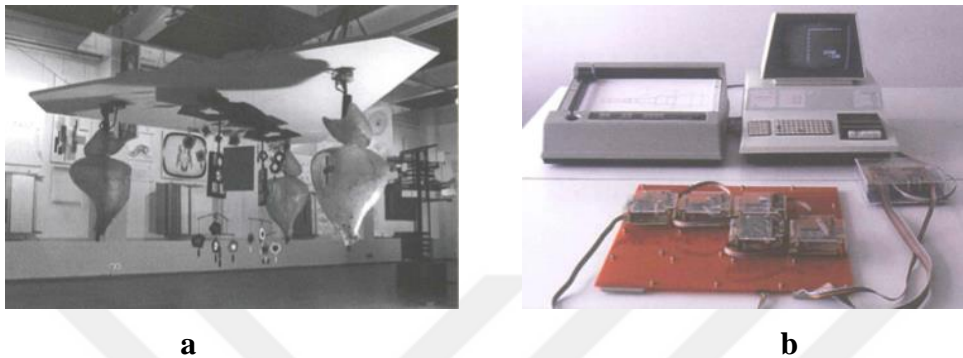
### 2.1. Responsive System Design

#### *The responsive design theory*

The theoretical background of responsive design has its foundations on developments at computer and machine technologies. The roots of the responsive design theory lie in cybernetic control systems that were developed by Norbert Wiener. Cybernetic control systems dealt with the study of human/machine interaction on the basis of feedback, control and communication principles (Mindell, 2000). The human-machine interaction theory triggered the developments in artificial intelligence (AI) and information technologies (IT). These developments induced robotics and adaptive systems to progress, which are the corner stones of the development process of responsive system design (Fox and Kemp, 2009).

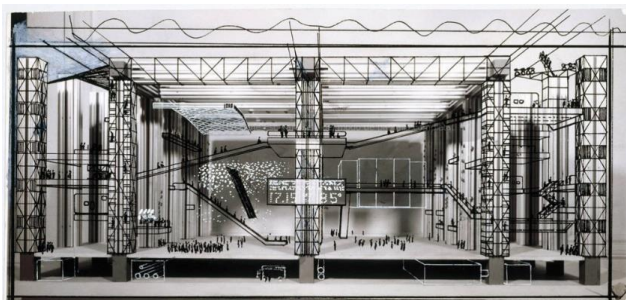
The primary responsive design practices were seen in 1960s, as technological developments and interdisciplinary collaboration taking place between the designer, engineer and cybernetician started to show up. Gordon Pask first materialized the human-machine interaction in ‘The Colloquy of Mobiles’ in 1968 (Figure 2.1.a). In

this installation, a communication between mobiles (the tools and the machinery) and visitors was sustained by computer systems. John and Julia Frazer, along with Cedric Price, designed another cybernetic project in 1976, which was referred to as ‘The Generator’ (Figure 2.1.b). The group created a programmable modularized computer system that was capable of responding to altering requirements.



**Figure 2.1:** The Colloquy of Mobiles Installation (a) and Generator interface (b) (Dunn, 2012).

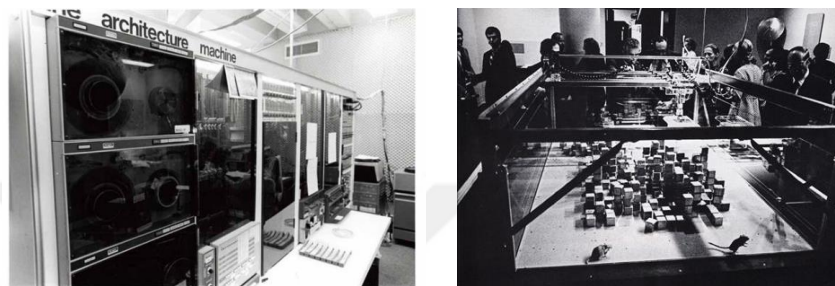
In 1962, Cedric Price and Gordon Pask designed ‘Fun Palace’, a project that can today be referred to as the initial prototype for responsive design (Figure 2.2). The aim of this project was build a ‘fun laboratory’ with machines. The installation responded to visitors’ requests and movements by transforming its movable spaces through control systems (Url-3).



**Figure 2.2:** Fun Palace illustration plan and interior perspective (Url-3).

Based on theoretical developments and implementations, Nicholas Negroponte coined the term ‘Responsive Design’ in 1970’s. A responsive design aims to integrate computing power into a built environment and hence render the parts of the building communicative with their environment (Negroponte, 1970). The responsive systems transforms the static space into an adaptive environment. As a result,

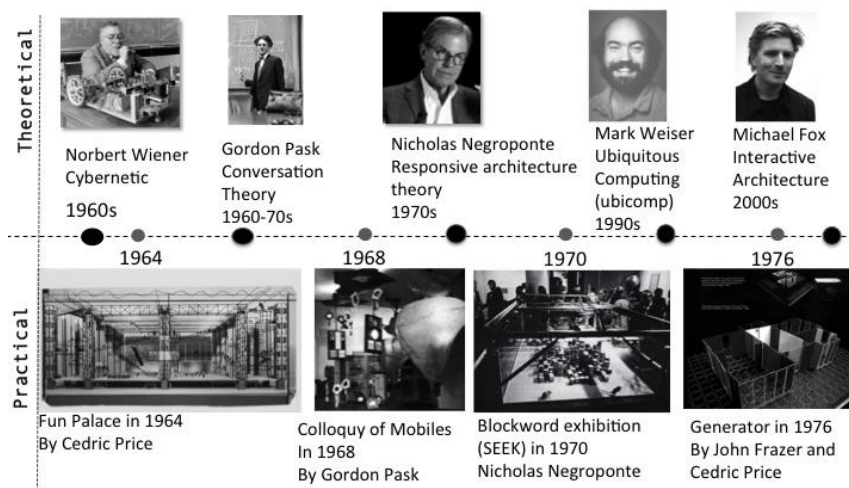
architecture becomes an evolutionary machine through responsive systems, as Negroponte (1970) states. Negroponte developed the SEEK project (Blockword) and exhibited it in the Jewish Museum, New York in 1970 (Figure 2.3). SEEK was the first implementation to bring human-machine interaction into a space (Url-2). The interaction of the gerbils with their living space was controlled by the designer through robotic arms, with which the designer located the boxes and ensured interaction.



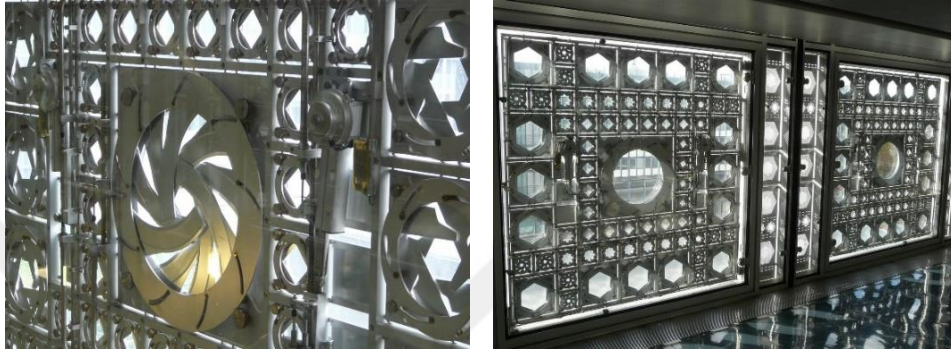
**Figure 2.3:** SEEK exhibition images (Url-2).

Charles Eastman described the basis of responsive design components by using the analogy of thermostat; sensors, actuators and control mechanism in 1972 (Kolarevic and Parlac, 2016). Mark Weiser (1991) reduced the physical dimensions of responsive components to indistinguishable magnitudes. Weiser also coined the term ‘ubiquitous computing’. Ubiquitous computing facilitates the user-environment interaction and renders the system more pervasive (Weiser, 1991). The chronological progress of responsive design is displayed in the below Table 2.1

**Table 2.1:** The developments in responsive design.



The first responsive building system is the responsive façade of The Institut du Monde Arabe, which is designed by Jean Nouvel in 1988. Nouvel designed a light-responsive façade system through photosensitive mechanical diagrams which were inspired by *mashrabiya*, as displayed in Figure 2.4 (Jodidio, 2012). The aim of designing a responsive façade is to filter the sunlight, minimize the solar gain and provide privacy to users.



**Figure 2.4:** Light responsive façade system (Url-4).

### ***Responsive design definition***

The eventual integration of responsive systems into architecture, on the background of which laid all previous developments in the history of responsive systems, came to occurrence in 1980's and since then, it gradually became prevalent. Sterk (2004) defines the ***responsive system*** as the system that has the ability to alter its own form in response to the changing conditions. According to Kolarevic and Parlac (2016), the responsive design domain has emerged as a response to the rigid, static and inflexible articulation of space.

Kolarevic and Parlac (2016) state that the building becomes 'alive' with the integration of responsive systems because then it senses its environment and adjusts itself accordingly. Yiannoudes (2010) argues that responsive systems stand between the living and the non-living; they remove the boundaries between the human and the machine; between the biological and the technological. Fox (2009) indicates the impacts of responsive design on the building and the user, as articulated below:

- Renders the design of adaptive, smart and sensitive spaces possible by enabling change in configuration in response to the shifts in environmental conditions or user requirements

- Improves building performance by optimizing environmental conditions
- Responds to environmental circumstances and acts as an intermediary agent in establishing a dialogue between the user and the environment towards ensuring user comfort.
- Expands environmental consciousness of users by creating awareness on environmental changes
- The continuous development pattern of responsive systems procures new aesthetical features to buildings, as Meagher (2015) points out.

### *Components of responsive systems*

Responsive system senses and measures the changing conditions via its sensors. It ‘thinks’ and determines which response to be given through its control mechanism (its ‘brain’) and responds with changing shape, through actuators. Components of a responsive system (Figure 2.5) render a space more sensitive, more intelligent and adjustable to the user and the environment.



**Figure 2.5:** The sensor and actuator parts (a) and controllers (b) for the responsive system (Fox, 2009).

A *sensor* is a device detects the external stimuli and transforms it into digital data (Fox, 2009). The type of the sensor can vary according to the received stimulus type such as; light, sound, thermal, humidity, touch and motion sensor.

An *actuator* is the kinetic part of the system and composed of the robotics and mechanical components. An actuator alters the form of the system through robotic devices. Actuator is activated by the electrical signal which comes from the control

systems; it converts the input signal into the mechanical movement (Addington and Schodek, 2005). The processed data is transmitted into the actuators for the mechanical actuation. Common actuator types are electromechanical, hydraulic and pneumatic.

A **control mechanism** receives data from the sensors, process data and controls the movement of the kinetic parts according to the data (Fox, 2009). Nordenson (1995) asserts that the control mechanisms are the brain of the system and make the kinetic design components intelligent and adaptive. Fox (2009) states the significance of control mechanism “without control mechanisms a kinetic environment is like a body without brain: incapable of moving”.

In control mechanisms, the response is managed through programming. In order to program the control mechanisms different software can be utilized. Arduino is the most preferable program since it presents simple and accessible open-source platform (Url-5). Arduino utilize a simple programming derived from Processing and hardware parts; microcontroller, the sensory and robotic devices.

Jeng (2012) attributes the key principles for the responsive design as **sensitivity**, **smartness** and **responsiveness** by considering the function of its components, as shown in the Table 2.2. **Sensitivity** derives from the detection of the stimuli through sensory systems and exchanging the stimuli into data for processing. **Smartness** derives from the controlled and processed data through the control systems in order to adapt the system to environmental conditions. **Responsiveness** derives from the form transformation through actuator devices by converting data into motion (Jeng, 2012). Metaphorically, the sensory network resembles the sensory organs, the control mechanism resembles the neural systems and brain, the actuator resembles muscular system in human body.



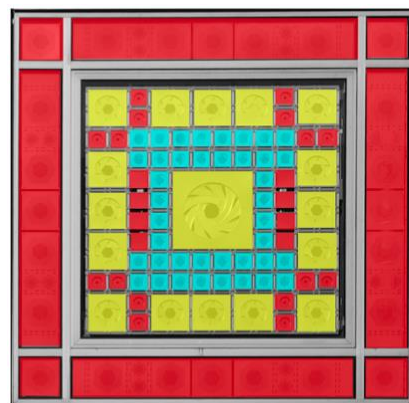
**Table 2.2:** The key principles of the responsive design (By the author).

<b>Key principles</b>	<b>Sense</b>	<b>Think</b>	<b>Response</b>
<b>Process</b>	Perceive the agent	Control data	Data converted to motion
<b>Medium</b>	Sensory systems	Computational tools and control mechanisms	Robotics actuators
<b>Purpose</b>	sense the environment	Control the response to adapt	Make responsive through shape change



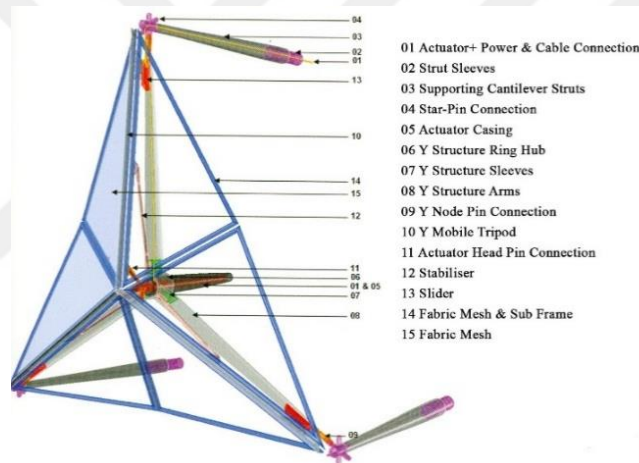
### ***Mechanical responsive systems***

In current use, responsive systems operate with mechanical components (sensor, actuators, micro controller and robotics equipment). The dependency to mechanical components in responsive systems results with the inevitable need for maintenance, due to the fragile characteristics of mechanical components. For instance, the mechanical diaphragms in the Institut du Monde Arabe experienced longevity problems, required maintenance and hence, failed to function; as Meagher (2015) analyzed. Illustrated in Figure 2.6, Meagher’s (2015) analysis indicates the non-functional diaphragms with red color and the functional ones with yellow and blue color.



**Figure 2.6:** The analysis of non- functional responsive façade of Arab Institute (Meagher, 2015).

The mechanical components of the responsive system constitute a complex mechanism. Displayed in Figure 2.7, the responsive tripod actuator mechanism on the façade of Al-Bahar Tower (designed by Aedas Design Group) exemplifies this complexity. The mechanical components are activated by energy use. As they consume energy, mechanical-based responsive systems cannot be qualified as sustainable systems (Maragkoudaki, 2013). As Sample (2012) claims, the deficiencies that arise from dependency to mechanical components prevent the responsive design from becoming prevalent. As an alternative, natural responsive systems are researched towards avoiding mechanical dependency at responsive systems. Since responsiveness is conducted in material level in the nature, designers take the material potential into regard in designing energy efficient responsive systems.



**Figure 2.7:**Theparts of the complex responsiveunit (Fortmayer &Linn, 2014).

## 2.2. The Classification in Responsive Systems

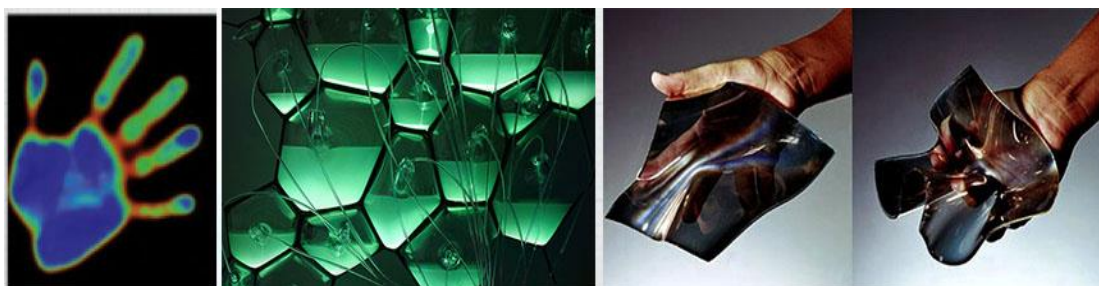
The current tendency in responsive system design is the shift from mechanical transformation to material reformation. Material is included in the development of responsive systems as an active agent, through the involvement of smart materials, to eventually establish responsive material systems. Responsive systems are classified according to their use of material. The comparison can be seen in Table 2.3: The mechanical based responsive design refers to active systems (1); the smart material based responsive design refers to hybrid systems (2); and the material based responsive design refers to passive systems (3).

**Table 2.3:**Comparison of the responsive systems types.

Active Responsive Systems	Hybrid Responsive Systems	Passive Responsive Systems
Use mechanical components for the responsiveness	Integrate smart materials with mechanical components	Use material behavior for the responsiveness
Material remains limited not used in responsiveness	Material facilitates the responsiveness (used sensor or actuator)	Material generates the responsiveness
Requirement of the energy supply and mechanics	Decrement in requirement of the energy supply and mechanics	Any requirement of the energy supply and mechanics

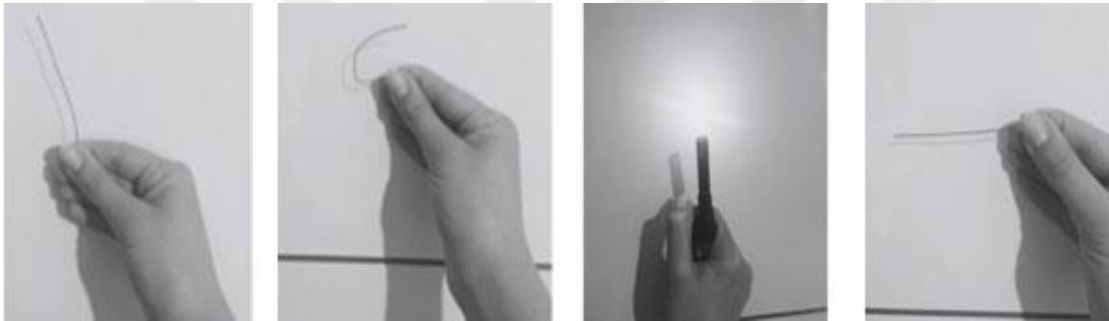
**Hybrid Responsive Systems**

Hybrid responsive systems integrate smart materials with responsive components by combining cybernetic processes with smart material properties (Ou, 2014). Smart materials can be defined as materials that sense the changes in their environment, process the sensed information and act accordingly (Kroschwitz, 1992). Piezoelectric materials, shape memory alloys and chromic materials set precedent to smart materials (Figure 2.8). As Schröpfer (2012) states, smart materials conduct responsiveness in material level by changing property or exchanging energy, in response to external influences. The energy-exchanging smart materials can be computationally controlled and enhanced. Thus, energy-exchanging smart materials can be employed in development of responsive systems (Addington and Schodek, 2005).



**Figure 2.8:**Smart material samples (Url-10, Url-11, Url-12).

Operating as sensors and/or actuators, smart materials replace mechanical components in hybrid responsive systems. For instance, a thermo-chromic material can be used as a sensor to detect temperature in hybrid responsive systems: The material changes its color in response to temperature changes. With their capability to change in form in response to external stimuli, smart materials replace actuators in hybrid systems. Utilization of smart materials in function of actuators removes the mechanical joints, hinges and motors from the system. For instance, Nitinol (alloy of Nickel and Titanium) is the best-known shape memory alloy (SMA) which is used as an actuator in hybrid responsive systems. Nitinol wire can be bended in any shape. When exposed to heat, the bended Nitinol wire reverts to its initial shape (see Figure 2.9), due to *shape memory effect*. (Addington and Schodek, 2005).



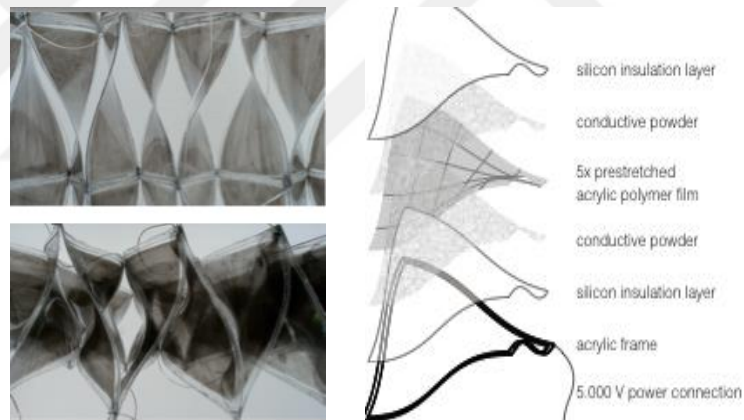
**Figure 2.9:**The shape memory effect of Nitinol wire (By the author).

Designed by Rob Ley and Joshua Stein, Reef Installation was exhibited at Storefront for Art and Architecture in 2009. The installation, inspired by sea reef, displays the way that a smart material integrates with mechanical responsive systems (Url-14). It recognizes the presence of a user and responds by altering the shape of the Nitinol wire, as illustrated in Figure 2.10 (Url-14). Nitinol presents an organic fluid movement without mechanized motion by remembering its initial shape. Mechanical systems are used to manage the interaction between clustered surfaces. When a user gets into the envelope, the envelope is stimulated by this mechanism. The Nitinol wire is induced and actuates the surfaces in response to the user's movement (Url-15).



**Figure 2.10:**Reef installation (Url-14).

Apart from the substantial use of smart materials as actuators or sensors, a responsive smart *composite* can also be produced through combining different smart materials. In Shape\_Shift experimental installation, designed by Zürich Responsive Design Studio, Electro Active Polymer (EAP) was produced as a smart composite (Url-16). EAP substitutes the actuator and responds to external stimuli by converting electrical energy into mechanical force (Figure 2.11).



**Figure 2.11:** EAP material structure(Url-16).

### 2.3. Material Based Responsive System

Hybrid responsive system is a translation stage from mechanical to material approach in responsive design. However, smart materials are man-made materials and they have limited availability (Holstov et al., 2015). These circumstances were regarded in conducted researches: The interest tends towards natural materials in responsive systems. Architects examine responsiveness in natural systems. Conducted researches focus on the material's *behavior* rather than its *shape* (Hensel, Menges

and Weinstock, 2010). Researches reveal that responsiveness in nature is achieved in material level. Natural systems involve movement for adaptation and responsiveness, without the presence of muscles (Jeronimidis, 2004). The response capacity is ingrained in the material itself in natural systems (Menges and Reichert, 2012). Therefore, 'material thinking' gains importance in responsive systems. As an instrument for responsiveness, material behavior is examined and utilized. Menges (2012a) defines this novel exploratory and open-ended design process as *material based responsive design*. Material based responsive design approach transforms responsiveness from a concept with mechanical basis to a biological paradigm, as Menges and Reichert (2012) indicate.

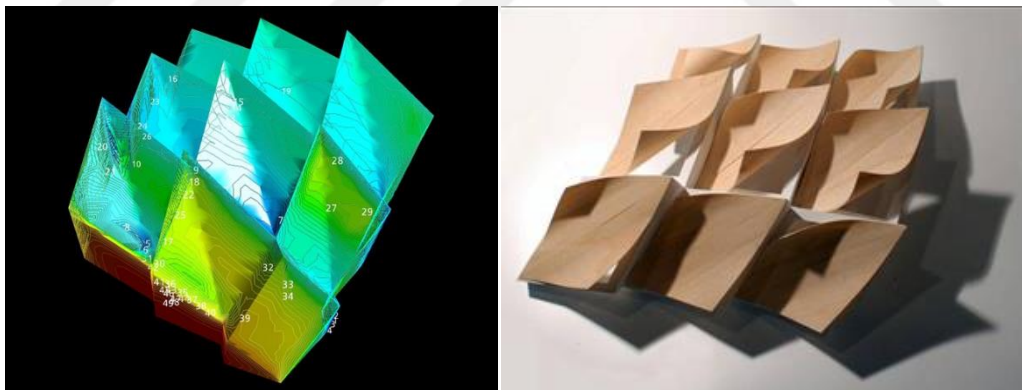
In this approach, a responsive *material system* is developed, which comprises of an overall interaction between material behavior, form, structure, energy and environment. Menges (2008a) defines material system as “understanding of form, material, structure and environment not as separate aspects, but rather as complex interrelations that are embedded in and explored through integral computational process” (p.56). Material becomes the generative driver in material systems. “The material structure transforms into the machine itself in material system design”, as Menges points out (Url-19). The form and response of the material system emerges on the ground of the material behavior (Menges, 2008a). The material system requires neither energy nor mechanical components as it leverages the embedded responsiveness of the material. Therefore, these responsive systems can be referred as *passive responsive systems* in this thesis. Responsive material systems present sustainable and energy efficient solutions for responsive architecture.

## **2.4. Material Computation**

Computational design methods contribute to the exploration of material potential. According to Schröpfer (2012), “Computational design has impacted architectural design in multi-faceted ways” (p. 171). In responsive material systems, computational design methods are used to instrumentalize the material. The material and the computation process complement each other: Computation refers to the processing of information and material has the capacity to compute through its inherent behavior (Menges, Fleischmann, Knippers, Lieanhard and Schleicher 2012).

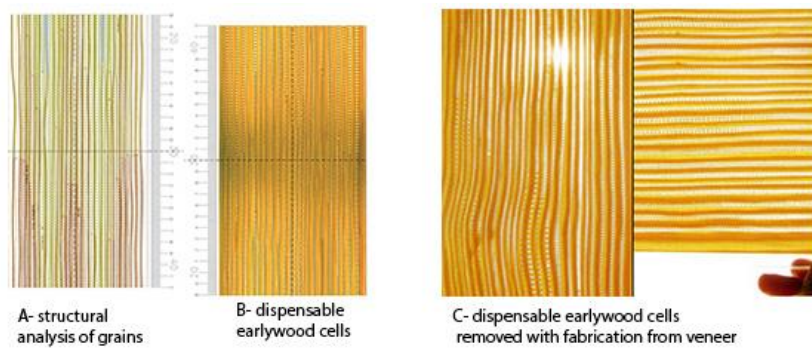
The integration of material and computation allows the exploration of a novel term, *material based design computation* or *material computation*. In material computation, material behavior is analyzed and programmed with computational tools.

Neri Oxman (2010) defines material based design computation as “a set of computational strategies supporting the integration of form, material and structure by incorporating physical form-finding strategies with digital analysis and fabrication” (p.3). Material computation processes the information from material behavior and feedbacks to the environment via computational tools. The framework of material computation requires the parametric setup based on material constraints and evaluation on material-environment interaction (Menges, 2008b). The material is analyzed, calculated and arranged to serve the desired function and to develop material systems. Computational analysis tools define the material behavior through simulations, instead of just representing its physical properties in a digital model. Figure 2.13 sets a precedent for the simulation of hygroscopic behavior of wood material.



**Figure 2.12:**The humidity analysis of the wood veneer in CFD (Computer Fluid Analysis Program) (Url-17).

The inherent properties of the material are computed and manipulated through computational design tools. In the example (Figure 2.14), the wood grain structure is analyzed with analysis tools and manipulated by removing the dispensable earlywood grains through laser cutter, towards obtaining transparent undulated wood element (Url-18).



**Figure 2.13:**The processed wood veneer (Url-18).

Material system emerged via computation tools, as a result of the interrelation between the generative form and material behavior (Menges, 2008b). The form of the system is generated through algorithms (Url-19). Furthermore, with its consideration of material behavior, material computation process renders the eventual fabrication of the generated form possible

## **2.5. Examples of Responsive Material System**

Responsive material systems can employ material behavior to achieve responsiveness by developing artificial responsive composites. Composites may consist of different materials or different specifications of the same material. Hovsepian (2012) defines composite materials as; “Any two materials that are combined together in a single bulk material in order to obtain the best properties from both materials” (p. 332). Composites have multi-layered structures and each layer has a different property (Enhoş, 2014). The difference between the layer properties enhances material performance (Enhoş, 2014). The main objective of producing a composite is to integrate different material properties with the aim of obtaining the desired performance.

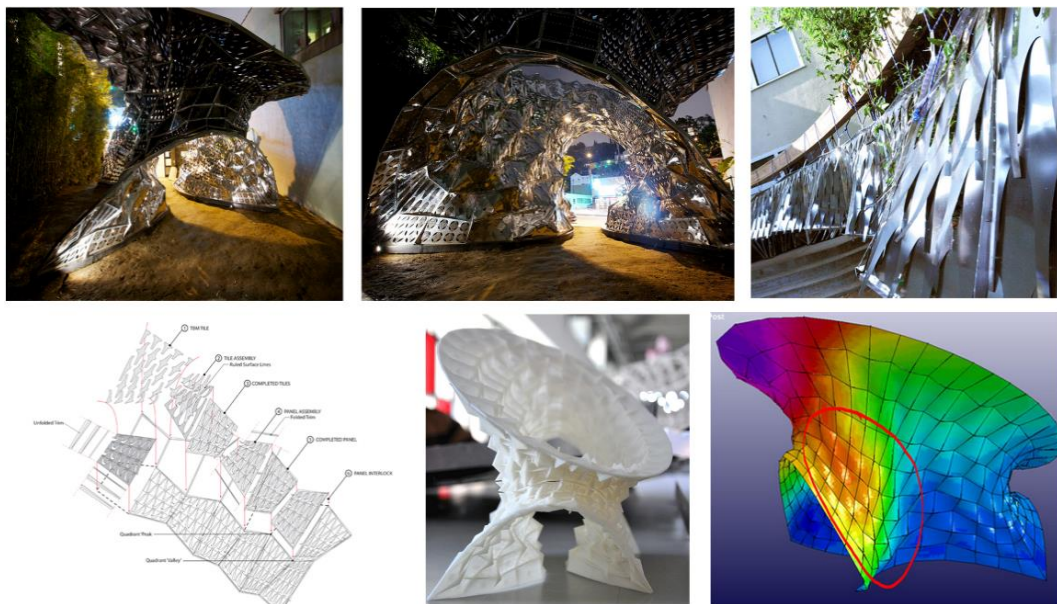
Different examples of responsive material systems are examined below to observe how they employ material behavior via composite development. The examined composite materials are thermo-bimetal (Nickel and Magnesium metals) and Hygromorphic composite (wood and polymer). Both composites utilize the difference in their layer properties to improve responsiveness. Based on the extensive examination, this study suggests a proposal for a responsive material system design.



### ***Bloom installation with thermo-bimetal***

Sung (2012) develops a new thermo-responsive component referred as thermo-bimetal. Thermo-bimetal is derived from the lamination of two different metals (Nickel and Magnesium), each of which has different expansion coefficients (Sung, 2012). The thermo-bimetal strips respond to the changes in temperature through curling movement. The curling is the consequence of the expansion coefficient difference of the two metals. As the composite is exposed to heat, one of the two metals with the higher expansion coefficient expands more than the other, leading the bimetal to curl (Sung, 2012).

Sung designs an environmentally responsive installation named ‘Bloom’ by using thermo-bimetal components at the Materials & Applications Gallery in Silver Lake in 2012 (Figure 2.15). Bloom performs as a sun-tracking instrument with smart thermo-bimetal strips (Sung, 2012). The strips are inserted to the body of the installation according to the position of the sun and to curling direction (Sung, 2012). The thermo-bimetal strips curl in response to the air temperature; thus, the space is ventilated without any mechanical component. As the temperature increases, the strips are curled and the canopy openings expand, which eventually brings airflow and shading (Url-20). When the temperature falls, the strips are curled in the opposite direction and the openings narrow (Url-20).



**Figure 2.14:** Bloom installation and design process (Url-20, Url-21).

In ‘Tracheolis’ project, Sung (2012) designs breathing concrete blocks inspiring the trachea system (the breathing system) of grasshopper (Url-21). The 3D printed concrete blocks with smart thermo-bimetal components allow the airflow as shown in Figure 2.16(Sung, 2014).

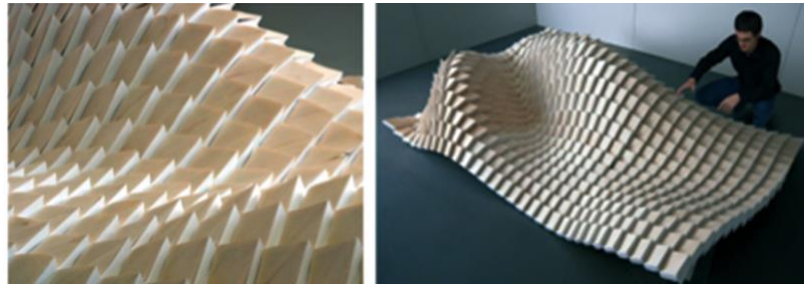


**Figure 2.15:** The conceptual drawings of Tracheolis (Url-22).

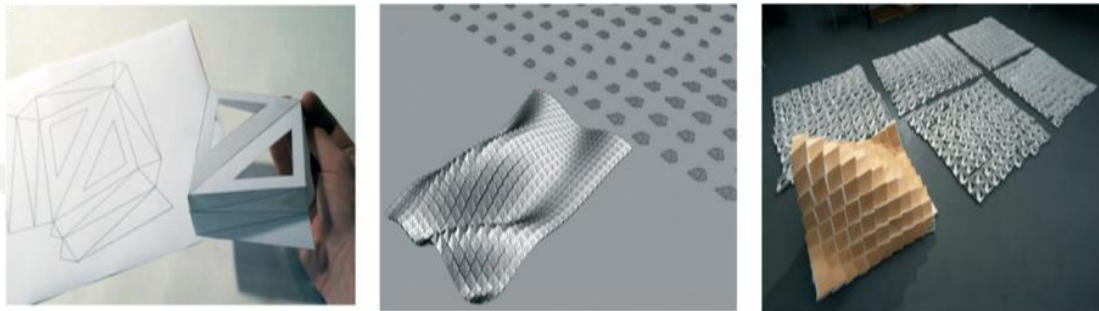
***Responsive Surface with hygromorphic composite***

Utilizing the material behavior of wood, Menges and Reichert (2008c) develop a responsive composite. A semi-synthetic bilayer composite is derived from the combination of wood and polymer. The composite uses the hygromorphic property of wood. The composite can therefore be defined as a ‘hygromorphic composite’. Responsive Surface (Figure 2.17), designed by Menges and Reichert (2007), presents a responsive material system that uses a semi-synthetic composite (Menges, 2008c).

Responsive Structure displays how the material’s responsive capacity can transform the material into the sensor, the actuator and the regulator of the system, without consuming any energy (Menges, 2008c). The structure of Responsive Surface has two main parts: A parametric sub-structure with a folded system and moisture-sensitive veneer composite elements as responsive material (Figure 2.18). The composite elements are triggered by humidity alterations and change shape: They swell in humid air and curve outwards, they shrink in dry air and curve inwards, all without energy supply (Menges, 2008c).



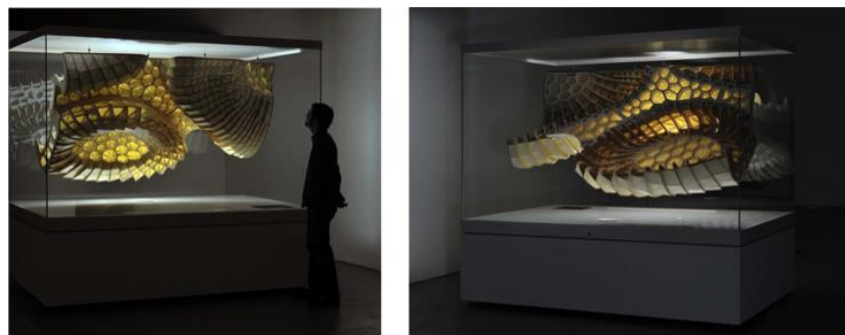
**Figure 2.16:** Responsive Surface physical model (Url-17).



**Figure 2.17:** Responsive Surface design development (Url-17).

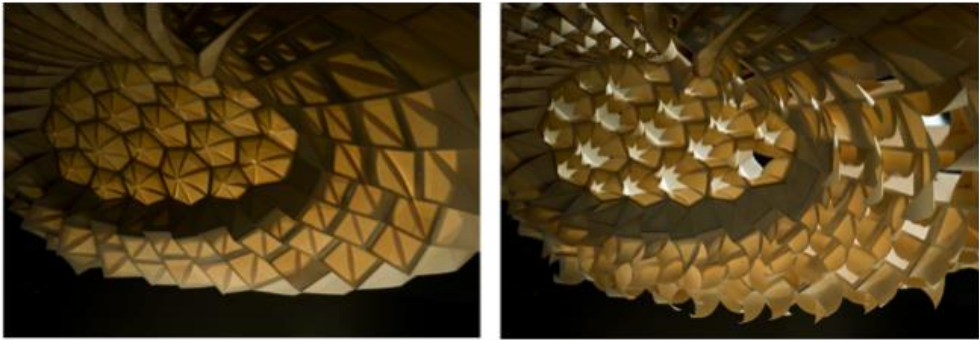
### *Hygroscope with hygromorphic composite*

Menges and Reichert design Hygroscope as a responsive material system by using hygromorphic composite in Centre Pompidou in 2012 (Figure 2.19). This responsive system installation is suspended within a humidity-controlled glass case. The humidifier and dehumidifier technology (Figure 2.21), embedded within the base of case, regulates the climate in the case. The climate regulation is driven by two influencing factors; one being the relative humidity of Paris city, and the other being the visitor density in the room, as it effects the absolute humidity content (Menges, 2012b).



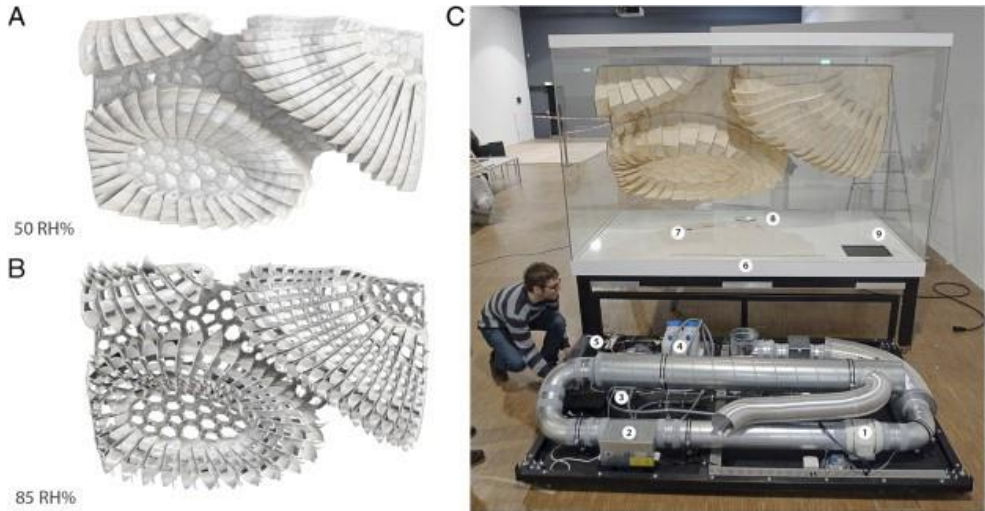
**Figure 2.18:** Hygroscope installation in humidity controlled glass case (Url-19).

The complex form is generated through the integration of intrinsic material performance and extrinsic environmental data (Menges, 2014). According to Menges and Reichert (2012), this installation presents the virtual extension of the exterior climate of Paris and visitor density in Pompidiu (Url-19). Hygromorphic composite veneers curves inwards or outwards, in response to the controlled microclimate.



**Figure 2.19:** Responsive behavior of hygromorphic wood composites (Url-19).

On the ground of the examined precedents, the hygromorphic composite is selected in this study to be employed as the responsive material since it introduced the embedded behavior of natural material. On this basis, understanding the wood-inherent properties becomes a key parameter for developing a responsive composite material. Next section (Section 3) focuses on inherent material properties and presents examples of responsive materials.



**Figure 2.20:** The simulation and working mechanism of Hygroscope units (Menges et al., 2014).

### 3. WOOD AS A MATERIAL SYSTEM

Wood takes the traces of the natural system since it grows and develops in the nature. Wood displays adaptive movement due to its embedded material properties. In this study, the inherent material properties of wood are utilized to achieve responsiveness in material system design. Wood, as a suitable natural material, is selected as it has numerous qualities in terms of availability, utilization and construction, as listed below in a more detailed manner:

- Sustainable and renewable properties due to its natural origin,
- Versatile material, multifunctional and large area of use
- High availability, ease of utilization and assembly,
- Low cost and low environmental effects during production,
- Potential to take shape easily through cutting, bending and carving methods,
- Easy and affordable machine processing for manufacturing and digital fabrication techniques (like CNC and laser cutting),
- Wide range of connection options to expand the surface (finger joint, dove tail etc.),
- Means to combine with other materials (like composite production).

#### 3.1. Explorations at Embedded Material Properties

Wood interacts with nature and changes its behavior, due to its inherent material properties. The *hygroscopic* (ability to take or yield moisture) and *anisotropy* (directional dependency of material characteristics) are the embedded properties of wood, each of which indicates responsive material behavior. The first characteristic, hygroscopic, renders the wood material responsive to humidity. Wood receives the moisture and swells in humid air, while it yields the moisture and shrinks in dry air. The second characteristic, anisotropy brings dimensional changes that arise from the alterations in humidity.

The dimensional change of wood, derived from hygroscopic and anisotropy, has been accepted as a deficiency since it causes deformations in wooden products. The wood material has been being exposed to special processes such as drying methods in

purpose of restricting dimensional change and stabilizing the moisture content (Menges, Reichert and Correa, 2014). It is worth to mention that wood processing methods constitute 70% of the world's total energy consumption (Menges et al., 2014). This study however, in contrast to the general acceptance, makes a use of hygroscopic actuation and anisotropy; rendering them the key elements of the responsive material system. Therefore, understanding the inherent properties of wood material becomes an essential parameter in developing a responsive material system, which is the basic inquiry of the thesis.

### **3.1.1. Hygroscope (Humidity transition)**

Wood expands or contracts in response to humidity alterations, due to its *hygroscopic* property. A hygroscopic material takes moisture from atmosphere in dry air and yields the moisture when in humid air to balance the moisture content between wood fibers and environment (Menges, 2014). The humidity transition is achieved by changing the water content of wood fibers; this leads to the *dimensional changing* in wood, namely *swelling* and *shrinking*. Water exists in wood in two ways; as *bound water* in wood cells or as *free water* in fiber cavities (Winandy, 1994).

As the relative humidity content gets higher, wood takes in the moisture; thus the water content in wood fibers increases. Wood fibers absorb the water until they are saturated; then the water content in fibers reaches to the fiber saturation point (FPL, 2010). At fiber saturation point (FSP), the free water in cell cavities move to wood cells via diffusion and therefore, the bound water content in wood cells becomes saturated. At FSP, wood does not exhibit any dimensional changes; it neither shrinks nor swells. Above FSP, the fiber walls enlarge due to the increment of water and the wood plank *swells*. As the relative humidity content gets lower, wood yields the moisture; thus, the water content decreases until the FSP in wood fibers. Below the FSP, fiber walls tighten due to reduction of water and wood plank *shrinks*. The type of the wood determines the fiber saturation point and hence, the shrinkage and swelling capacities. The fiber saturation point (FSP) ranges between 20 and 30%, according to the type of wood (Winandy, 1994).

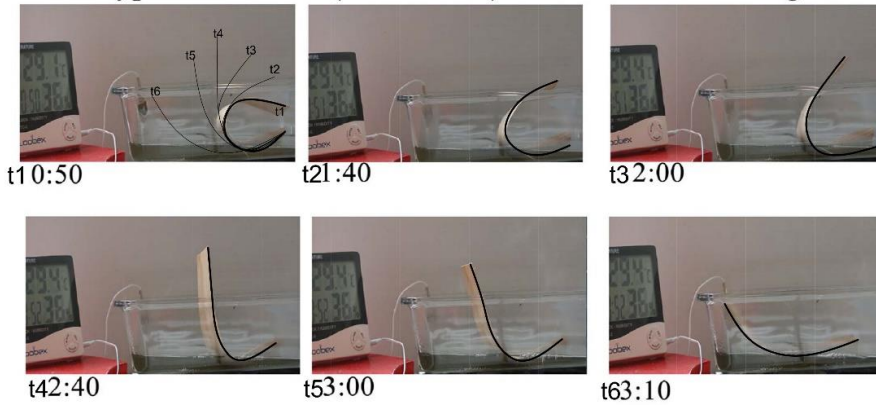
The humidity transition cycle aims to balance the moisture content between the wood fibers and the environment. Therefore, humidity transition continues until the wood reaches the equilibrium moisture content (EMC). If the relative humidity content is 40%, the humidity transition will continue until the humidity content in wood fibers reaches 40%. As Winandy (1994) states, equilibrium moisture content (EMC) is the balance point between the humidity content of the wood and the environment. The EMC achievement threshold depends on the wood type, the temperature and the relative humidity content (Winandy, 1994). The moisture content in wood is calculated via the following formula (**Formula 2.1**) (Winandy, 1994):

$$\text{Moisture Content (MC)} = \frac{\text{Moist weight} - \text{Dry weight}}{\text{Dry weight}} \times 100 \quad (2.1)$$

When the wood gains or loses moisture, it swells or shrinks. The shrinkage amount is proportional with the moisture content change in the wood; one percent decrease in humidity content causes wood to shrink at the rate of one over thirty (1/30) (FPL, 2010). On the contrary; one percent increase in humidity content causes wood to swell at the rate of one over thirty (1/30) (FPL, 2010). On this basis, the amount of the dimensional change can be predicted through the moisture content in wood. For instance, if the wood plank loses 5% of its moisture, it will shrink at a rate of 5/30. If the wood gains 5% moisture, it will swell at a rate of 5/30.

An experiment is conducted to understand the dimensional change that is pursuant to hygroscope. An oak veneer sample is partly immersed in, curved and dried out. After the drying process, the glass case that contains the water is heated to increase the humidity level within the case. A humidity sensor is used to detect the change in temperature and the humidity content. The shape transformation as a result of hygroscope is analysed in Figure 3.1. The veneer takes water from the case and reaches to its FSP. When it exceeds the FSP, it swells and bends outwards. The shape transformation process of the oak veneer sample is recorded with captures as displayed in Appendix A.1. The same experiment is conducted also with teak and walnut veneer samples, as shown in Appendix A.2.

Wood type: Oak wood (Hard wood) Grain direction: Tangential



**Figure 3.1:** Hygroscopic movement of oak wood.

The moisture content ranges from approximately 25% to 50% in green wood, depending on the type of wood. Wood is dried through air-drying and kiln drying methods in order to stabilize the moisture content in wood fibers. In air drying method, wood is left to dry by itself in the open air, as wood contains about 20-25% moisture in hardwood and %15-20 in softwood types (FPL, 2010). In kiln drying on the other hand, the wood is dried in kiln, as it contains around 6-8 % moisture in both hardwood and softwood types (FPL, 2010).

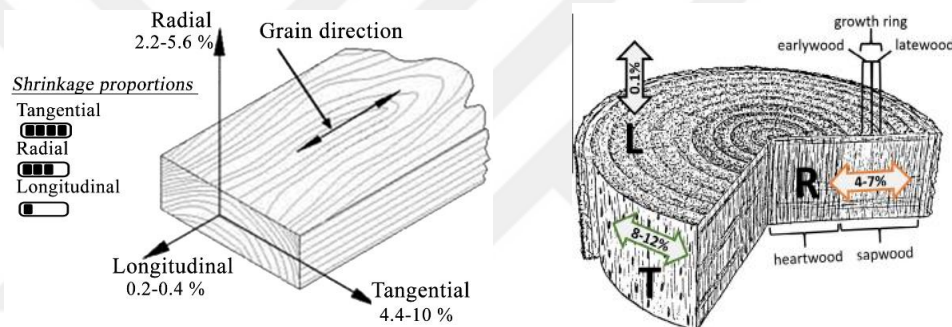
### 3.1.2. Anisotropy (Grain directionality)

Wood has a fibrous material structure and displays different properties in different grain directions. The fibrous character makes the wood an *anisotropic* material. Anisotropy denotes the directional dependence of material's characteristics; its grain directional structure leads material to exhibit different behavior in different directions. Anisotropy provides wood to change its dimension with hygroscopic in humidity alterations.

Wood has a fibrous structure and displays different properties in different grain directions. The fibrous character makes the wood an *anisotropic* material. Anisotropy denotes the directional dependence of material's characteristics; its grain directional structure leads material to exhibit different behaviors in different directions. Anisotropy provides wood to change its dimension with hygroscopic at different states of humidity.

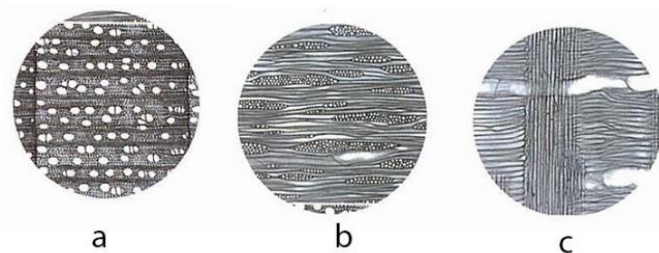


As Winandy (1994) states, the direction of wood fibers and growth rings in the wood varies along three axes; *tangential*, *radial* and *longitudinal* directions. The *tangential axis* is perpendicular to the grain direction and parallel to growth rings. The *radial axis* is perpendicular to growth rings and normal to the grain direction. The *longitudinal axis* is parallel to the grain direction (Winandy, 1994). The amount of dimensional change varies along these three axes (rad., long., rad.) as displayed in Figure 3.2. As Winandy (1994) states, the amount of dimensional change is between 0.1 and 0.2 % in the longitudinal direction, which is usually left out due to being too slight. In the radial direction, the dimensional change varies from 2.2 to 5.6 % and it is between 4.4 and 10 % in the tangential direction, as shown in the graph (Figure 3.3) (Winandy, 1994).

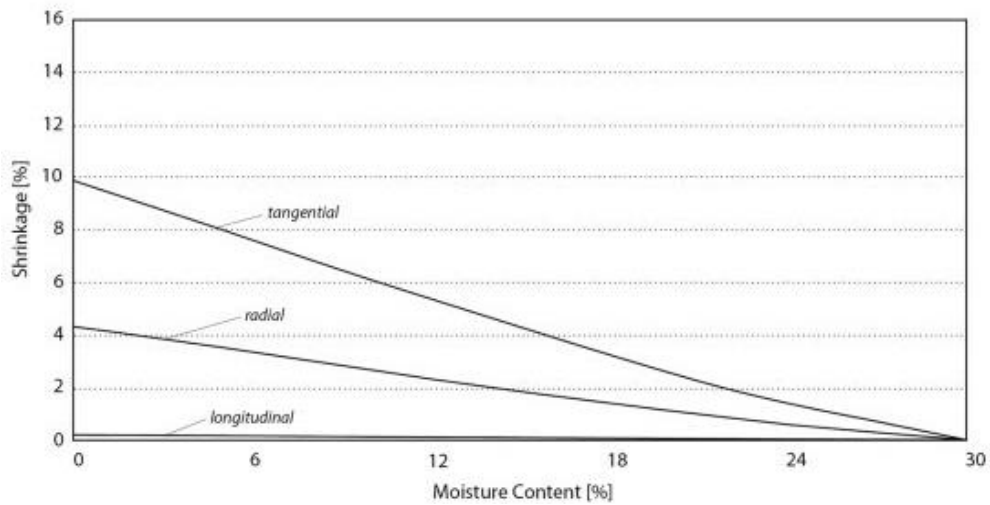


**Figure 3.2:** Projection of maximum shrinkage percentage in each of grain direction in wood batle (Winandy, 1994) and wood trunk (Holstov et al., 2015).

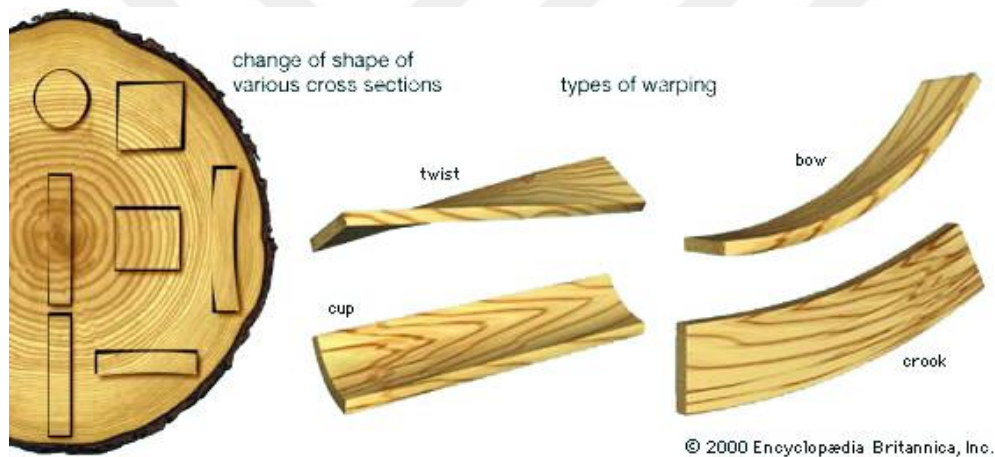
Menges and Reichert (2012) examine the cell arrangement of maple wood with microscope in longitudinal (a), tangential (b) and radial (c) directions (Figure 3.3). The researchers (2012) assert that the variation along three axes is derived from different cell alignments in each axis. The cutting section varies the distortion of wood planks as demonstrated in Figure 3.4. In response to humidity alterations, different warping types occur in wood planks due to grain directionality.



**Figure 3.3:** Microscopic photographs of maple (Menges and Reichert, 2012).

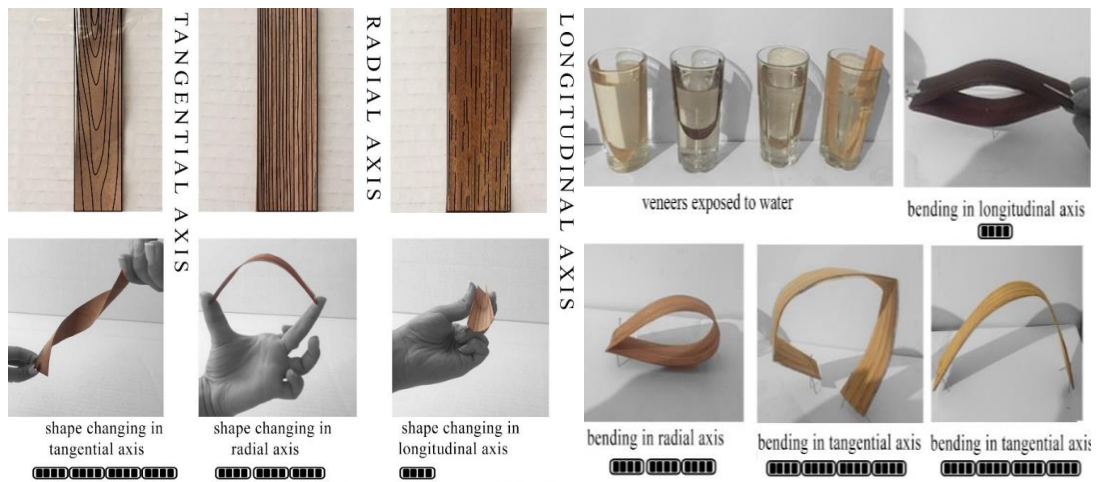


**Figure 3.4:** The graph showing the shrinkage amount in different grain axis (Mengeset et al., 2014).



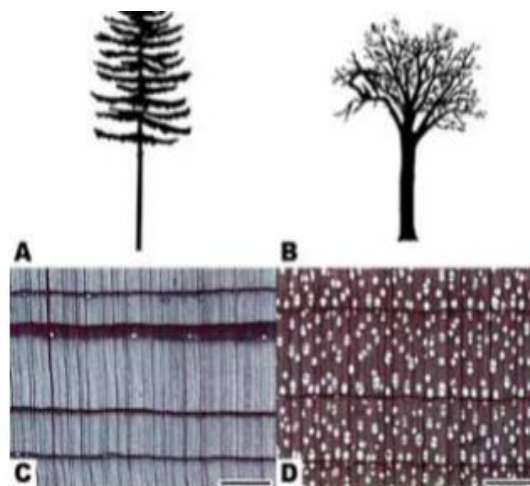
**Figure 3.5:** Distortions of wood due to swelling and shrinking (Url-23).

An experiment (Figure 3.6) is carried out to understand the anisotropic property-based distortion in wood veneer. The veneers with different axes (tang, rad, long) are bent and immersed in water. They are kept in water for a certain amount of time until they obtain the desired shape. As a result of the experiment, the veneer in tangential axis reveals to be the most easily bendable veneer. The veneer in radial axis is more bendable than the longitudinal one. Finally, the longitudinal one is the least bendable veneer. Distortion abilities of the three different types are ranked as illustrated in Figure 3.6. It can be argued that the tangential veneer distorts the most, the radial veneer comes in the middle and the longitudinal veneer distorts the least.



**Figure 3.6:** The experiment to test the anisotropic character of wood (By the author).





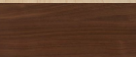









Wood type is a significant agent in identifying dimensional change. Wood types are divided into two parts as softwood and hardwood in terms of fiber structure and property. The structure and property differences of softwood and hardwood are displayed in Figure 3.7. Based on the references, generally hardwood types takes and yields the moisture easier than softwood, out of the exceptions. The shrinkage percentage of hardwood types is higher than that of softwood types. Based on data taken from the Forest Product Laboratory (FPL), Table 3.1 illustrates the shrinkage amount of several hardwood and softwood types in different grain directions.



**Figure 3.7:** The difference in the hardwood and softwood species (FPL, 2010)<sup>1</sup>.

<sup>1</sup>A shows the form of a generic softwood tree, B shows shows the form of a generic hardwood tree, C shows transverse section of a softwood tree and D shows shows transverse section of a hardwood tree.

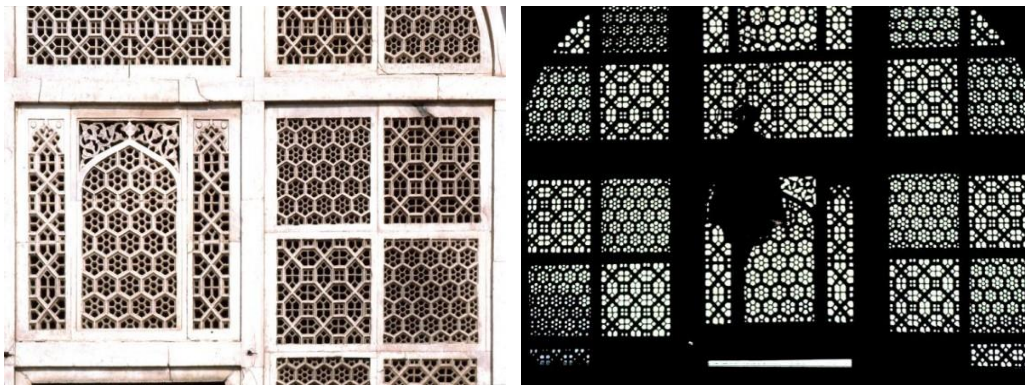
**Table 3.1:** The shrinkage table according to wood types ( Adapted from, FPL, 2010)<sup>2</sup>.

No	Wood type	Wood species	Wood figures	Grain directionality	Percentage of shrinkage %	Volumetric Percentage of shrinkage %
HARDWOODS		Beech (Kayın)		Tangential	11,9	17,2
				Radial	5,5	
		Birch, Yellow (Huş ağacı)		Tangential	9,2	16,8
				Radial	7,2	
		Ash, Black (Dişbudak)		Tangential	7,8	15,2
				Radial	5	
		Maple, Sugar (Akçaağaç)		Tangential	9,9	14,7
				Radial	4,8	
		Walnut, Black (Ceviz)		Tangential	7,8	12,8
				Radial	5,5	
		Oak, White (Meşe)		Tangential	8,8	12,7
				Radial	4,4	
		Poplar, Yellow (Kavak)		Tangential	8,2	12,7
				Radial	4,6	
		Chestnut, Black (Kestane)		Tangential	7,1	11,5
				Radial	3,7	
SOFTWOODS		Larch, Western (Karaçam)		Tangential	9,1	14
				Radial	4,5	
		Spruce, Red (Ladin)		Tangential	7,8	11,8
				Radial	3,8	
		Pine, Red (Çam)		Tangential	7,2	11,3
				Radial	3,8	
		Fir, Balsam (Göknar)		Tangential	6,9	11,2
				Radial	2,9	
		Cedar, Yellow (Sedir)		Tangential	6	9,2
				Radial	2,8	
Redwood		Tangential	4,9	7		

### 3.2. Humidity Responsive Systems Using Wood

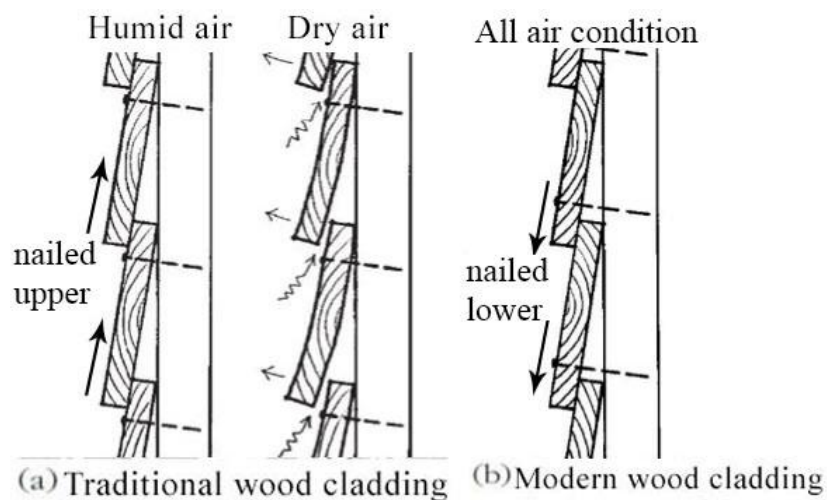
The shrinking behavior of wood has been accepted as a deficiency in construction industry. However, there are a few practices in architecture that took advantage from hygromorphic structure of wood. The traditional Islamic wood latticework, known as *mashrabiya*, benefits wood's hygromorphy (Figure 3.8). Fathy (1986) asserts that the regulation of light, airflow, temperature and humidity are accomplished by the calibration baluster sizes of the latticework (cited from Hensel, 2011). The increment in the size of balusters enhances humidification and cooling, Fathy (1986) claims. Mashrabiya use the hygroexpansion of wood in architectural scale by calibrating the balusters on the basis of its hygroscopic properties.

<sup>2</sup>Forest Product Laboratory (FPL), (2010). Wood Handbook, Wood as an Engineered Material.pp.6.



**Figure 3.8:** Traditional wood latticework, mashrabiya (Url-24).

Another inspirational precedent is the typical wood cladding in Norwegian boathouses which utilized the wood material behavior as a responsive building component in the 19<sup>th</sup> century (Larsen and Marstein, 2000). While the modern wood cladding is air-impermeable, the traditional type was air-permeable, in purpose of providing ventilation. The tangential axis wooden planks are nailed to the upper edges. The nailed wood planks twist upwards in dry weather to ensure natural ventilation. In humid weather, the planks straighten to ensure protection against water and humidity, as demonstrated in Figure 3.9 (Larsen and Marstein, 2000). The wooden planks and mashrabiya reveal how the hygroscopic behavior of wood is utilized for climate responsive design. The calibration and orientation are achieved on the basis of material behavior; thus the material properties are employed for responsiveness in the architectural scale.



**Figure 3.9:** Wooden paneling of boathouses in Nordmore, Norway (Larsen and Marstein, 2000).

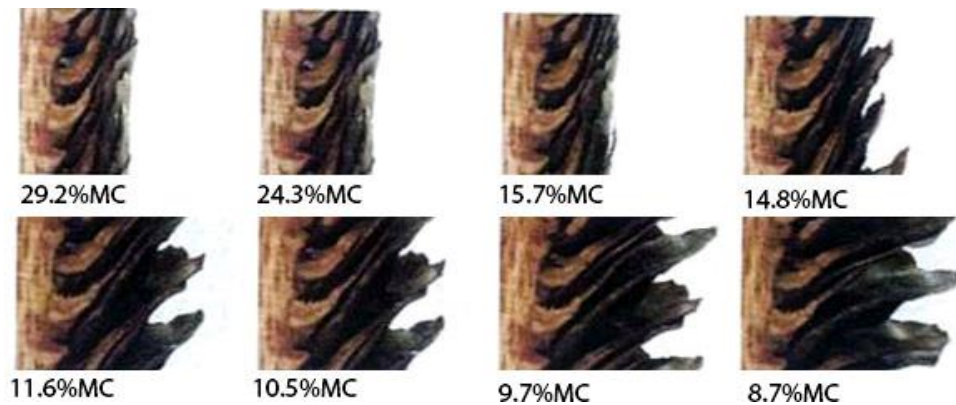
### *Humidity responsive system in nature*

In nature, pinecone scales are referred to as an inspiration for humidity responsive systems. As Dawson, Vincent and Rocca (1997) state, pinecone scales open by shrinking in dry air and close by swelling in humid air. Pinecones act like this to release their seeds in the optimum humidity conditions. This actuation mechanism continues, even when the cone is dead as an organism (Correa, Menges, Reichert, 2014). This fact indicates that the responsive movement of the cone originates in material's intrinsic capacity (Dawson et al., 1997).

An experiment is carried out to observe the humidity reaction of cone scales (Figure 3.10). In the experiment, a pinecone scale is put into hot water and another into cold water, for 15 minutes. The scale of the cone that is put into water moves inward and closes while the scale of the other cone remains open. The actuation rate of the scale that is put in hot water is higher than that of the one in cold water. As the experiment proves, the responsiveness is embedded in the material. Kremsa, Nakagi and Santiago (2009) analyze the actuation mechanism of cone scales in a detailed way, using microscope for particular humidity contents, as displayed in Figure 3.11 (cited from Menges et al., 2014).

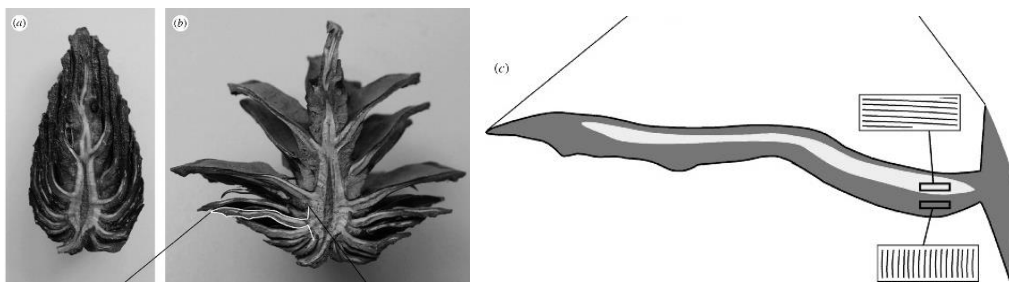


**Figure 3.10:** An experiment to observe the humidity reaction of the pinecone scales (By the author).



**Figure 3.11:** The hygroscopic analysis of the cone scales (Kremsa et al., 2009).

The actuation mechanism of cone scales (Figure 3.11) is derived from the bilayer structure as well as the material's hygroscopic capacity (Dawson, Vincent and Rocca, 1997). Fibers of the outer layer lie in parallel direction while the fibers of the inner layer are in longitudinal direction, as illustrated in Figure 3.12 (Correa et al., 2014). As Dawson, Vincent and Rocca (1997) explain, the *outer layer* is more sensitive to humidity than the inner layer and this results in it to exhibit a higher change in dimension. Thus, this layer is denoted as the *active layer*. The *inner layer* on the other hand, is less sensitive to humidity and exhibits a relatively limited dimensional change. This layer is denoted as the *passive layer*. The difference between the layers' hygroexpansion capacity leads the cone scales to open or close in response to humidity (Dawson et al., 1997).



**Figure 3.12:** The bilayer structure of the pinecone (Burgert and Fratzl, 2009).

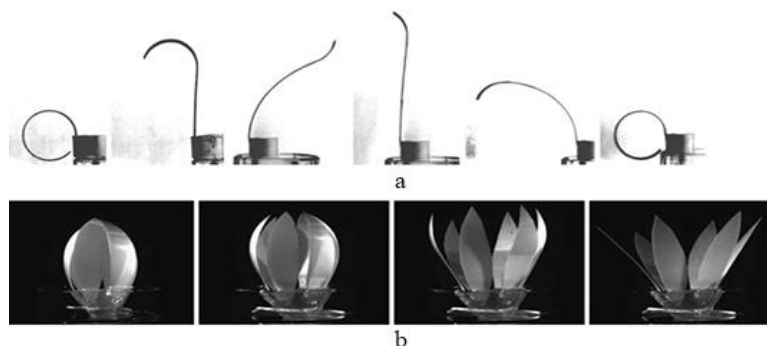
The bilayer structure of pinecone scales shares similarity with thermo-bimetal, in terms of actuation mechanism. Both materials consist of two layers with different response capacities against moisture and heat. Nevertheless, the stimuli that they respond to are different: The bimetallic strip curves in response to temperature changes while the bilayer scale curves in response to moisture changes.

### 3.4. Examples of Humidity Responsive Composite

Responsive material studies utilize hygromorphic composite as the responsive material, integrating pinecone's actuation principle with hygroscope and anisotropy properties of wood. Since the composite employs hygroscope in wood material for responsiveness, it can be named as a *hygromorphic* composite. In the hygromorphic composite, the active layer responds to humidity and changes in dimension, while the passive layer does not respond to humidity and exhibits limited change in dimension. Hygromorphic composite benefits from this difference in creating responsiveness.

Former responsive material studies are examined in terms of material selection, design and production methods. All case studies handle responsive material system development; yet their design processes and methods show alteration. These design processes serve as a model for humidity responsive material system proposal presented in this study.

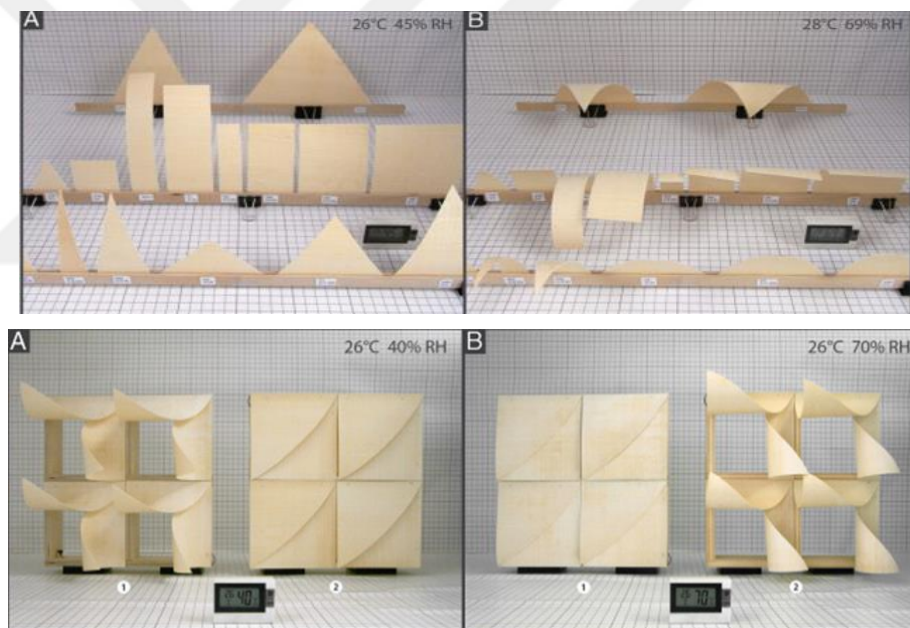
Reyssat and Mahadevan (2009) offer a simple bilayer composite by using paper and polymer that are adhered to each other with epoxy. In dry environment, the paper-plastic bilayer composite bends inwards (in direction of the paper side). In humid environment however, the composite bends outwards; in direction of the polymer side (Figure 3.13.a), (Reyssat and Mahadevan, 2009). The researchers also developed a floral-resembling model with bilayer petals. When the bilayer petals are dipped in water, they open because of swelling and the floral-like model 'blooms'. When the water is drained, the petals close by shrinking and the floral mimicking model tilts (Figure 3.13.b).



**Figure 3.13:** The humidity response process of the composite (a) and the controllable blooming and wilting of the petals (b), (Reyssat and Mahadevan, 2009).



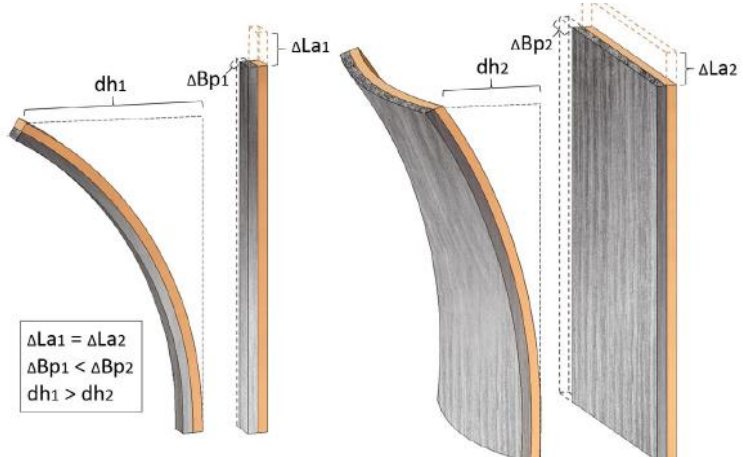
Correa Reichert and Menges (2014) develop another humidity responsive system with a semi-synthetic responsive composite that consists of wood (active layer) and polymer (passive layer). Menges and other researchers (2014) employ a quarterly cut maple wood veneer as the active layer. They produce a specific synthetic composite mixture of glass fiber bond with epoxy and use the produced polymer as the passive layer. The researchers perform several experiments based on different material parameters (wood type, fiber direction, dimensional consideration, environmental control) to understand the responsive composite behavior, as shown in Figure 3.14. Responsive Surface and Hygroscope, which are examined in Section 2.6, are the projects that employ hygromorphic composite in humidity responsive material system design. The variation in geometric arrangement of composites provides different movement patterns, as displayed in Figure 3.14.



**Figure 3.14:** The experiments to analyze the material behavior (Correa, Reichert and Menges, 2014).

Holstov, Bridgens and Farmer (2015) develop an artificial moisture-sensitive (hygromorphic) composite that consists of an active layer of wood and a passive layer of either a synthetic or a natural material. The researchers use a rotary-cut beech wood veneer as the active layer since this wood qualifies with the greatest hygroexpansion (has the ability to shrink/swell through hygroscope). They utilize polymer-based material (such as Polyethylene Terephthalate (PET) and Polycarbonate (PC) and glass fibre-reinforce composites (GFRP)) as the synthetic

passive layer. The researchers use wood veneer in the longitudinal grain direction as the natural passive layer by aligning it as perpendicular to the active wood layer. The natural passive layer has a lower hygroexpansion than the active wood layer. The responsive actuation principles of both natural and synthetic composites are illustrated in Figure 3.15.



**Figure 3.15:** The response principle of the bilayer composite (Holstov et. al, 2015).

According to the researchers, the thickness ratio is relevant with response time. The response rate of the thin composite is higher than that of the thicker composite material. The optimum response time is 20 minutes from dry to wet state and 3 hours from wet to dry state. The developed responsive prototypes with hygromorphic composite are illustrated in Figure 3.16 (Holstov et al., 2015).



**Figure 3.16:** Humidity responsive system prototypes by using hygromorphic composites (Holstov et. al, 2015).

#### 4. RESPONSIVE COMPOSITE MATERIAL DEVELOPMENT

This study aims to explore a responsive material system that utilizes the responsive composite material in parametric form. A semi-synthetic composite is produced as responsive material by combining wood and polymer. The bilayer structure of the composite is similar to that of pinecone scales; wood being the active and polymer being the passive layer. The main purpose of producing composite is to take advantage of the difference between the humidity sensitivity of layers.

The responsive composite material development is conducted in five stages; (1) material selection (2) production of the composite, (3) experiment setup, (4) conducting the experiment analysis methods, (5) material experiments, and (6) evaluation on the experiments; as shown in Table 4.1. The experiments are analyzed through numerical and observational methods to evaluate the responsiveness behavior. The optimum material parameters are identified according to the evaluations on material experiments. Material behavior is improved by adjusting the parameters.

**Table 4. 1:** The stages of the responsive material development.

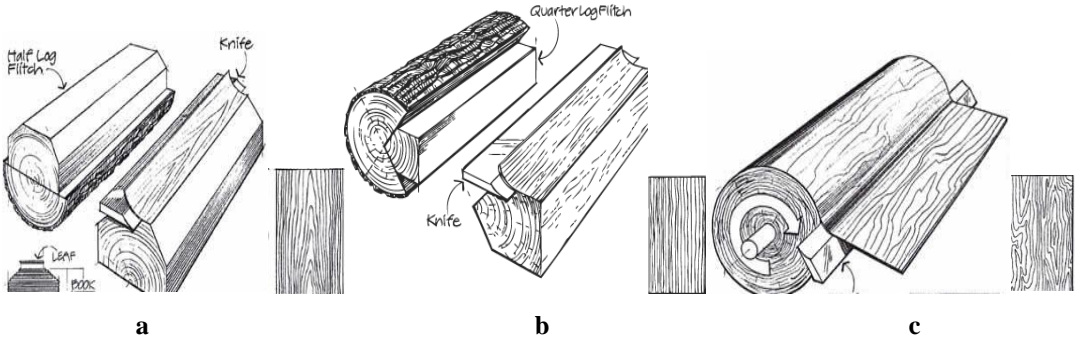
<b>Material Selection</b>	<b>Composite Production</b>	<b>Experiment Setup</b>	<b>Analysis Methods</b>	<b>Material Experiment</b>	<b>Experiments Evaluation</b>
-Wood -Polymer -Epoxy (bonding)	-Bonding wood and polymer with epoxy for bilayer composite	-Simplified Humidity box -Experiment Setup (wood tray-template)	-Empirical Analysis -Numerical Analysis	-Polymer type -Wood type -Grain orientation -Fibered polymers	-Improve material performance by adjusting the parameters

The difference of the conducted study is the execution and evaluation of the material experiments. The methodology of this study relies on learning by doing experiments. The material experiments test the material parameters and based on the result the optimum parameter is decided for the composite. A simplified humidity box is developed to test the composite material. A response graph is drawn for empirical analysis to observe the responsive behavior. It is worth to mention that the setup and execution of the material experiments is specific to this study within the simplified humidity box. The observational analysis method is specific to this experimental study. Apart from that, in this study the passive polymer layer is manipulated and

become anisotropic material by adding fibers. This can be included as the contribution of the conducted study to example studies.

**4.1. Material Selection for Responsive Composite Material**

Wood material is sensitive to humidity changes and is defined as the *active layer*. In this study, wood veneer is used as the active layer. The *wood veneers* comprise of thin slices of wood that are obtained from the tree trunk peel; the wood taken from the tree trunk is then sliced with different techniques (Url-25). The difference among cutting methods renders it possible to make different patterns on veneer surfaces, thanks to the grain direction of wood (Figure 4.1). In plain cut method, for instance, the log is cut parallel to the center while in rotary cut method, the log is rotated and then cut. In quarter cut method on the other hand, the log is quartered and cut (Url-25)<sup>3</sup>. Different cutting methods are used to obtain different grain axes (*tan, long, rad*) in wood veneer (FPL, 2010). Longitudinal axis veneer is parallel to the fibers and obtained through quarter cutting method (FPL, 2010). Tangential axis is perpendicular to the grain but tangent to the growth rings and it is obtained via plain cutting method (FPL, 2010). Radial axis veneer is perpendicular to the grain in the radial direction but normal to the growth rings and it is obtained via rotary cutting method, as illustrated in Figure 4.1 (FPL, 2010).



Plain (flat) cut for tangential veneer    Quarter cut for radial veneer    Rotary cut for radial veneer

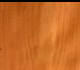



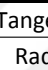
**Figure 4.1:** Different wood veneer cutting methods (Url-26).

The cutting method determines the grain axis in the wood veneer and the grain direction affects the veneer’s shrinkage rate against humidity alterations. The shrinkage rate in the tangential axis is higher than that of the other axes (radial and

<sup>3</sup> For detailed information, Url-26: <<https://www.youtube.com/watch?v=AdYDsIhy2VU>>

longitudinal axes), as shown in Table 4.2. For instance, the shrinkage rate in tangential axis is 11.9%, while the same in radial axis is 5.5%. Therefore, the selected wood veneers are cut in *tangential axis* which is achieved via *plain cut* method. The type of the active layer is selected according to the shrinkage capacity (hygroexpansion) of wood. Hardwood wood types display a higher dimensional change in response to humidity with a few exceptions, as mentioned in Section 3.1.2. Among the species of hardwood; *Beech*, *Ash*, *Maple* and *Oak* are tested for active layer selection, as displayed in Figure 4.2.

**Table 4.2:** The shrinkage table in selected wood types (Adapted from FPL, 2010)<sup>4</sup>.

Wood Species	Wood figures	Grain directionality	Percentage of shrinkage %	Volumetric Percentage of shrinkage %
Beech (Kayın)		Tangential	11,9	17,2
		Radial	5,5	
Ash, Black (Dişbudak)		Tangential	7,8	15,2
		Radial	5	
Maple, Sugar (Akçaağaç)		Tangential	9,9	14,7
		Radial	4,8	
Walnut, Black (Ceviz)		Tangential	7,8	12,8
		Radial	5,5	
Oak, White (Meşe)		Tangential	8,8	12,7
		Radial	4,4	

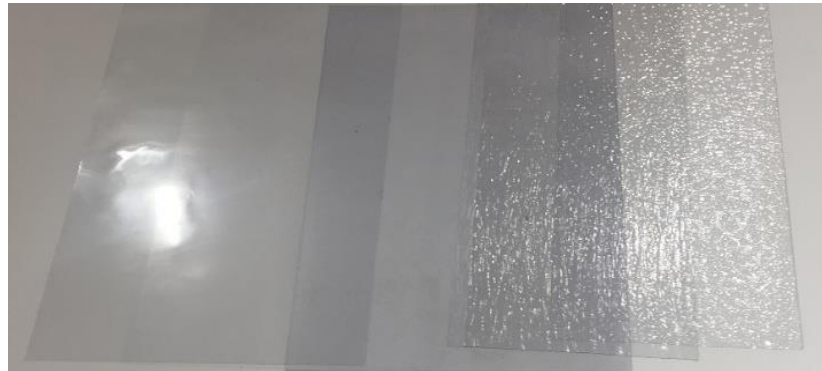


**Figure 4.2:** Selected wood veneers as active layer.

Synthetic polymer based material is non-sensitive to humidity changes and thus, the polymer material is defined as the *passive layer*. Among various types of polymer materials; *Polycarbonate (PC)*, *Polyethylene terephthalate glycol-modified polymer*

<sup>4</sup>Forest Product Laboratory (FPL), (2010). Wood Handbook, Wood as an Engineered Material.pp.6.

*and Polyvinyl Chloride (PVC)* qualify for passive layer selection. Polymer sheets are used as the passive layer in this study, as displayed in Figure 4.3.



**Figure 4.3:** Selected polymer sheets as passive layer.

The active and passive layers are bonded through an adhesive material. A resistant and durable adhesive, which will resist to humidity and prevent any splitting of the two layers, is required. In this study *epoxy resin* is used as the *adhesive* to bind the layers together. The selected materials for the production of the responsive composite are listed in Table 4.3.

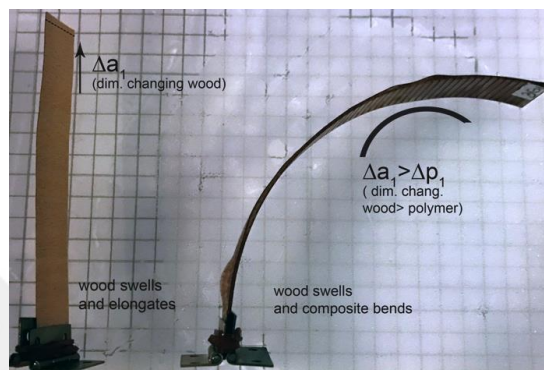
**Table 4. 3:** Table of the selected material for the composite.

Active Layer	Adhesive	Passive Layer
-Beech -Maple -Oak -Ash	+ -Epoxy Resin	-Polyvinyl Chloride (PVC) -Polycarbonate (PC) -Polyethylene terephthalate glycol-modified (PETG)

#### 4.2. Production of the Responsive Composite

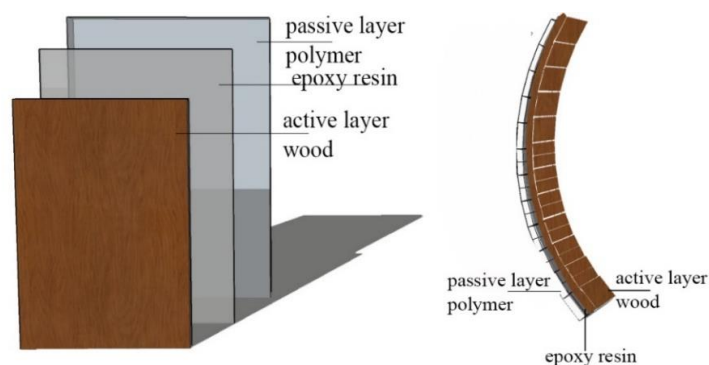
A bilayer composite is produced as the responsive material by adhering the wood veneer (the active layer) with the polymer sheet (the passive layer) with epoxy, as shown in Figure 4.6. The composite material curves as per its responsiveness to humidity. As the humid content increases, the active wood layer absorbs moisture, swells and elongates. The passive polymer layer does not exhibit any changes and limits the hygroscopic elongation by remaining stable. This results the bilayer composite to curve.

The bilayer composite and a single piece of wood veneer are exposed to humidity for an hour. As seen from Figure 4.4, the composite material bends while the wood veneer elongates in response to humidity. Wood veneer absorbs the moisture, swells, elongates and becomes 2 mm longer in 60 minutes. In the composite though, the wood layer cannot elongate because of the polymer and this results the composite wood to bend in the polymer direction. The elasticity of the polymer facilitates the curving.



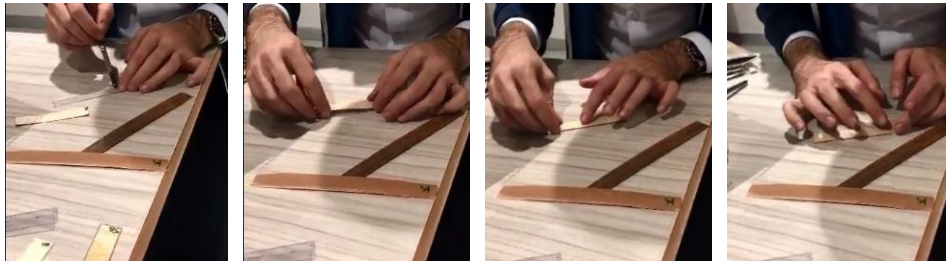
**Figure 4.4:** The comparison of the response principle of the composite and wood.

For the production of the composite samples, the active (wood veneer) and passive (polymer) samples are cut in the same dimension; 16 cm of height and 2 cm of width. The thickness of composite layers is measured with a caliper tool prior to adherence. Thicknesses of the wood veneers range between 0,45 mm to 0,6 mm while the same of the polymer layers range between 0.15 to 0,95 mm.



**Figure 4.5:** The layers of the bilayer composite.

For the adhesive material, a mixture, made up of epoxy resin and cure in specific proportions<sup>5</sup> is prepared and homogenously distributed on the polymer surface (Figure 4.6), to prevent imperfections on the composite. The drying process of the epoxy resin takes approximately 24 hours. The production of the composite is attained with the collaboration of the material scientist.



**Figure 4.6:** The application process of the adhesive solution with brush.

### 4.3. Material Experiments

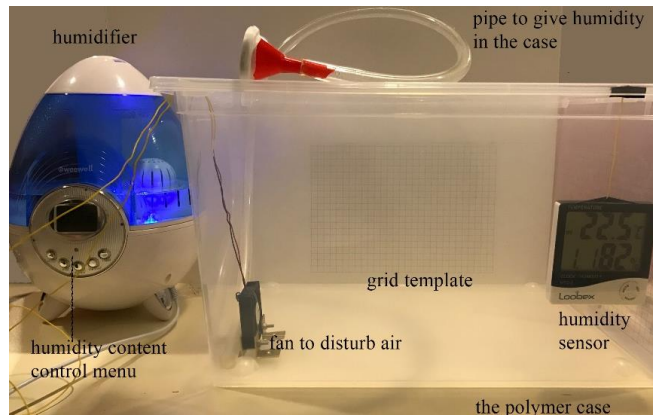
#### *Experiment Setup*

The experimental study is conducted in Istanbul Technical University and Kemerburgaz University Material Laboratories, in collaboration with a material scientist. A range of experiments is performed in a controlled environment, using a humidity (climate) chamber. In a humidity chamber, a humidifier controls the humidity, a fan provides the airflow and a sensor detects the humidity content and the temperature. The humidity content is set at 80% and the temperature is set to be room temperature (24-25 °C). The temperature remains constant at room temperature (24-25 °C) and any changes in temperature is ignored in the conducted experiments. A simplified humidity box, inspired by climate chamber, is developed as displayed in Figure 4.7.

---

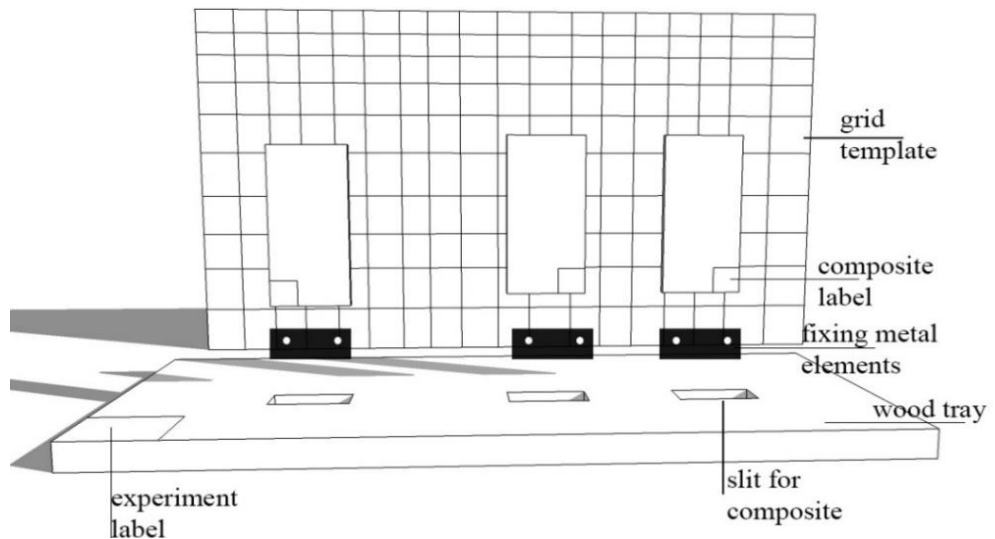
<sup>5</sup>The ratio of epoxy resin and cure is three to one (3/1). A syringe is used to measure the material rates. 3 milliliters of epoxy is mixed with 1 milliliter of cure with syringe in a pot. The total amount of the applied epoxy resin is about 4 - 5 grams.



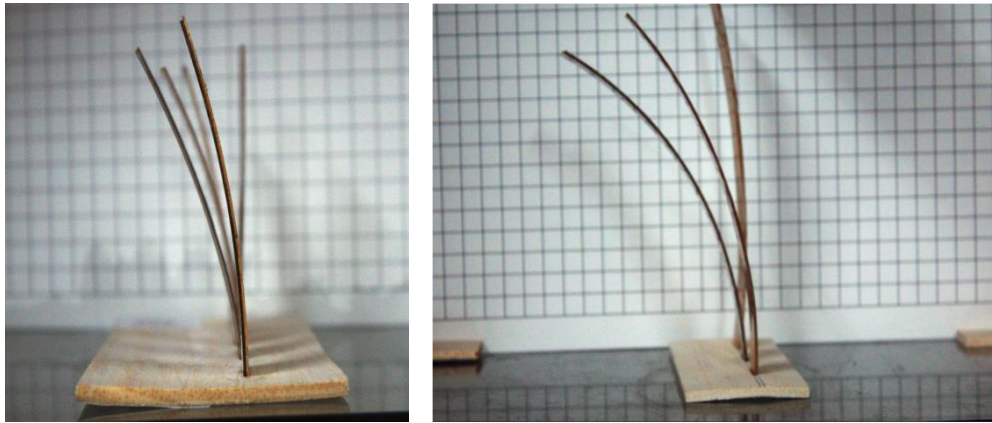


**Figure 4.7:**The simplified humidity chamber.

The humidity content of the box is regularly detected by the humidity sensor and adjusted by the humidifier device. The fan controls the airflow by homogenously distributing the moisture content that accumulates below the chamber. The working period of the fan is adjusted to five seconds per twenty-five seconds. The actuation mechanism of the fan is controlled via Arduino (see Appendix B). The relative humidity content is set at  $80 \pm 5\%$ . The conditioned humidity (80%) is the upper limit of the acknowledged indoor thermal comfort condition. This rate also is the highest humidity content observed in Istanbul, according to the references. Figure 4.8 illustrates the diagram of the experiment setup. Based on the setup, the composite samples are arranged for material experiments, as displayed in Figure 4.9.



**Figure 4.8:** The diagram for the experiment setup.



**Figure 4.9:** The arranged composite samples for material experiments.

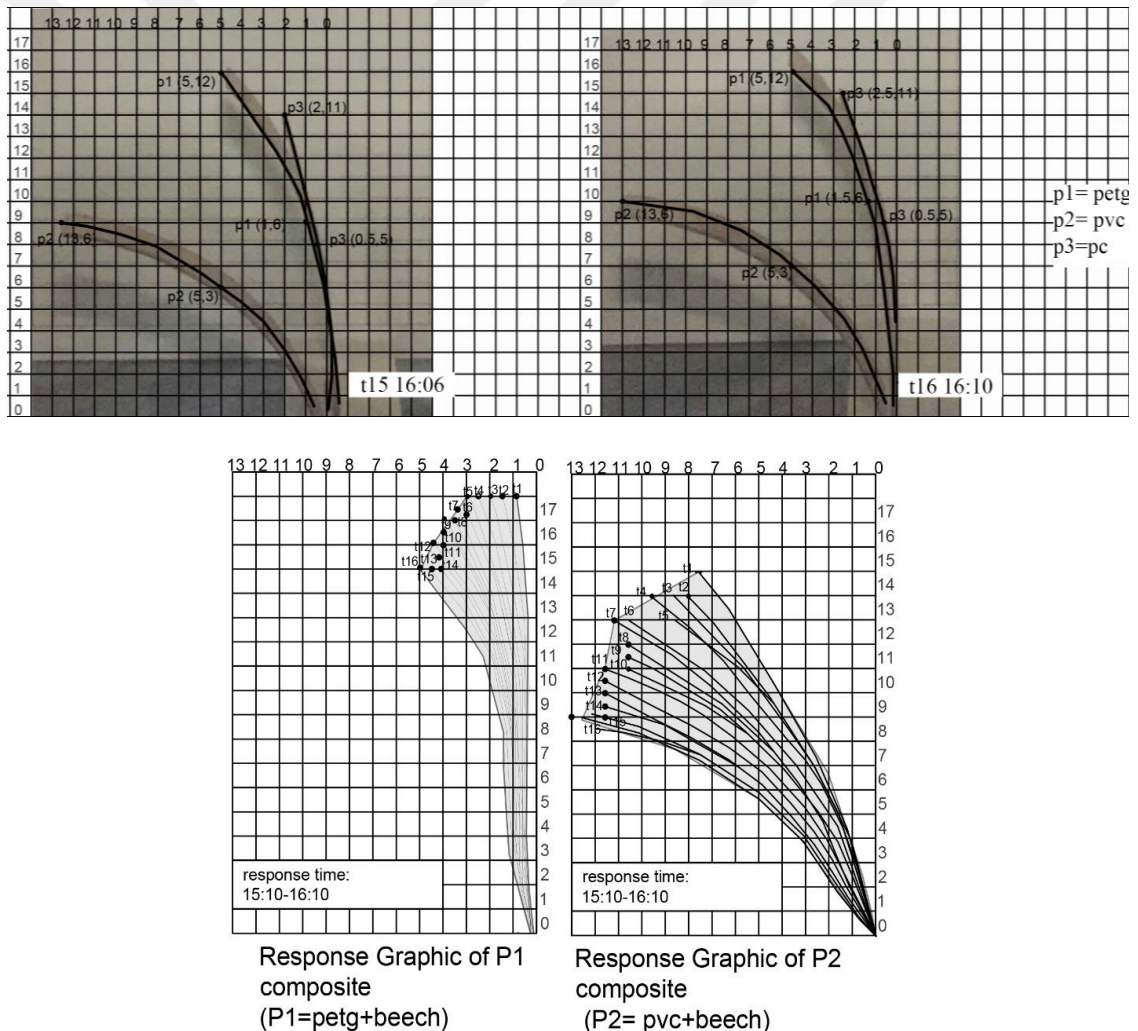
In this study, material experiments are carried out to understand composite behaviour. The parameters that affect composite behavior are indicated as (1) polymer type, (2) wood type, (3) grain orientation of wood, (4) fibered polymers. These parameters (Table 4.4) are tested in conducted experiments. The tested composite samples are categorized and labeled as per each experiment, as shown in Table 4.4. In addition to above parameters, the thickness of composite layers also changes from experiment to experiment. The responsive behavior of the composite improves through the adjustment of these parameters.

**Table 4.4:** The experiment phases according to the affecting parameters.

<i>Experiment 1</i>	<i>Experiment 2</i>	<i>Experiment 3</i>	<i>Experiment 4</i>
<i>Polymer type</i>	<i>Wood type</i>	<i>Grain orientation</i>	<i>Fibered polymers</i>
Test the effect of polymer type	Testing the effect of wood type	Testing the effect of grain direction of wood	Testing the effect of fibers on polymer
<b>P<sub>1</sub></b> (PETG+beech)	<b>1P<sub>2</sub></b> (Maple+PVC)	<b>3D<sub>1</sub></b> (cutparallel d.)	<b>3G<sub>1</sub></b> (distance b. fibers 2.5mm)
<b>P<sub>2</sub></b> (PVC+beech)	<b>2P<sub>2</sub></b> (Ash+PVC)	<b>3D<sub>2</sub></b> (perpendicular d.)	<b>3G<sub>2</sub></b> (distance b. fibers 5mm)
<b>P<sub>2</sub></b> (PC+beech)	<b>3P<sub>2</sub></b> (Beech+PVC)	<b>3D<sub>3</sub></b> (cut diagonal d.)	<b>3G<sub>3</sub></b> (distance b. fibers 10mm)
	<b>4P<sub>2</sub></b> (Oak+PVC)		

### Analysis methods of the experiments

Two types of analysis are conducted in this study; *empirical (observational)* and *quantitative (numerical)* analysis methods. In the observational analysis, the curvature change is analyzed and a response graph is drawn to compare the responsive behavior of composite samples. Each experiment takes 60 minutes and captured in shots per every 4 minutes. The curvature change of the composite material is defined in each caption and a response graph is drawn, as shown in Figure 4.10. The response graph is used to evaluate the composite responsive behaviour. The responsiveness of each composite material is put into comparison through the response graph.



**Figure 4.10:** The defined curve of the composite materials and the response graph.

The observational (empirical) analysis is justified by numerical analysis. The curvature change of the composite, derived from responsive behaviour, is estimated. Holstov and other researchers (2015) adapt Timoshenko's theory for bi-metal thermostats to predict the curvature change since the bilayer structure of the composite shares similarities with bi-metal thermostats. By using the formula shown below (**Formula 4.1**), the empirical process is justified. In this study, the curvature change coefficient values ( $f(m,n)$ ) are used to compare the responsive behaviour of composite materials. The calculations are displayed in Appendix C<sup>6</sup>.

$$K = \frac{1}{R} = \frac{\Delta a \cdot f(m,n) \cdot \Delta MC'}{t_{total}} + \frac{1}{R_0}$$

$$\Delta a = a_a - a_p = \text{difference of hygroexpansion} \\ = \text{active l. hygroexp.} - \text{passive l. hygroexp.}$$

$$f(m,n) = \frac{6(1+m)^2}{3(1+m^2) + (1+m.n)\left(m^2 + \frac{1}{m.n}\right)}$$

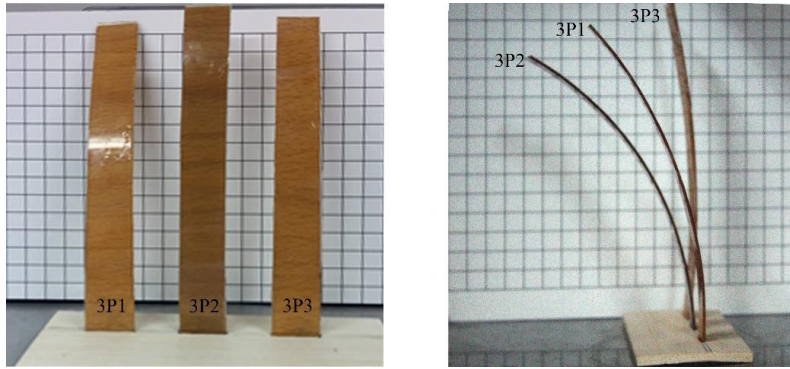
$$m = \frac{t_p}{t_a} = \frac{\text{thickness passive l.}}{\text{thickness active l.}} ; \quad n = \frac{e_p}{e_a} = \frac{\text{elasticity coef. passive l.}}{\text{lasticity coef. active l.}} \quad (4.1)$$

### Experiment 1: Testing the polymer types

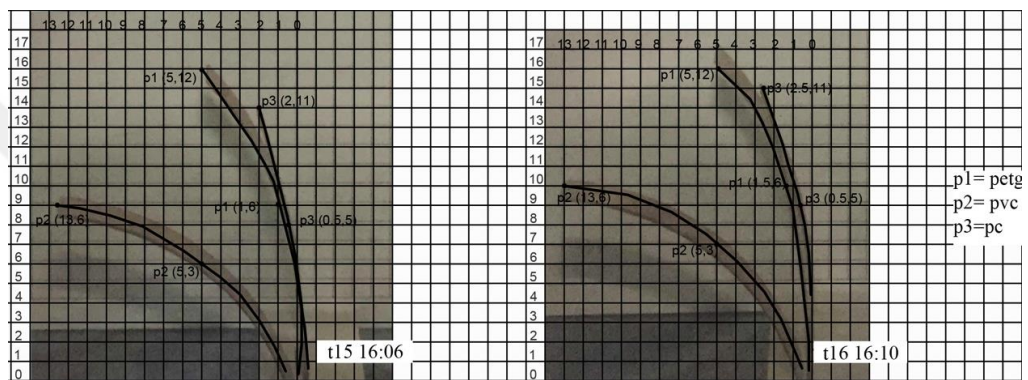
*Polyethylene Terephthalate Glycol-Modified* (PETG), *Polyvinyl chloride* (PVC) and *Polycarbonate* (PC) are tested as *passive* layers of the bilayer composite (Figure 4.11). This experiment aims to analyze how different polymer types affect the responsiveness of the composite. The tested composite samples are grouped and labeled according to the polymer types that are used in the experiment, as shown in Table 4.4 (P<sub>1</sub> denotes PETG, P<sub>2</sub> denotes PVC and P<sub>3</sub> denotes PC).

---

<sup>6</sup>Hygroexpansion value ( $a$ ), moisture content change ( $\Delta MC$ ), active and passive layers' thicknesses ( $t_a$  and  $t_p$ ), elastic modulus (stiffness) of active-passive layers ( $e_a, e_p$ ), radius of curvature of the composite ( $R$ ), stiffness and thickness ratios of layers ( $n$  and  $m$ ), and the initial curvature of the element ( $1/R_0$ ).



**Figure 4.11:** The composite samples with different polymer types.

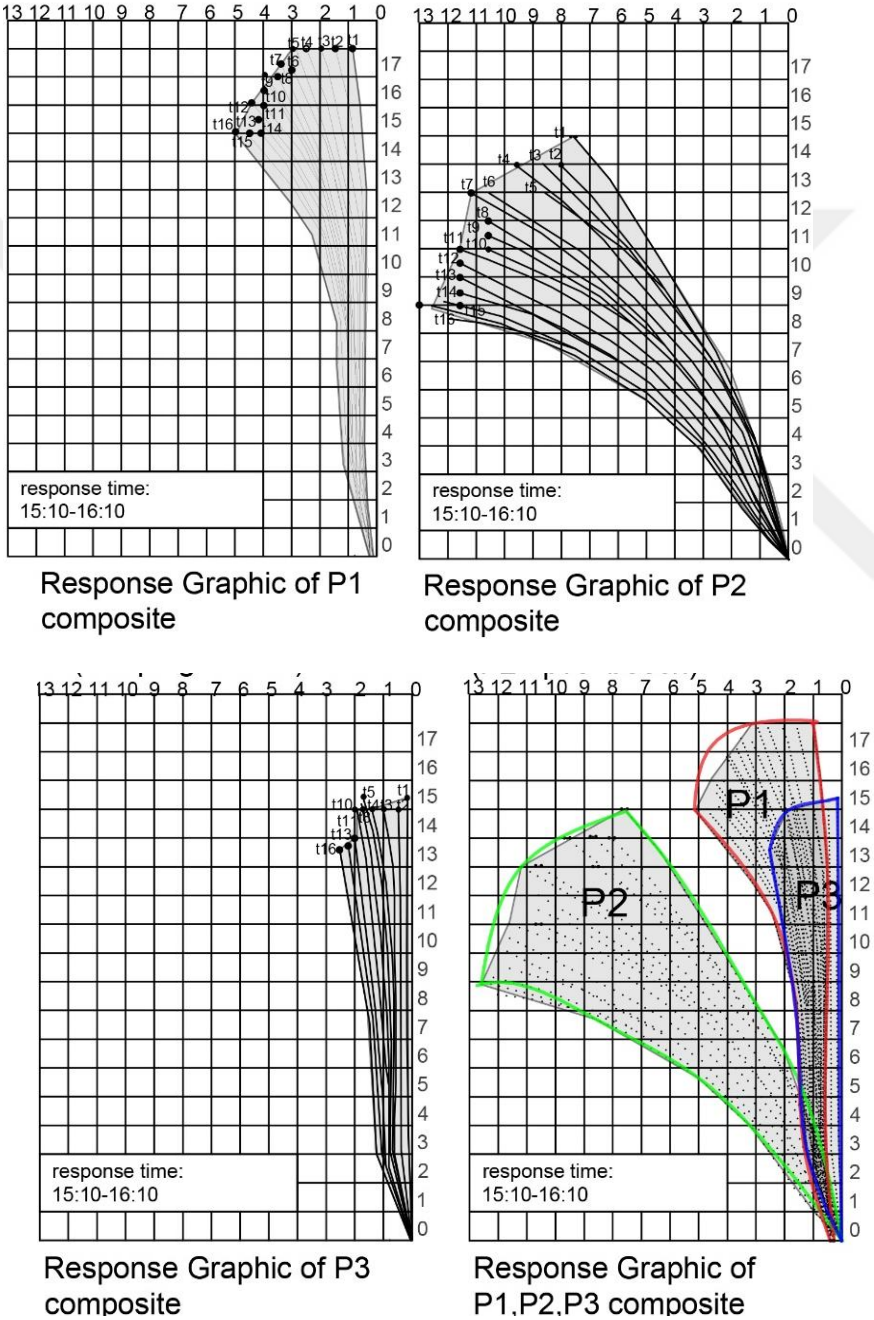


**Figure 4.12:** The defined curvature of composite in one caption (in  $t_{15}$  and  $t_{16}$ ).

The experiment takes 60 minutes and the composite samples are captured per every 4 minutes, as shown in Appendix D. The curvature change of the composite material is defined in each caption, as shown in Figure 4.12. A response graph is drawn through the identified curves (Figure 4.13). According to the response graph;  $P_2$  (beech and PVC) achieves the maximum curvature change,  $P_1$  (beech and PETG) achieves a higher curvature change than  $P_3$  (beech and PC); and  $P_3$  achieves the minimum curvature change, in 60 minutes. Based on the empirical analysis,  $P_2$  (beech and PVC) is the most responsive composite while  $P_1$  (beech and PETG) comes in the middle and  $P_3$  (beech and PC) is the least responsive composite ( $P_2 > P_1 > P_3$ ). Moreover, as the response graph displays, the curvature change is more obvious in the first 32 minutes, between  $t_1$  and  $t_8$ .

The results obtained from the empirical analysis are justified through quantitative methods, using **Formula 4.1**. The thickness and elasticity coefficient values are given in Table 4.5. Accordingly, the thickness and elasticity proportions (stiffness) are calculated and the curvature change coefficient is found, as shown in Table 4.6.

The calculations are given place in Appendix C. In order to enable a comparison on the curvature change value of composite materials, the thickness of the samples is regarded to be at a standard of 0.85 mm. Based on the calculations, the curvature change coefficient graph is drawn for each composite material, as illustrated in Figure 4.14. This graph (Figure 4.14) demonstrates how the curvature coefficients of composites change according to the thickness ratio.



**Figure 4.13:** The response graph of the samples in Experiment 1 (P<sub>1</sub>,P<sub>2</sub>,P<sub>3</sub>).

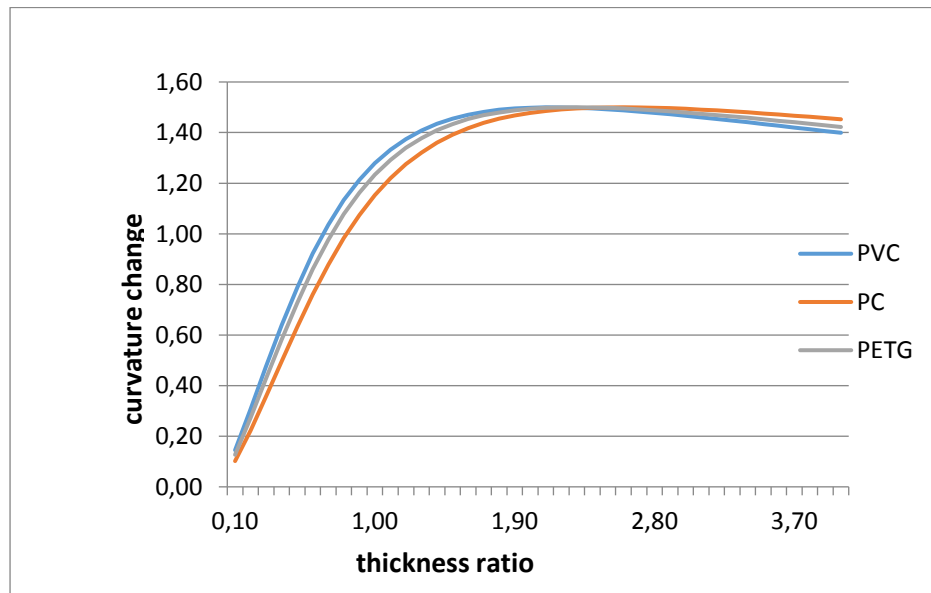
**Table 4.5:** Thickness and elasticity values of used polymer types and wood veneer.

<i>Materials</i>	<b>PETG</b>	<b>PVC</b>	<b>PC</b>	<b>Beech</b>
<i>Thickness</i>	0.85mm	0.85 mm	0.85 mm	0.85 mm
<i>Elasticity</i>	2.19 GPa	3.25 GPa	2.2 GPa	15GPa

**Table 4.6:** Curvature change coefficient  $P_1$ ,  $P_2$  and  $P_3$  with elasticity and thickness proportions.

	$P_1$ (PETG+Beech)	$P_2$ (PVC+Beech)	$P_3$ (PC+Beech)
<i>Thickness ratio (m)</i>	1.89	1.89	1.89
<i>Elasticity ratio (n)</i>	0.19	0.22	0.15
<i>Curvature change coefficient (f(m,n))</i>	1.488	1.494	1.464

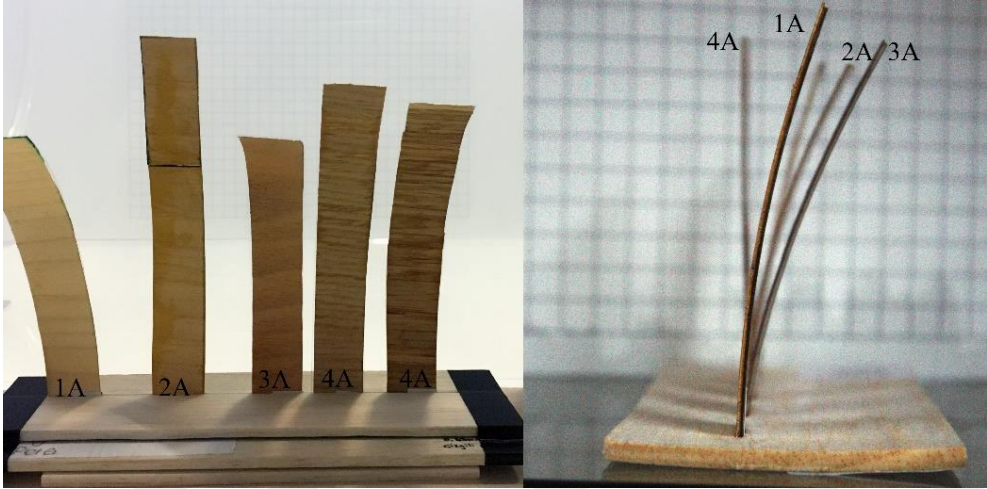
On the ground of the experiment results, *PVC polymer type* is selected to comprise the *passive layer* of the composite material of the designed material system. The thickness becomes one of the parameters to influence the curvature change, as seen in **Formula 4.1** and in the curvature change coefficient graph in Figure 4.14. The thickness of polymer layers is reduced in the following experiments.



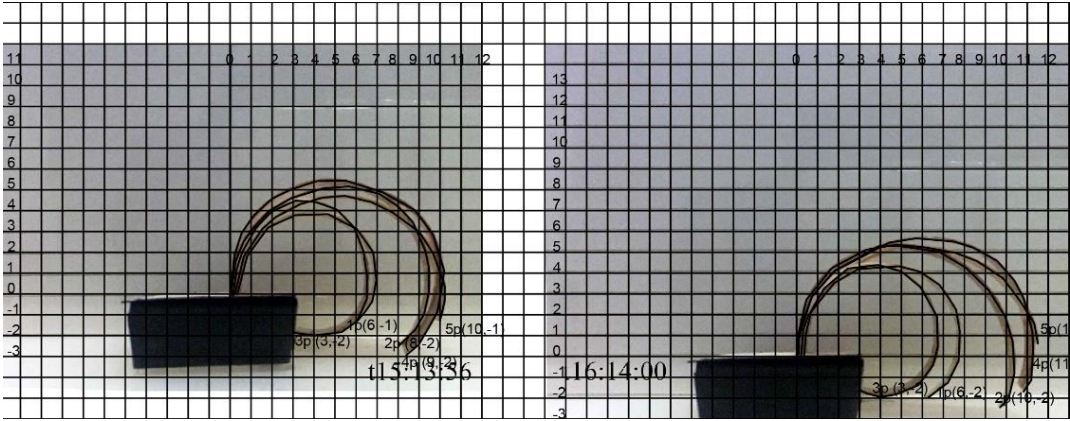
**Figure 4.14:** The curvature change coefficient graph of polymer types.

**Experiment 2: Testing wood types**

*Maple, Beech Oak* and *Ash* are tested as *active* layer candidates of the bilayer composite (Figure 4.15). This experiment tests how different wood types affect composite behavior. These composite samples are labeled in numerical order according to the wood types, as shown in Table 4.4 (Numbers denote the wood types and P<sub>2</sub> denotes the PVC polymer. Maple wood is represented with 1P<sub>2</sub>, Ash wood with 2P<sub>2</sub>, Beech wood with 3P<sub>2</sub> and Oak with 4P<sub>2</sub>).



**Figure 4.15:** The composite samples with different wood types.

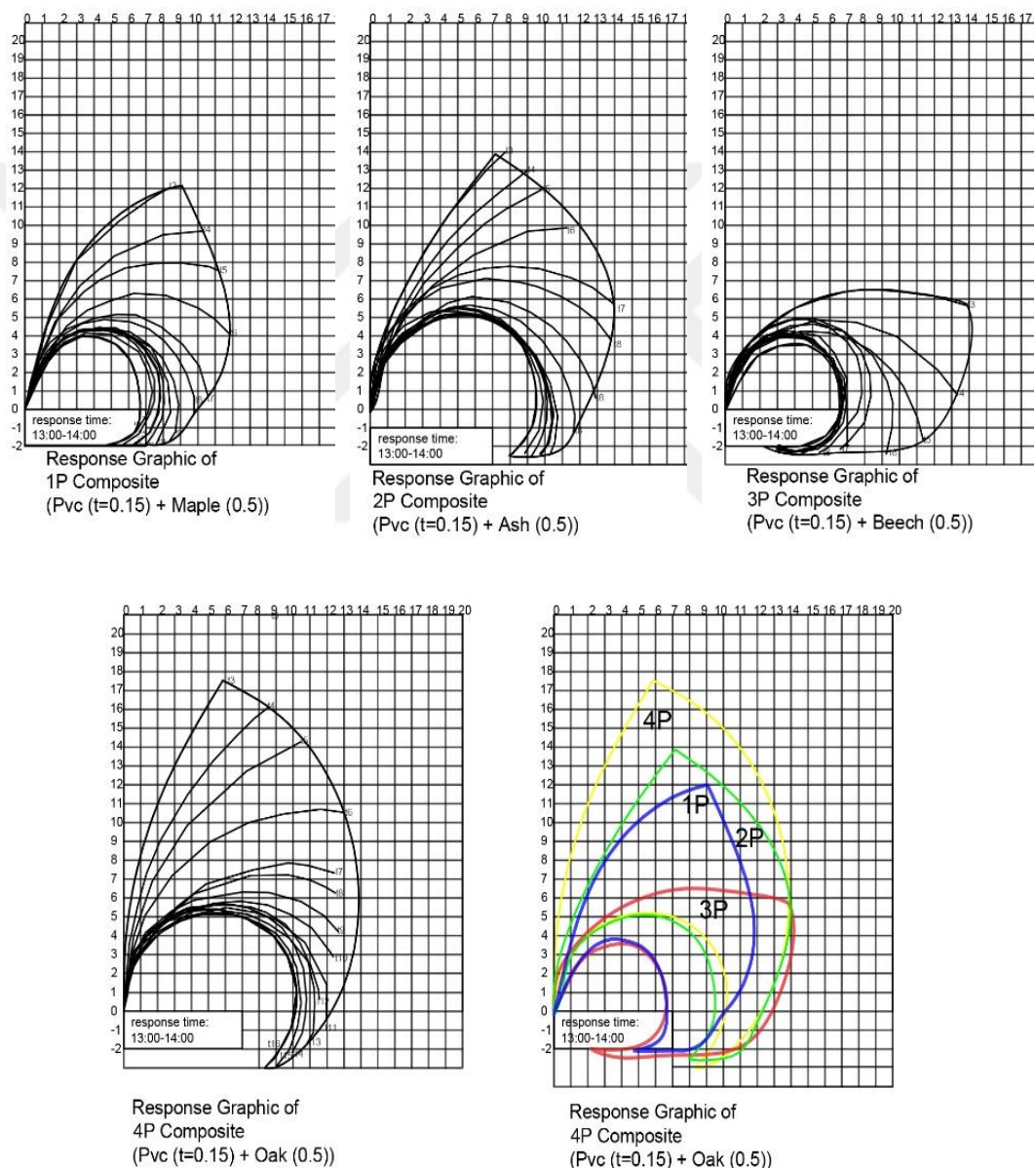


**Figure 4.16:**The defined curvature of composite in one caption (in t<sub>15</sub> and t<sub>16</sub>).

The experiment takes 60 minutes and the composite samples are captured in shots per every 4 minutes, as shown in Appendix E. The curvature change of the composite material is defined in each caption, as displayed in Figure 4.16. A response graph is drawn through the defined curves in Figure 4.17. According to the



experiment results, beech reveals to have the highest shrinkage capacity among the samples. Maple has a higher shrinkage capacity than ash and ash has a higher shrinkage capacity than oak (Beech>Maple>Ash> Oak). The shrinkage percentages of the wood types can be viewed in Table 4.2. This experiment reveals that the responsive behavior shows alteration according to the wood type, even with different kinds of the same wood type: Two different kinds of oak wood are used (4P<sub>2</sub> and 5P<sub>2</sub>) in the experiment and the curvatures of these composites showed difference.



**Figure 4.17:** The response graph of the samples in Experiment 2 (1P<sub>2</sub>, 2P<sub>2</sub>, 3P<sub>2</sub>, 4P<sub>2</sub>).

As the response graphic shows (Figure 4.17), the 3P<sub>2</sub> (Beech and PVC) sample achieves the maximum curvature change within the shortest period of time (20 minutes). The 1P<sub>2</sub> (Maple and PVC) sample displays a higher curvature change than 2P<sub>2</sub> (Ash and PVC). 2P<sub>2</sub> (Ash and PVC) displays a higher curvature change than 4P<sub>2</sub> (Oak and PVC). Based on the empirical analysis, 3P<sub>2</sub> (Beech and PVC) reveals to be the most responsive sample, while 1P<sub>2</sub> (Maple and PVC) comes the second. 2P<sub>2</sub> (Ash and PVC) is the third most responsive sample and 4P<sub>2</sub> (Oak and PVC) is the fourth (3P<sub>2</sub>> 1P<sub>2</sub>> 2P<sub>2</sub>> 4P<sub>2</sub>). Based on the results of this experiment, **Beech (3P<sub>2</sub>)** is selected for this material system study. Besides the curvature change of the composite materials, the response graph also provides information about response times. The curvature change gains speed after the first 12 minutes (t<sub>3</sub>). The change is more obvious in the first 20 minutes, i.e. between t<sub>3</sub> and t<sub>8</sub>. The response time of the 3P<sub>2</sub> (Beech+ PVC) composite takes **32 minutes**.

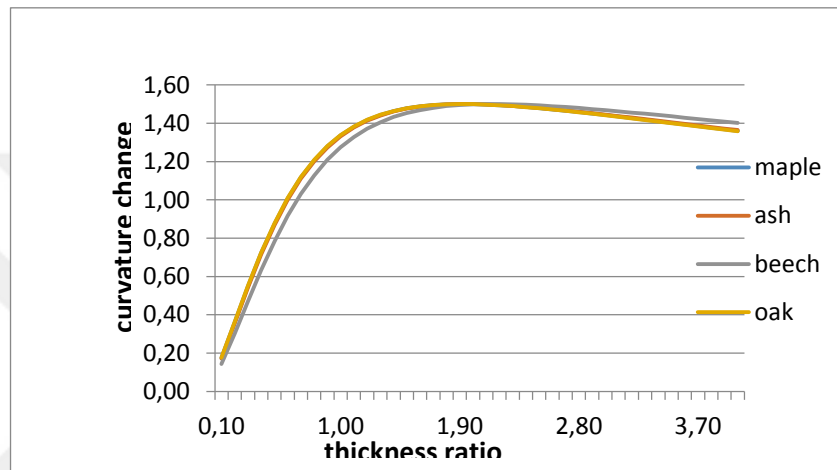
The results obtained from the empirical analysis are justified through quantitative methods, using **Formula 4.1**. The thickness and elasticity coefficient values are given in Table 4.7. The thickness and elasticity proportions of the samples are calculated and the curvature change coefficient is found, as shown in Table 4.8. The calculations are given in Appendix C. Based on the calculations, a curvature change coefficient graph is drawn for each wood type (Maple, Ash, Beech, Oak) (Figure 4.18). This graph (Figure 4.18) displays how the curvature coefficient changes in different thickness ratios.

**Table 4.7:** Thickness and elasticity values of used wood veneer types and polymer.

<i>Materials</i>	<b>Maple</b>	<b>Ash</b>	<b>Beech</b>	<b>Oak</b>	<b>PVC</b>
<i>Thickness</i>	0.60 mm	0.60 mm	0.45 mm	0.60 mm	0.15 mm
<i>Elasticity</i>	12GPa	12.20GPa	15GPa	11.9 GPa	3.25 GPa

**Table 4.8:** Curvature change coefficient  $P_1$ ,  $P_2$  and  $P_3$  with elasticity and thickness proportions.

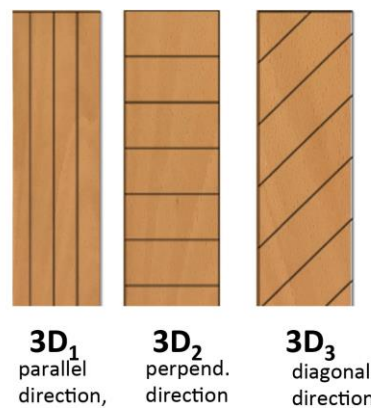
	<b>1P<sub>2</sub></b> <b>(PVC+Maple)</b>	<b>2P<sub>2</sub></b> <b>(PVC+Ash)</b>	<b>3P<sub>2</sub></b> <b>(PVC+Beech)</b>	<b>4P<sub>2</sub></b> <b>(PVC+Oak)</b>
<i>Thickness ratio(m)</i>	0.25	0.25	0.33	0.25
<i>Elasticity ratio(n)</i>	0.271	0.266	0.217	0.15
<i>Curvature change coefficient f(m,n)</i>	<b>0.457</b>	<b>0.451</b>	<b>0.525</b>	<b>1.464</b>



**Figure 4.18:** The curvature change coefficient graph of the used wood types.

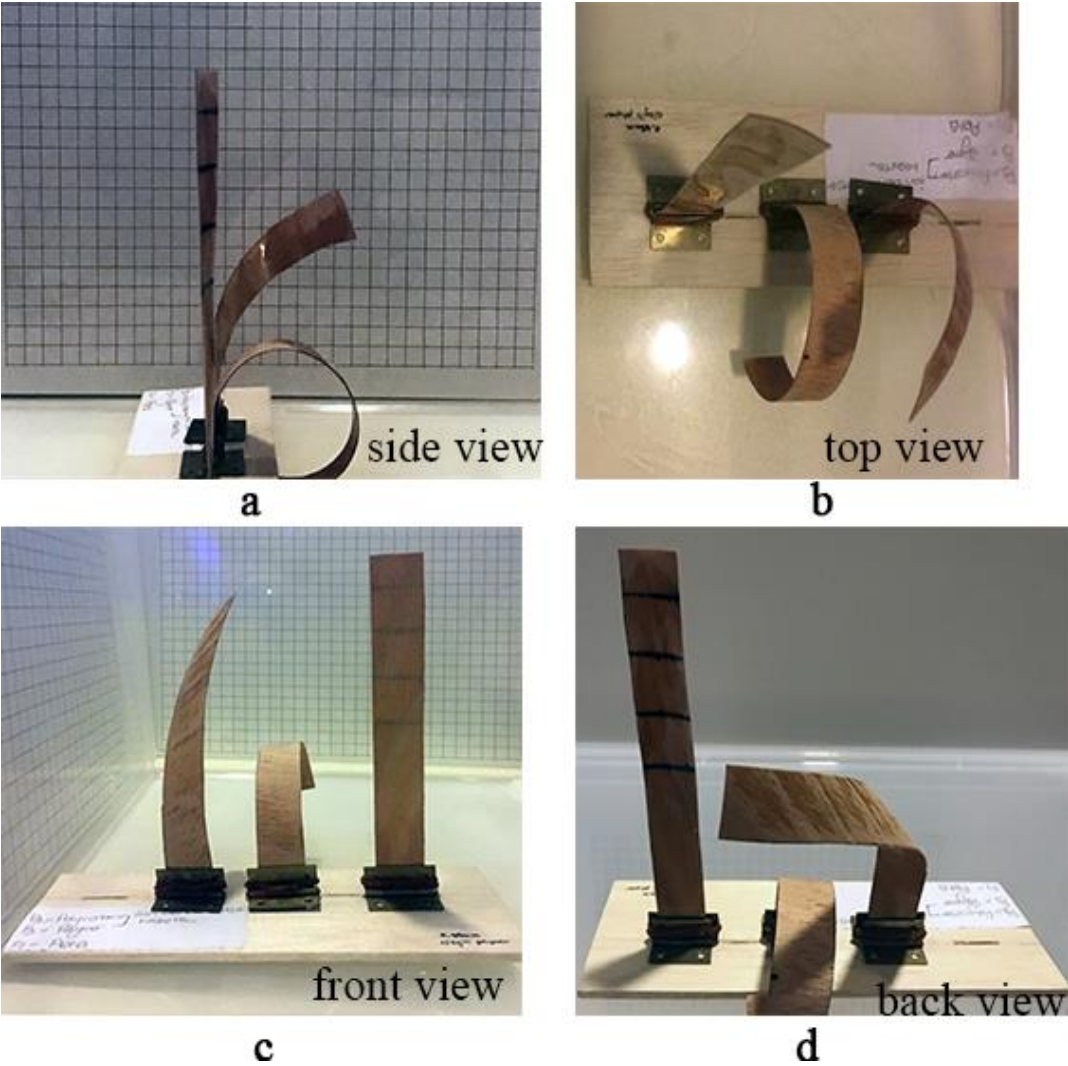
### Experiment 3: The grain orientation of wood veneer

In purpose of understanding how the grain orientation affects responsiveness in a composite, a beech veneer sample is cut in three different ways: In parallel to the grain direction, in perpendicular to the grain direction and in diagonal to the grain direction (Figure 4.19).



**Figure 4.19:** The cutting direction of the samples.

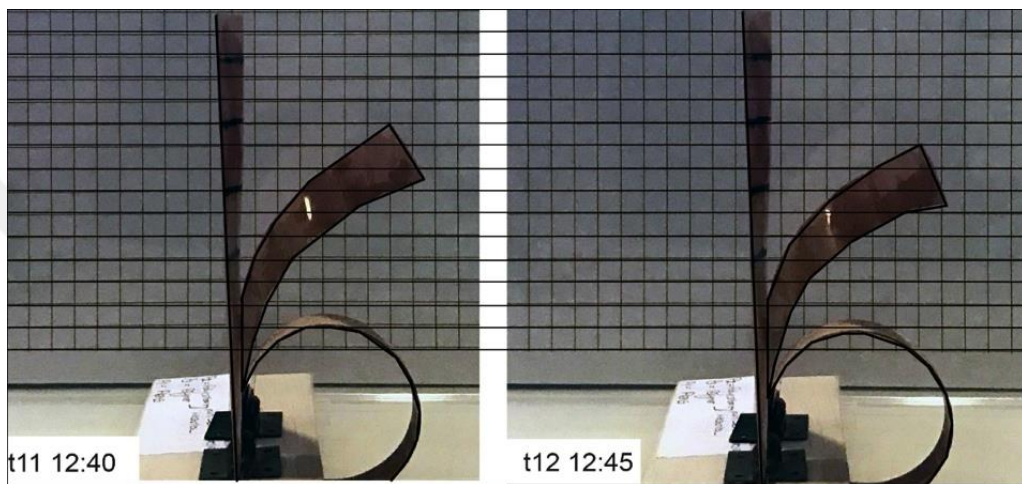
These composite samples are labeled in numerical order (3D<sub>1</sub> denotes the parallel direction, 3D<sub>2</sub> denotes the perpendicular direction and 3D<sub>3</sub> denotes the diagonal direction). An experiment is conducted with the aim of testing the effect of the grain direction on the responsive behavior of the composites. The experiment period takes 60 minutes and the composite samples are captured in shots per every 4 minutes, as shown in Appendix F. Figure 4.20 displays from different views the eventual form that the composites take at the completion of the experiment.



**Figure 4.20:** The shape transformation of composite samples from different views.

As seen in Figure 4.21, the orientation of the wood layer does make a change on the shape of the composite materials, since the hygroscopic elongation differs in different grain directions. The shape transformation in sample 3D<sub>3</sub> (cut in diagonal direction) is different from the transformation in other samples (3D<sub>1</sub>, 3D<sub>2</sub>). The

experiment results exhibit that the sample cut in perpendicular direction achieves ( $3D_1$ ) the highest curvature change in the shortest period. The sample that is cut diagonally to the grain direction ( $3D_3$ ) achieves a higher curvature change than  $3D_2$ , in a shorter period. The sample cut in parallel to the grain direction ( $3D_2$ ) achieves the lowest change of curvature in the longest period ( $3D_2 > 3D_3 > 3D_1$ ). The *tangential veneer* samples that are cut in *perpendicular to the grain direction* is selected for the responsive material system.



**Figure 4.21:** The shape transformation of composite samples due to anisotropy.

#### **Experiment 4: Testing the fibered polymer (anisotropic polymer)**

The previous experiments take advantage of the anisotropic and hygroscopic properties of wood. In this experiment (Experiment 4), polymer material properties are modified. Being an isotropic material, polymer exhibits same properties at all directions. The polymer only becomes anisotropic through the addition of fibers by laser cutting. The fibered polymer layers are bond with wood veneer and anisotropic composite materials are obtained.

The distance between the fibers differs in each sample, being 2.5mm, 5mm and 10mm respectively, as displayed in Figure 4.22. In the first sample ( $3G_1$ ), the distance between fibers is 2.5 mm. In the second sample ( $3G_2$ ), the distance is 5 mm and in the third sample ( $3G_3$ ), the distance is 10 mm. An experiment is carried out to test how polymer fibers affect the responsive behavior of the composite. The experiment takes 60 minutes and the composite samples are captured in shots per every 4 minutes, as shown in Appendix G. The curvature change of the composite

material is defined in each caption, as displayed in Figure 4.23. A response graph (Figure 4.24) is drawn through the defined curves.

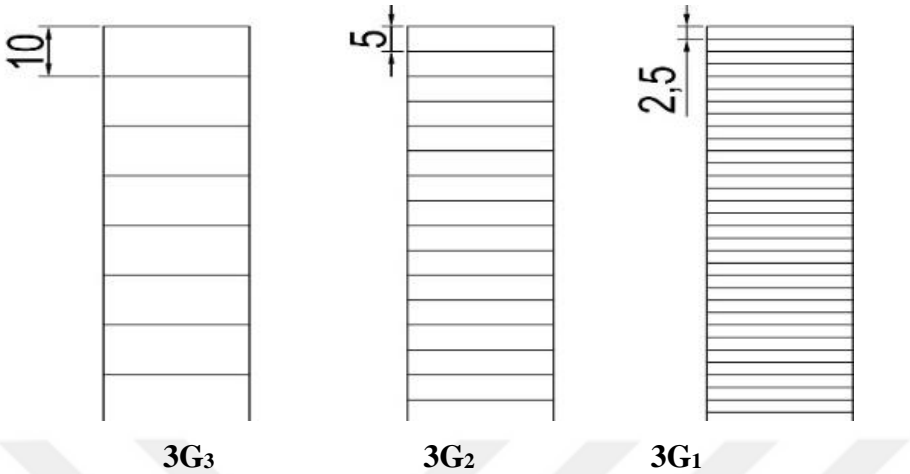


Figure 4.22: The distance between the grains in 3G<sub>3</sub>,3G<sub>2</sub> and 3G<sub>1</sub>.

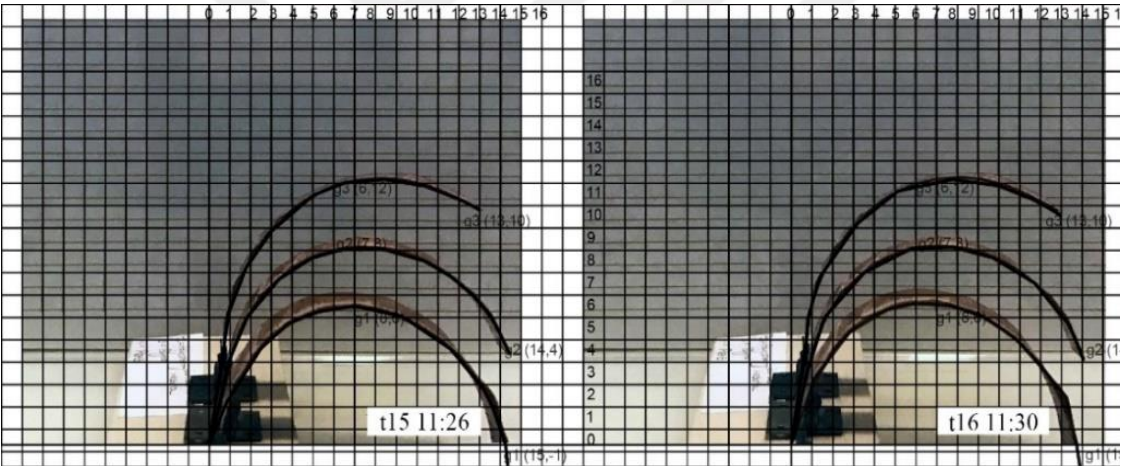
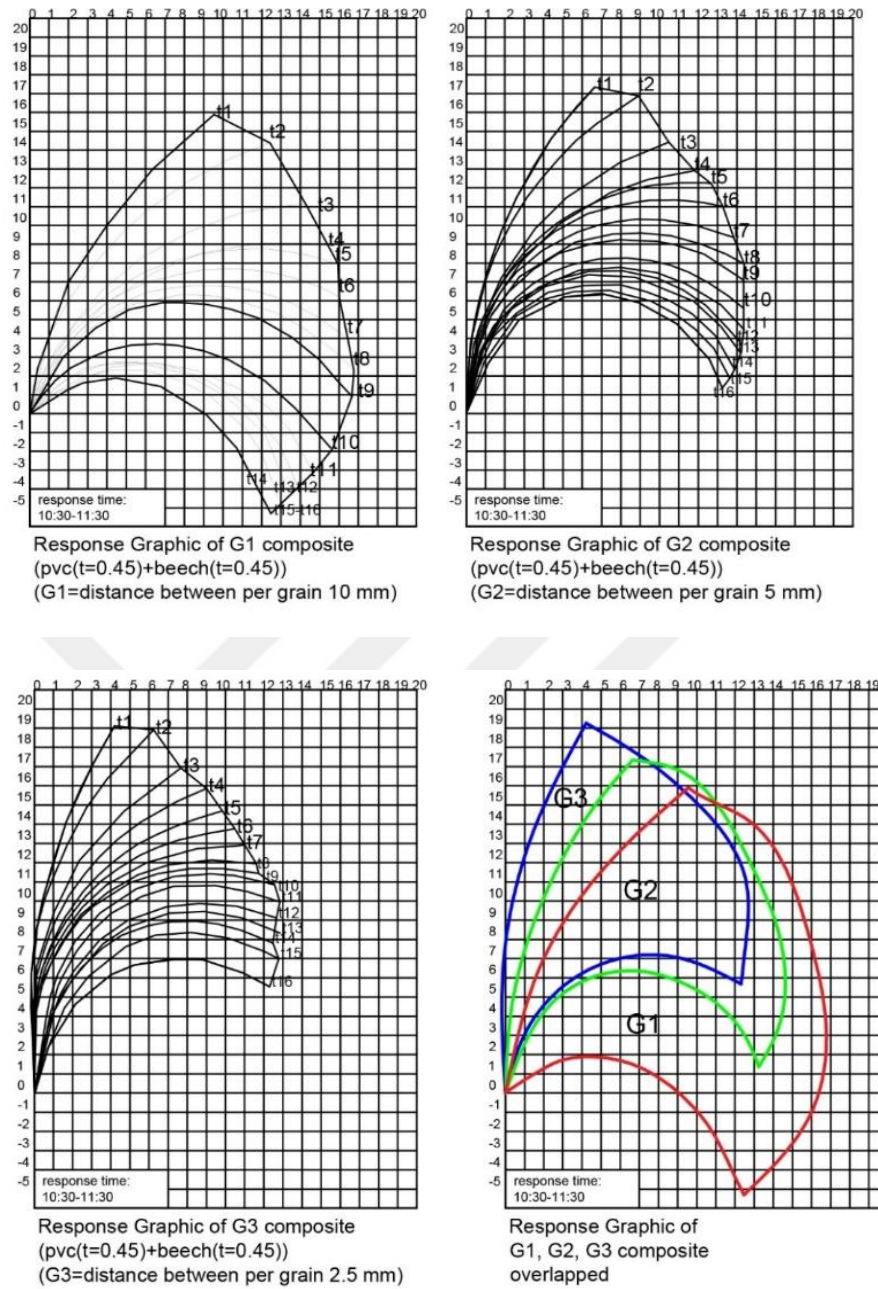


Figure 4.23: The fibered composite samples.

According to the response graph (Figure 4.24), 3G<sub>1</sub> achieves the highest curvature change. 3G<sub>2</sub> achieves a higher curvature change than 3G<sub>3</sub>, which achieves the lowest curvature change. The experiment reveals that the denser and with higher quantity the grain is, the higher the curvature change will occur within a shorter period. Thus, it was decided that the passive layer for the material system would comprise of *the fibered polymer layers* with the fiber distance of 2.5 mm. It can be noted that this method facilitates responsiveness and enhances the curvature change of the composite material.

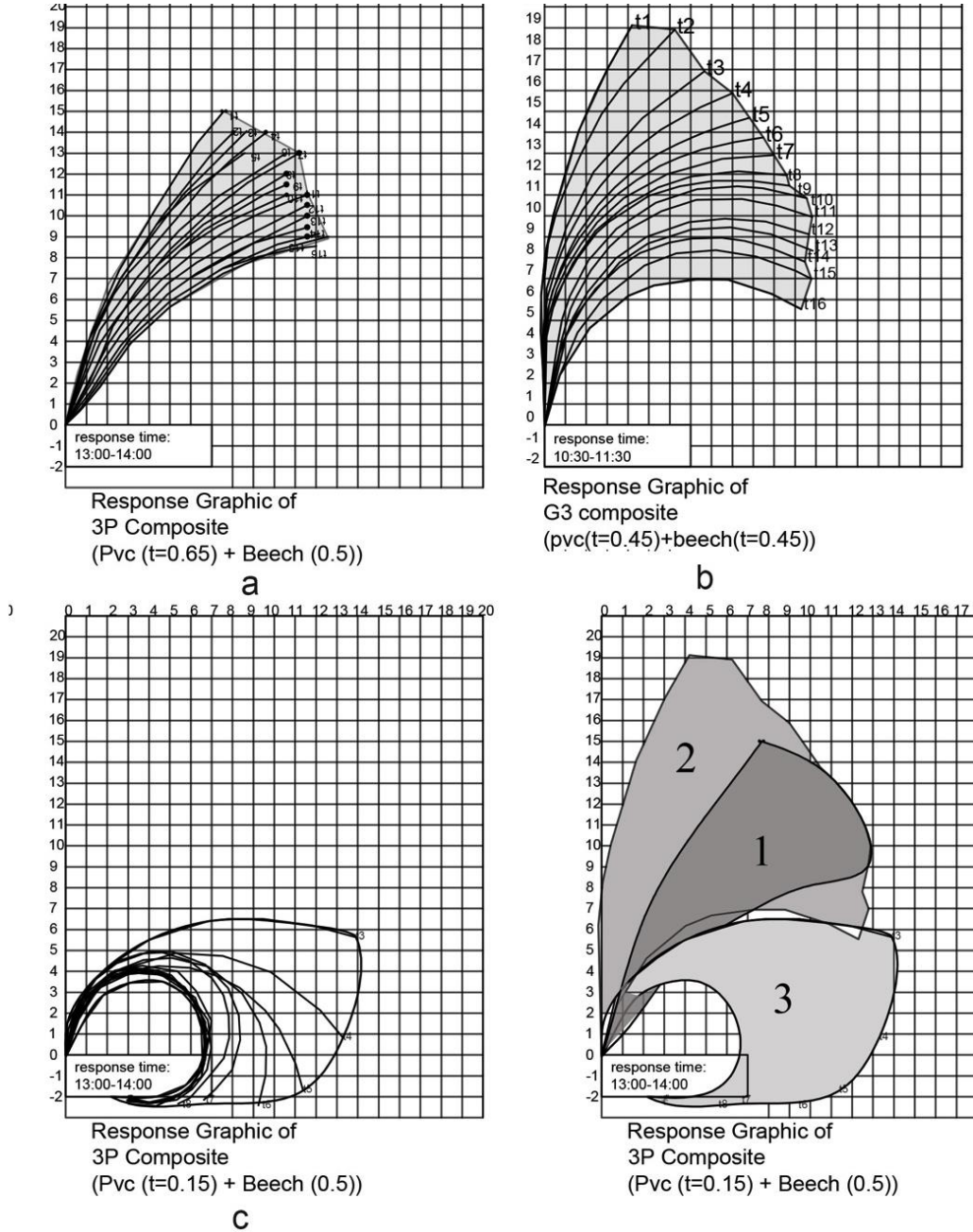


**Figure 4.24:**The response graph of the samples in Experiment 4 (3G<sub>1</sub>, 3G<sub>2</sub> and 3G<sub>3</sub>).

### The thickness of polymer layers

Thickness of the layers appears to be an influent parameter on curvature change. Thus, the thickness of the polymer layer is reduced in the following experiments, in an aim of understanding how thickness affects the responsiveness of the composite. The thickness of the polymer used in the first experiment is 0.65 mm. This value is reduced to 0.45 mm and 0.15 mm respectively, in the following experiments. The composite material with the thinner polymer layer, achieves a higher curvature

change. The empirical analyses of the experiments show that any decrease in thickness causes the response time to shorten and the curvature to bend further. In order to analyze the effect of thickness, three different composite samples, the first polymer layer being 0.65 mm thick, the second being 0.15 mm and the third being 0.45 mm thick are compared, as seen in Figure 4.25, The thinner polymer achieves a higher change in curvature in the shortest period. While the thickest composite ( $P_2$ ) curves in 60 minutes, the thinnest composite ( $3P_2$ ) curves in 32 minutes.



**Figure 4.25:**The response graphic to compare the thickness of the polymer.



### 4.3. Evaluation on Material Experiments

Responsive composite material benefits the anisotropy and hygromorphy properties of wood to achieve responsiveness. The influential characteristics of material behavior are tested through material experiments (wood types, polymer types, grain direction, polymer with fibers and layer thickness). The main objective of the experiments is to understand the material behavior and ensure improvement through adjusting the parameters. On the basis of the evaluation of conducted experiments, the optimum parameters for responsive material are listed below;

- Among the tested polymer types (PETG, PVC and PC); the **PVC** polymer is selected to function as the passive layer of the composite (PVC>PETG>PC).
- Among the tested wood types (maple (1), ash (2), beech (3) and oak (4)); **beech** is selected to function as the active layer of the composite, since it possesses a higher hygroexpansion (shrinkage) percentage and exhibits a higher dimensional change (3>1> 2> 4).
- The selected polymer (PVC) thickness is **0.15 mm**, since it is understood that the thinner the polymer is, the shorter the response time and the higher the curvature change will be.
- Among different cutting directions of the wood veneer (perpendicular cut (1), parallel cut (2) and diagonal cut (3)); the **tangential veneer** samples that are cut **perpendicularly to the grain direction** are selected to for the responsive composite material (1 > 3> 2).
- **The fibered polymer layer** is employed to facilitate the curvature change by adding fibers through laser cutting. Among the tested fibered polymer types, the selected one is the polymer with **denser fibers**, the distance of which is **2.5 mm**.

The optimum parameters for the composite material are shown in **Table 4.9**. Based on the parameters, the curvature radius of the most responsive composite is calculated through the application of **Formula 4.1**, as shown in Appendix C. The curvature radius of the most responsive composite is found as **24,2**. The material experiments show that seeing the responsiveness results of this composite takes **32 minutes**.

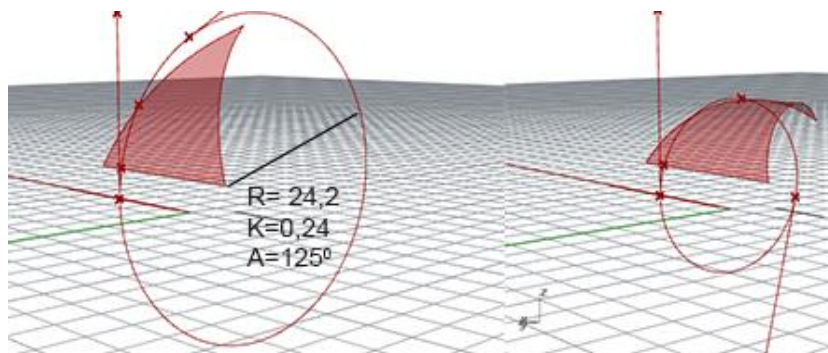
**Table 4.9:** The optimum parameters for optimum responsiveness.

<i>Parameters</i>	$\alpha_{\text{beech}}$	$\alpha_{\text{pvc}}$	$\Delta MC$	$t_{\text{beech}}$	$t_{\text{pvc}}$
<i>Values</i>	%11.9	0	(%80-%40)	0.45 mm	0.15 mm
	Thickness Rato(m)	Stiffness ratio (n)	Curvature Change f (m,n)	$t_{\text{total}}$	
	0.33	0.22	0.52	0.60	

$$K = \frac{1}{R} = \frac{\Delta a \cdot f(m,n) \cdot \Delta MC'}{t_{\text{total}}} + \frac{1}{R_0}$$

$$K = \frac{0,119 \cdot 0,52 \cdot 0,4}{0,60} + 0 = 0,041253 \quad R \cong 24,2 \quad (4.1)$$

The evaluation of experiment results rely on (i) empirical analysis and (ii) numerical analysis methods. The empirical method analyzes the curvature change of composite materials. The curving of the composite is defined and a response graph is drawn. In the numerical method, calculations are used to predict the curvature change of composite. The results from the observational analysis are justified through calculations. Calculation results that are obtained from quantitative methods enable the responsive behaviour of the composite material to be simulated via computational tools at further stages. The simulation of material behaviour can be furthered with material computation. Based on the numerical results, the curving action is simulated through computational design tools as shown in Figure 4.26. Grasshopper definition of the bending simulation of the composite is displayed in Appendix H.



**Figure 4.26:** Simulation of curvature of the composite material.

## 5. RESPONSIVE SYSTEM STRUCTURE





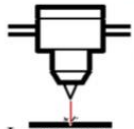
*Parametric design means designing the design (Burry, 2013).*

This study aims to develop a responsive material system, the responsiveness of which is achieved by the involvement of a specific responsive composite, which is developed in Section 4. A structure is designed for the responsive material, the form of which is generated on the basis of the parameters and their dependencies. This feature renders the structure *parametric*. Burry (2013) describes the parametric design approach as ‘designing the design’. The interrelation between the parameters defines the design process of the structure.

The progress of the parametric responsive system structure includes (1) the parametric design process and (2) the construction process of the structure. The parametric design process comprises of (1) sunlight analysis, (2) initial form generation, (3) form development. The construction process involves (1) joint detail, (2) fabrication and assembly of the units within (3) the installation of the responsive panels into the units. Computational tools are employed in the design progress of the responsive system structure.

The utilized design tools are grouped by Dunn (2012)’s usage purpose-based classification, as; *evaluative*, *explorative*, *descriptive* and *fabricative* design tools. Sunlight analysis is conducted through Ladybug (evaluative). Form generation is made through Rhinoceros (descriptive). Form development processes are run through Grasshopper (evaluative). The modules of the structure is arranged for fabrication with Fabtools (supportive) and fabricated with a laser cutter (fabricative).

**Table 5.1:** The classification of the used computational tools.

		<b>Used tools and purposes</b>				
P r o g r a m s  u s e d f o r	<i>Descriptive</i>	<i>Explorative</i>	<i>Evaluative</i>	<i>Supportive</i>	<i>fabricative</i>	
		 Rhinoceros	 Grasshopper	 Ladybug	 Fabtools	 Laser cutter
	the form of the surface	the form of the surface	the environmental analysis	unfolding and labeling the geometry	digital fabrication	

## 5.1. Design Process of Responsive System Structure

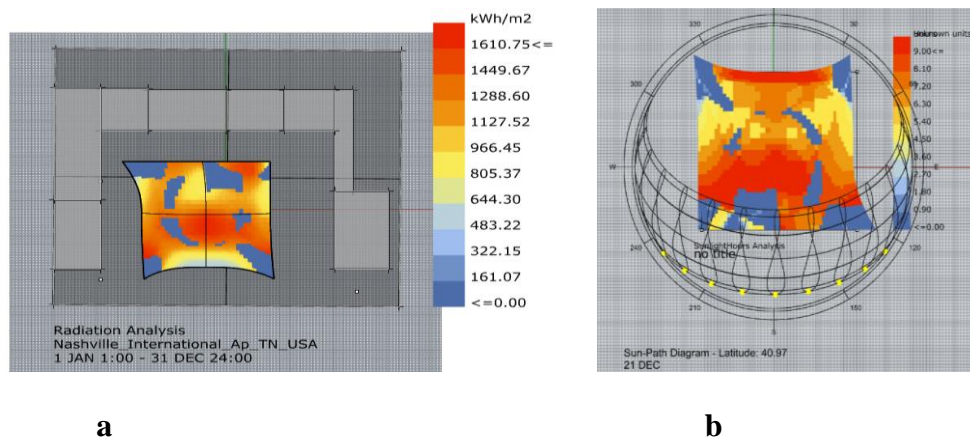
The design progress of the responsive system structure can be examined in three stages: (1) sunlight analysis, (2) initial form generation, (3) form development. Sunlight is acknowledged as the design parameter for the form generation and sunlight analysis is conducted through a simulation in Ladybug. The initial form of the system structure is generated in Rhinoceros, on the ground of the sunlight simulation analysis. The form parameters are modified through attractor points, the location of which is identified according to the sunlight simulation.

### *Sunlight analysis*

Sun radiation is one of the influent factors on relative humidity content. It triggers the temperature and the temperature affects relative humidity content. Therefore, the sunlight is taken into consideration as the design parameter in the form generation process.

The first step in drawing these simulation graphics is the import of the Standard Energyplus Weather Files (EPW) of the context to Ladybug, with the intent of obtaining weather information from the given location. Then the sun path command is specified and related with context parameters. Connecting the related parameters, Ladybug displays the sunlight and radiation analysis of the given context through graphical representation. The sun radiation (Figure 5.1.a) and sunlight analysis graphics are displayed (Figure 5.1.b) and the Ladybug definition is explained in Appendix I.

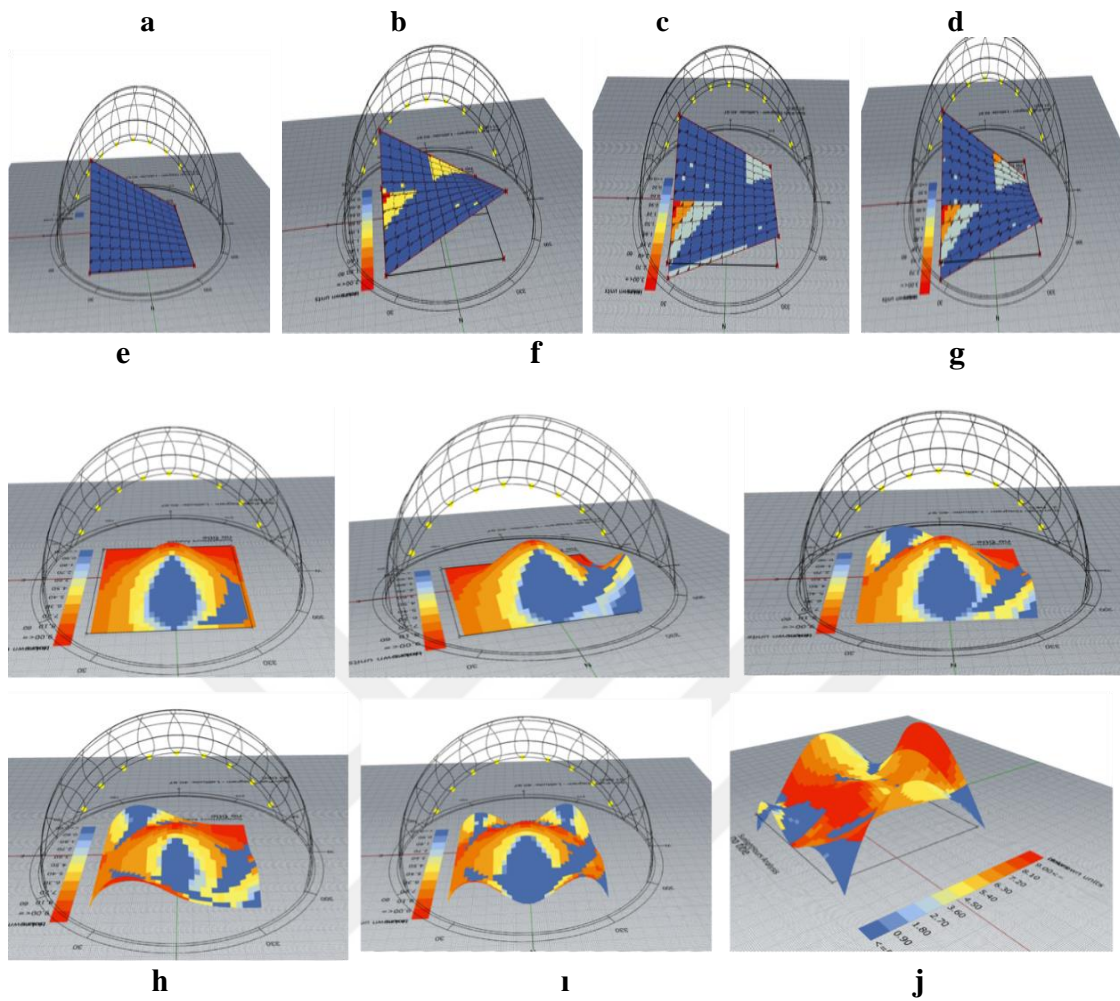
The amount of solar radiation (Figure 5.1.a) and sunlight (Figure 5.1.b) are indicated with colors in the analysis graphic: The surfaces with blue color on the geometry receive the sunlight for 2 hours maximum and the radiation by approximately 600 kWh/m<sup>2</sup> maximum, on December 21<sup>st</sup>. The yellow surfaces receive the sunlight for between 2-5 hours and the radiation between 600- 1000 kWh/ m<sup>2</sup>. The orange surfaces receive the sunlight for between 5-7 hours and the radiation between 1000- 1450 kWh/ m<sup>2</sup>. The red surfaces get the sunlight for more than 8 hours and the radiation between 1450-1600 kWh/ m<sup>2</sup>.



**Figure 5.1:** Sun radiation (a) Sunlight (b) analysis graphic on the geometry.

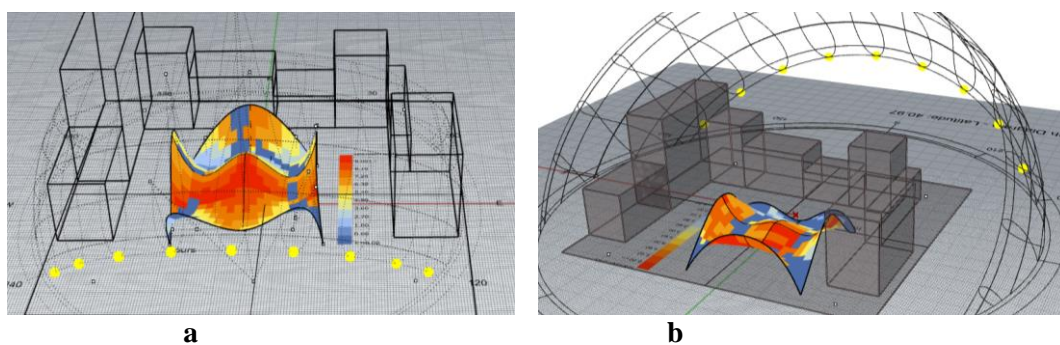
### *Initial form generation*

The form finding process is conducted through *Rhinoceros* program, which is used as a *descriptive* tool. During the form configuration, the sunlight simulations on the geometry are taken into consideration, as seen in Figure 5.2. In the basic Euclidian geometric form (Figure 5.2.a), the simulation represents no difference in color. This means that each surface receives the same amount of sunlight. As the geometry of the form alters through extrusion from corners (Figure 5.2.b, c, d), the represented colors begin to change in simulation. This means that the amount of the sunlight that falls on the surface differs in parallel to the alterations in the geometry. The basic geometry begins to transform into a curvilinear geometric model (Figure 5.2.e) by intersecting the non-uniform curves via loft operation and generating a NURBS (Non-Uniform Rotational Basis Spline) shape. The surface form will become more complex as the curve control points change (Figure 5.2.f, g, h, i, j). Accordingly, the simulation displays color changes as the curvilinear surface varies. By controlling the curves, the basic curvilinear form (Figure 5.5.e) develops a complex parabolic form (Figure 5.2.j). The resultant complex geometry is (Figure 5.2.j) selected for the structure of the system, according to the evaluation of the simulation. The surfaces of the complex form (Figure 5.2.j) receive different amounts and durations of sunlight in different hours, as seen in the simulation. The brighter surfaces receive sunlight for more than 5 hours and solar radiation for over 800 kWh/m<sup>2</sup> in a day. These surfaces are represented with orange and red color in the simulation.



**Figure 5.2:** The form finding process of the surface regarding to analysis.

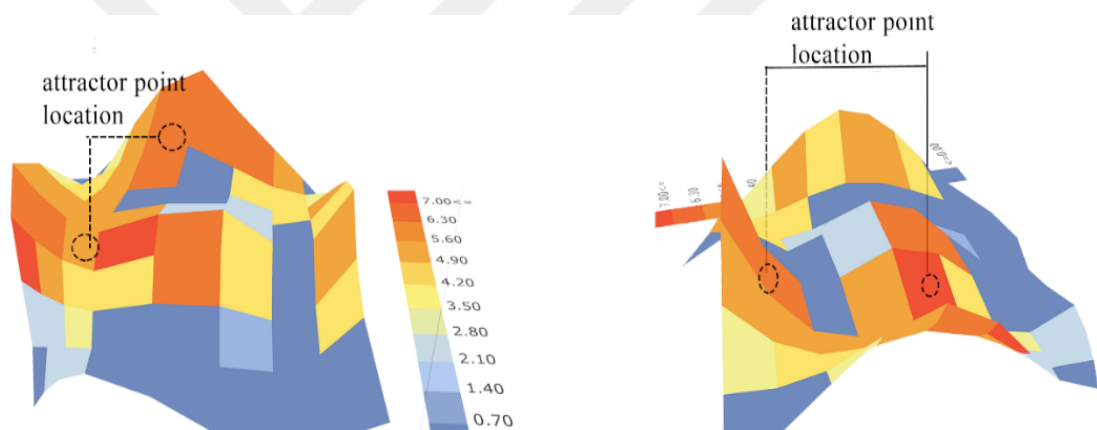
The built environment that surrounded the form (context), is included in the simulation. The built environment affects the amount of the sunlight and sun radiation at the designed surface as seen in Figure 5.3 since it casts a shadow over the surface.



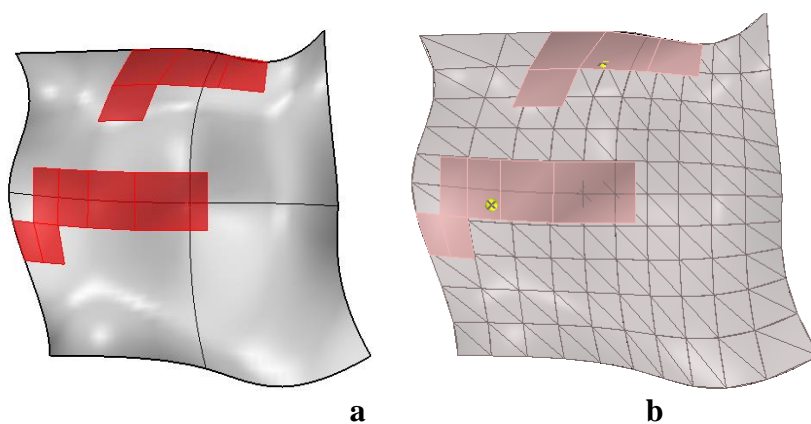
**Figure 5.3:** The sunlight analysis of the surface without (a) and within (b) the context.

### ***Form development***

The form parameters are modified according to the attractor points, via *Grasshopper*. The attractor point acts as a virtual magnet in Grasshopper, attracting object parameters such as scaling, form, color or rotation, as per the defined relation (Akos and Parsons, 2014). The sunlight analysis is used to determine the location of the attractor points that attract the defined parameter of the objects. In sunlight simulation, the surfaces that get the maximum amount of sunlight are represented in red and orange colors. These surfaces are specified (Figure 5.4) in order to help locating the attractor points. However, the interface of Ladybug does not allow making changes on the simulation graphic. Therefore, the specified areas are extracted from the model and turned into surfaces, as shown in Figure 5.5.a. The surface centers and the attractor points are located in the centers (Figure 5.5.b).

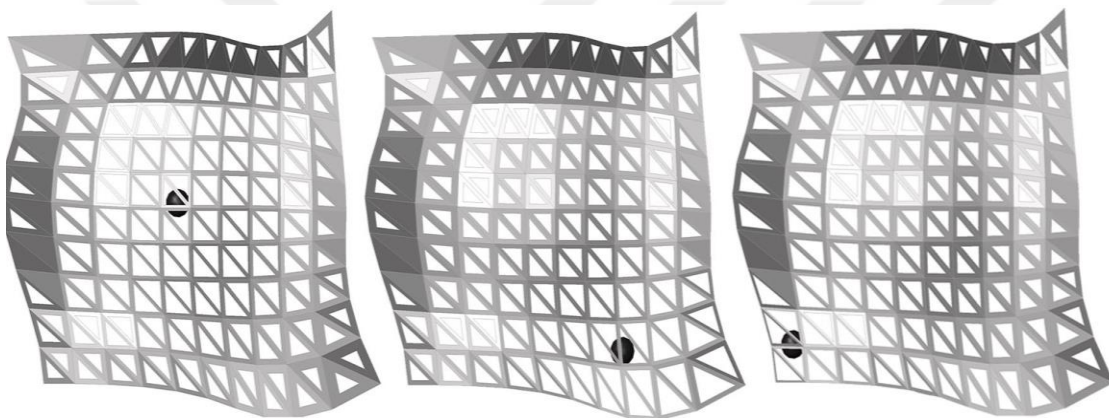


**Figure 5.4:** The extracted area according to sunlight analysis.



**Figure 5.5:** The extracted surfaces (a) and the attractor points located in centers of the surfaces (b).

The first stage of form development is subdividing the surface into units. The units are then modified according to the attractor points. The attractors affect the scaling parameter of the opening of each unit. The opening sizes vary according to the distance of the unit to the attractor points. The attractor points are located on the center of the brightest surfaces on the form, as shown in Figure 5.5. Figure 5.6 displays the effect of an attractor point on the openings' scale. The scale of the module openings depends to their distance to the attractor points: The units that are located closer have bigger openings while the units that are located farther have smaller openings. The relation between units' scale and the distance to centers is illustrated in Figure 5.6.



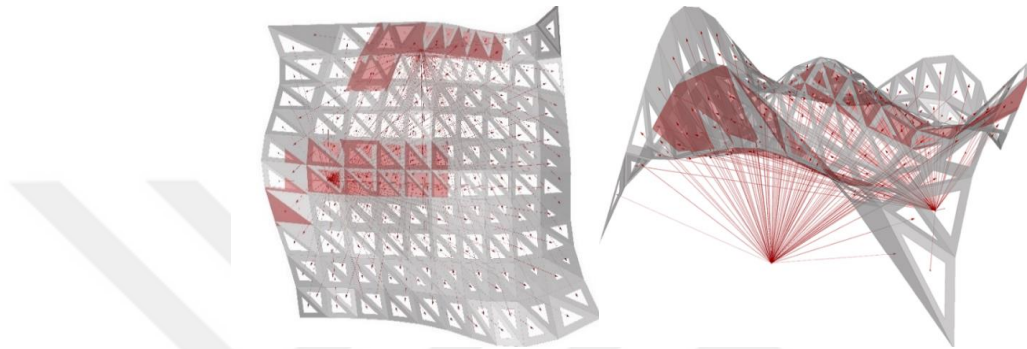
**Figure 5.6:**The relation between the scaling parameter and the attractor point.

The algorithms for the form development process are explained in Figure 5.8 and the resultant form is displayed in Figure 5.7. The form development process is accomplished through the definition made with Grasshopper, as displayed in Appendix J. The algorithms are explained in steps and are itemized below:

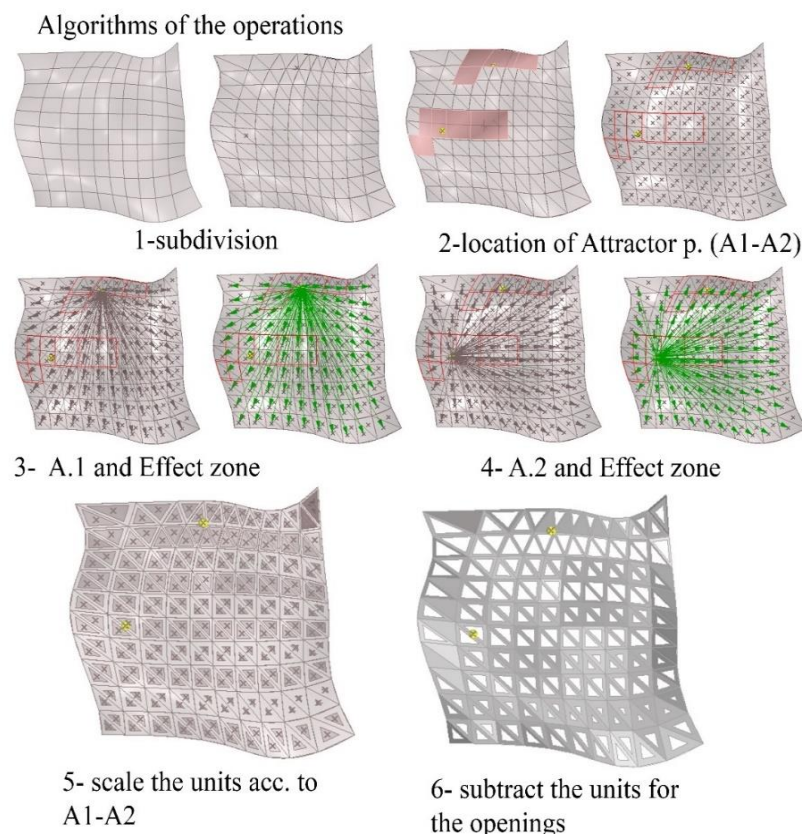
1. Subdivide the surface into sub-surfaces,
2. Find the area and the center of each subsurface,
3. Determine the location of the attractor points,
4. Calculate the distance between the attractor points and the centers of the modules,
5. Determine the distance value
6. Among the distances that were identified in Step 4, find the closest and farthest ones,



7. Modify the scale of each opening according to the distance value which was determined in Step 5,
8. Define the opening of the modules by scaling the modules themselves from the center
9. Assign the scaling factor to scale each opening according to the distance between their centers and the attractor points. Then subtract the scaled modules from the main module.

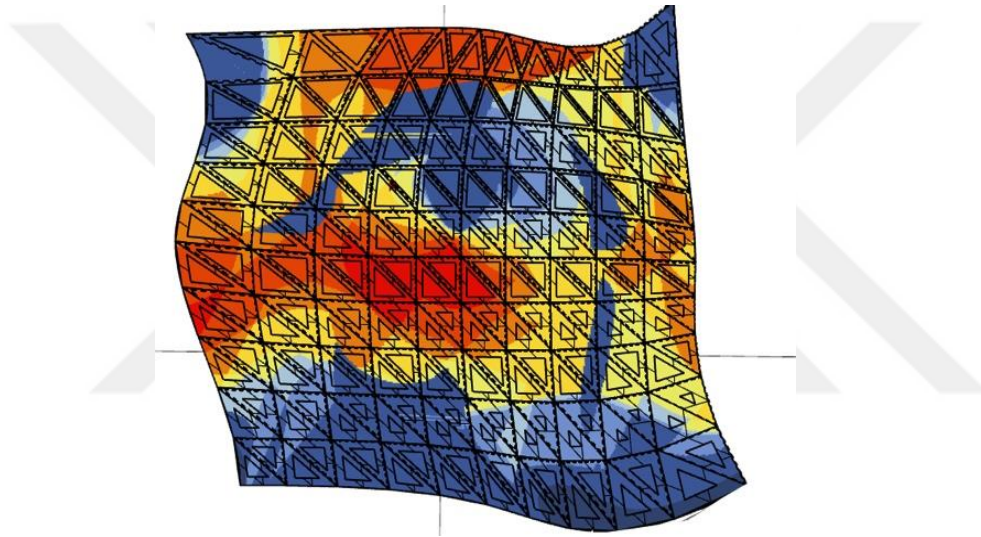


**Figure 5.7:** The final model of the structure according to attractor points (from the top view and perspective).



**Figure 5.8:** Algorithm of the formal operations.

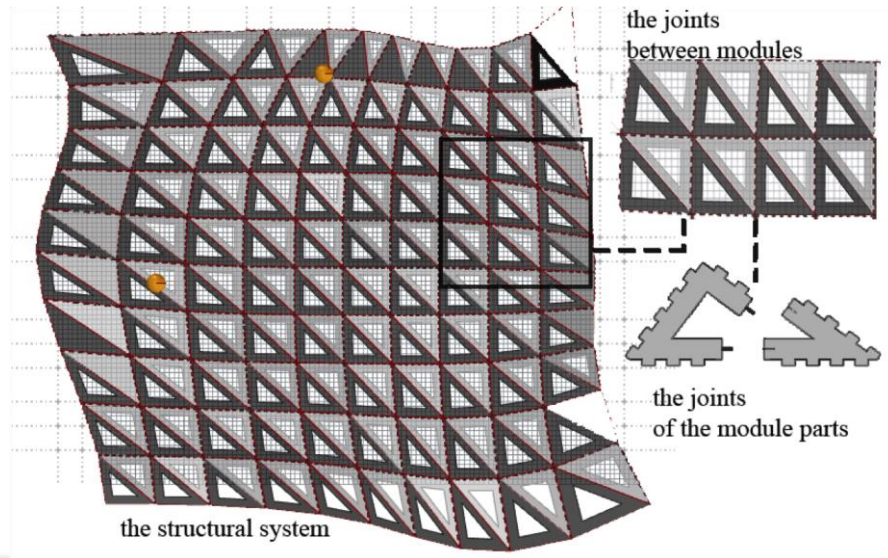
In result of the above-mentioned processes, the scale of each opening changes due to attractor point effect. The scaling rate varies according to the sunlight amount on the surface, since the location of attractor points were determined on the basis of the sunlight simulation. The brighter surfaces are located closer to the attractor points and thus, these surfaces have larger openings. They receive more amount of sunlight and they are affected more from humidity changes. The darker surfaces are located farther to the attractor points and thus, these surfaces have smaller openings. They receive less amount of sunlight and are affected less from humidity changes. The darkest surfaces have the smallest openings. The sunlight simulation and the resultant form are overlapped in Figure 5.9 in order to understand the relation between the scale of the openings and the sunlight simulation.



**Figure 5.9:**Overlapped sunlight analysis simulation and resultant form.

## **5.2. Construction Process of the Responsive System Structure**

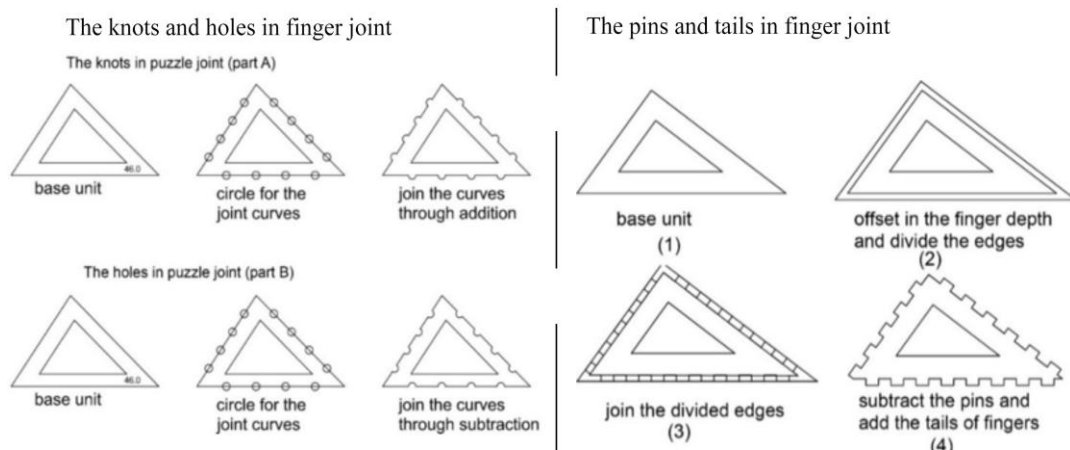
The construction process of the structure progresses is three stages; (1) joint detail design, (2) fabrication and assembly, (3) installation of the responsive panels into the structure. The structure comprises of modules and each module is made up two parts, as shown in Figure 5.10.



**Figure 5.10:** The modules of the structure and the parts the modules.

### *Joint detail design*

The modules are connected via joints. The joints are designed such as to minimize the use of adhesive or supporting materials throughout the assembly process. In this study, two joint alternatives are developed; puzzle joint (jigsaw joint) and finger joint. Finger joint is selected for the connection of the modules since this option involves more joints. The joints between modules are constructed (drawn and fabricated) via digital tools. The Grasshopper definitions for puzzle joint and finger joint are displayed in Appendix K and Appendix L, respectively. The design process of the puzzle and finger joints are illustrated in Figure 5.11.



**Figure 5.11:** The design progress of puzzle joint and finger joint detail.

Each triangular module is made up two parts that are connected through joints. Dividing the modules into smaller parts facilitates the assembly, disassembly and reassembly of the components. The partition renders the handling, transportation and reusability of the structure easier.

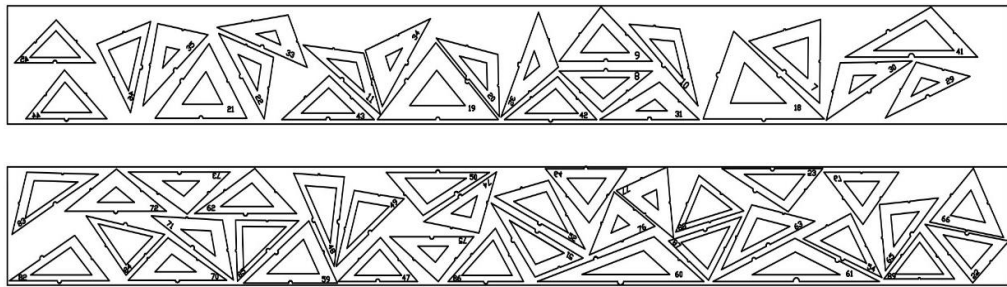
The physical model of each joint alternative is manufactured with the intent of being able to compare their connection durability, as displayed Table 5.2. According to table (Table 5.2), **Detail F**, among all the presented joint details, is selected. This joint type presents a more durable connection with more tails, as shown in the legend in Table 5.2.

**Table 5.2:** The joint detail alternatives.

NAME	MODEL	JOINT	JOINT DRAWING
DETAIL A █ %20			
DETAIL B █ %30			
DETAIL C █ %40			
DETAIL D █ %50			
DETAIL E █ %70			
DETAIL F █ %85			

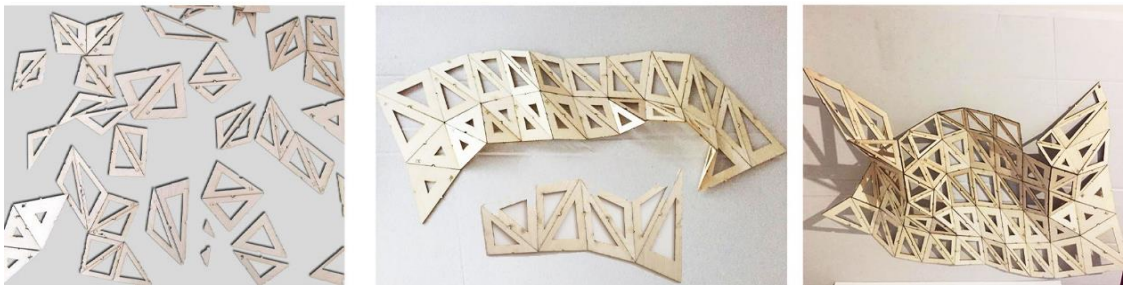
***Fabrication and assembly***

200 unique modules of the structure are prepared for digital fabrication and fabricated with a laser cutter. The surface units are unrolled, number-labeled with via Fabtools as displayed in Appendix M and arranged according to the dimension of the balsa wood sheet (10x100 cm) to minimize material waste, as shown in Figure 5.12.

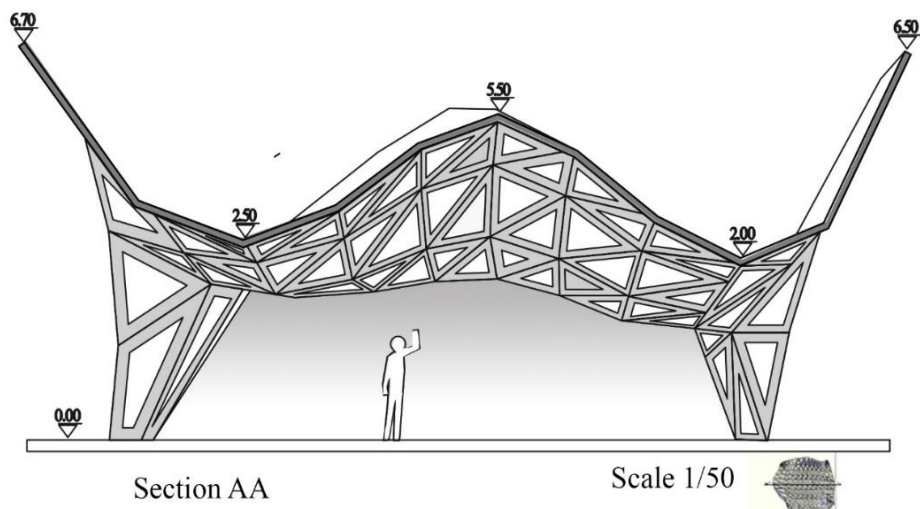


**Figure 5.12:** The fabrication layout that arranged for balsa wood sheet.

The fabricated modules are assembled from their joint details and number labels facilitate the assembly. The responsive structure model is constructed partially. Figure 5.13 displays the assembling stages of a partial model of the structure. The dimension of the structure is 10 meters in width and 10 meters in length while the height ranges between 2.00 meters and 6.50 meters, depending on the curvilinear form (Figure 5.14). The structure is consolidated with supportive footings as shown in the section drawing (Figure 5.14). The supportive footings carry the structural load.



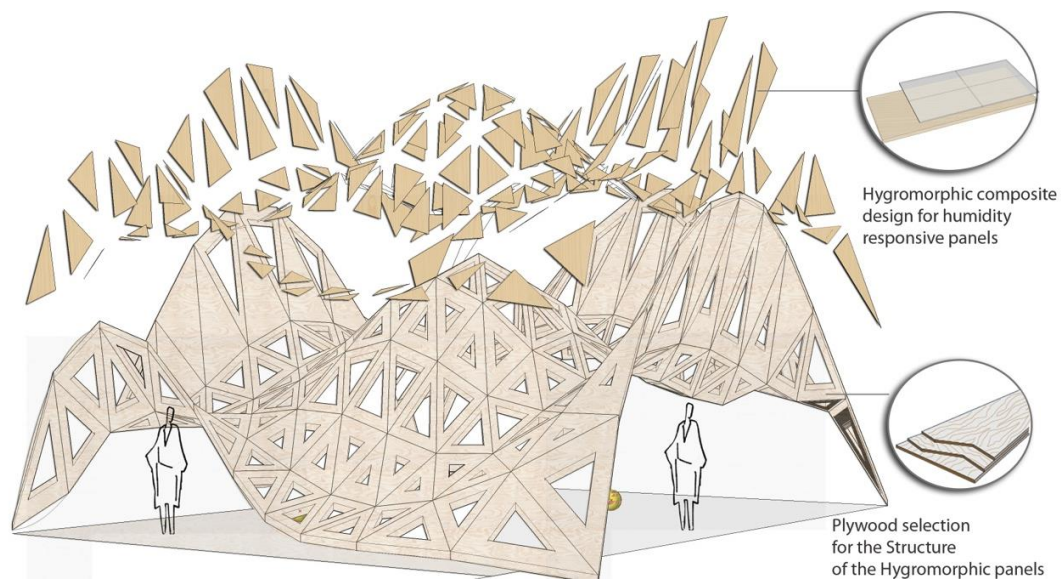
**Figure 5.13:** Partial physical model of the structure.



**Figure 5.14:** The section drawing of the structure.

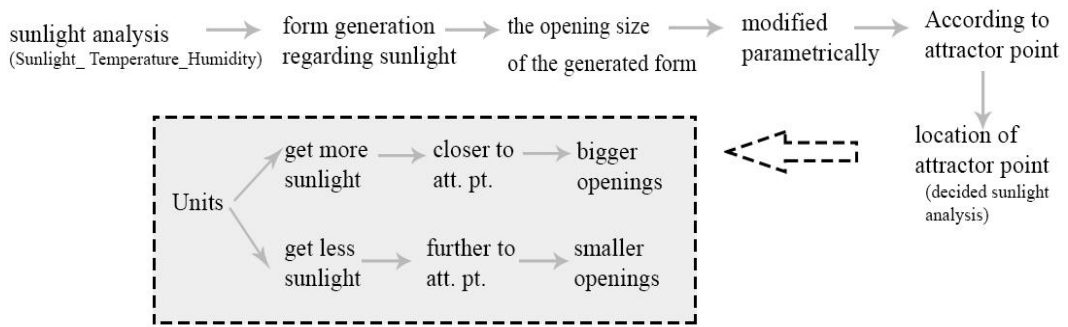
### ***Hygro\_Responsive Structure with responsive panels***

The responsive composite, developed in **Section 4**, is experimented in the parametric structure. The composite material is located at the responsive panels, which will in response to humidity alterations. The structural system is made up of plywood material and the panels are of composite material. The multi-layered structure of plywood material prevents shrinkage-based deformations (Figure 5.15). The geometry of the panels are arranged and the panels fabricated using composite material. The fabricated panels are installed into module slits.



**Figure 5.15:**The used material of the structure and responsive panels.

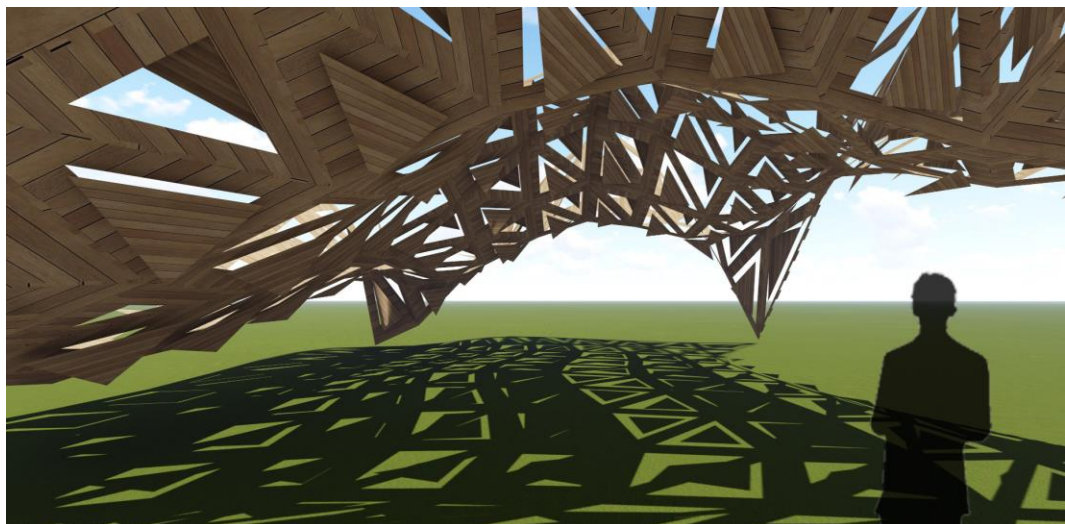
The composite panels have different sizes due to the attractor points' effect on the scaling factor, as mentioned in Section 5.1. As the opening sizes change, responsive panel sizes change, respectively. The increment in panel scales enhances the curvature change of panels since longer panels will curl more in response to humidity. Accordingly, brighter surfaces, receiving more sunlight and radiation, have larger openings and consequently, larger responsive panels. As the panels get larger, they curve more, in response to humidity. On the other way around, darker surfaces possess smaller openings, and therefore, smaller responsive panels. The smaller the panels get, the less they will curl less in response to humidity. The relation between the sunlight, form development and material response is explained in Figure 5.16.



**Figure 5.16:**The relation between the openings’ scale and panels’ response.

The responsive panels curl inward (in polymer direction) in humid air and the openings get close. In dry air though, the panels curl outward (in wood direction) and the openings get wider (Figure 5.16). As a result, airflow is regulated and natural ventilation is attained through humidity-driven movement of the responsive panels.

Observing the humidity-driven movement of the panels, the user can become knowledgeable on changes in humidity. Besides, the responsive behavior of the panels can create an *experiential effect* on the user. The response of the panels allows different forms of light penetration, as shown in Figure 5.17. As humidity changes, the panels curl and the amount of the light to diffuse alters. Furthermore, the structure has a potential for *multifunctional* utilization. It may present an adjustable space to host a large variety of user activities.



**Figure 5.17:**The light penetration in the structure.





## 6. CONCLUSION

The study presented in the thesis questions how the inherent properties of a specific material can be used to develop a responsive material system that does not require energy or mechanical support to work. The developed responsive composite material is integrated with a computationally developed form to create a specific responsive material system, which is named *Hygro\_Responsive Structure*. In this responsive material system, humidity becomes the movement driver for the responsive material and the sunlight acts as the design driver for form generation.

The responsive material development is conducted through experimental studies. The methodology of this study relies on learning by experiment. The outcomes of the experiments are analyzed and evaluated through empirical and numerical methods. It is worth to mention that the practice and evaluation of the material experiments is specific to this study within the simplified humidity box. In this study, passive layer of the composite becomes anisotropic through the addition of fibers. Another contribution of this study is composite production, effectuated through the manipulation of material properties. Material experiments will be enhanced in furtherance of the study. In the readily conducted experiments, changes in humidity are taken as basis. These experiments can be improved by taking temperature changing and its relation with relative humidity content into consideration. Different wood and polymer types might be experimented to ensure improved material behavior. Moreover, a bilayer material structure will be produced with two different materials, such as a metal type with a wood type.

This experimental study contributes to other studies by encouraging collaborative work. A specific set of experiments is conducted in collaboration with a designer and an engineer who are specialized in material studies. It can therefore be set forth that the experimental study is supported by designing and engineering disciplines. The responsive composite and the simplified humidity box are produced with the contribution of material scientists, each of whom is an expert in their own branch. The evaluation of the conducted material experiments is made through collaborative study: The empirical evaluations are made by the designer and the empirical analysis is justified with the calculations effectuated by the material scientist. The

collaborations form a foundation for further progress of experimental studies in the future.

The responsive material offers many opportunities to design responsive building systems. In this study, a composite material is utilized in the structure, the design process of which is accomplished through computational tools that take environmental parameters as basis. The composite panels are installed in the openings of the structure, the scaling factor of which is modified by attractor points. The variations of the openings' scales affect the size of the panels and therefore influence the responsive behavior. The aim of designing a parametric structure is to change the responsive behavior of the composite material by modifying the form of the structure. The panels respond to changes in humidity, curling inward in humid air and outward in dry air. The construction of the responsive system structure is open to discussions in further studies.

The humidity-driven movement of the panels provides airflow and enables the structure to have natural ventilation without consuming any energy since these results are achieved by utilizing the inherent responsiveness of the wood material. Therefore, the responsive material system can be referred to as an *energy efficient* system which requires neither energy nor mechanical components to work. The responsive material system presents an easily affordable and maintainable alternative with an energy efficient design against the adaptive systems that are activated via mechanical components. In further studies, the material system can be compared to mechanical responsive systems in terms of maintenance, construction costs and energy consumptions. The implementation of responsive material system will be discussed in further studies.

The further research of the study intends to focus on material computation. The material experiments will be expanded. On the ground of the results, the obtained material parameters will be conveyed and material behavior will be simulated in computational environment. The study can be furthered to develop a material computation plug-in to present the material parameters to the user. The user can therefore take initial design decisions based on the material behavior. The computation of material response enables the user to design according to material

parameters. Material and design will have a mutual interaction and become two parts of an integrated system rather than distinct concepts.

Recently, a wide range of researches and numerous experiments were conducted on material system design and computation. The study conducted in the thesis deals with how the inherent properties of material can be explored and employed to achieve. Material is used as a performative object rather than a concept with formative purposes in this study. The main objective is to encourage thinking in the material behavior in responsive design. The thesis study promotes to design a material system integrated with form and environment and enhanced with material computation.





## REFERENCES

- Addington M. and Schodek D.** (2005). *Smart Materials and New Technologies For Architecture and Design Professions*. Architectural Press, Oxford.
- Akos G. and Parsons R.** (2014). *The Grasshopper Primer Third Edition*. Mode Lab. The full text of this document is available here: <http://creativecommons.org/licenses/by-nc-sa/3.0/us/legalcode>.
- Armstrong R.** (2011). *Living Architecture: How Synthetic Biology can Remake our cities and Reshape Our Lives?* (Ted Talks).
- Benyus J.** (2007). *Biomimicry Guild. Innovation Inspired by Nature Work Book*, Biomimicry Guild.
- Burgert I. and Fratzl P.** (2009). Actuation systems in plants as prototypes for Bioinspired devices. *Philosophical Transactions of The Royal Society A*, 367. Retrieved from: <http://rsta.royalsocietypublishing.org/content/367/1893/1541>.
- Burry, M.** (2013). Between Intuition and Process: Parametric Design and Rapid Prototyping, in Kolarevic, B. [ed.] *Architecture in the Digital Age: Design and Manufacturing*. Spon Press, pp. 147-162.
- Colakoglu B., Durmisevic E., and Pasic A.** (2015). *Dynamic Architecture*. University of Twente, University of Sarajevo and Yildiz Technical University, published by University of Twente Netherlands.
- Dawson C, Vincent J.F.V, Rocca A.M** (1997). How pine cones open. Cited from *Actuation systems in plants as prototypes for bio inspired devices*. Burgert I. and Fratzl P. (2009). DOI: 10.1098/rsta.2009.0003. **Cited from Burgert I. and Fratzl P.** (2009). Actuation systems in plants as prototypes for bioinspired devices. *Philosophical Transactions of the Royal Society A*, 367.
- Dunn, N.** (2012). *Digital Fabrication in Architecture*. Laurance King Publishing, London.
- Enhoş, Z.** (2014). *Material Based Computation: Composites for a Responsive Façade Design* (M.Sc. Thesis) Istanbul Technical University, Graduate School of Science Engineering and Technology, İstanbul Turkey.
- Fortmeyer R., Linn C. D.** (2014). *Kinetic Architecture Designs for Active Envelopes*. Australia, The Images Publishing Group.
- Fox M.** (2000). *Sustainable Applications of Intelligent Kinetic Systems*.
- Fox M. and Kemp M.** (2009). *Interactive Architecture*. Princeton Architectural Press. New York.
- Forest Products Laboratory (FPL)**, (1957). United States Department of Agriculture Forest Service. Shrinking and Swelling of Wood in Use. No: 736.
- Forest Products Laboratory (FPL)**, (2010). *Wood Handbook, Wood as an Engineered Material*.
- Fathy, H.** (1986). *Natural Energy and Vernacular Architecture – principles and*

- examples with reference to hot arid climates. Chicago: The University of Chicago Press. **Cited from: Hensel M. U.** (2010). Performance-Oriented Architecture and the Spatial and Material Organization Complex. *FORMakademisk*. Vol.3, Nr.1, pp. 36-56.
- Hensel M. U.** (2013). Material Performance. *Performance-Oriented Architecture: Rethinking Architectural Design and Built Environment, Architectural Design Magazine*. Pp. 59-73.
- Hensel, M. & Sunguroğlu, D.** (2008). Material Performance in *Versatility and Vicissitude Performance in Morpho-Ecological Design, Architectural Design*, Profile No 192 Vol 78 No 2. pp. 34-38.
- Hensel M., Menges A. and Weinstock M.** (2010) Material Systems, Computational Morphogenesis and Performative Capacity. *Emergent Technologies and Design*. Routledge Press, USA and Canada. pp. 43-63.
- Hovsepian, S.,** (2012) Digital Material Skins: For Reversible Reusable Pressel Vessels.
- Holstov A., Bridgens B. & Farmer G.** (2015). *Hygroscopic Materials For Sustainable Responsive Architecture*. Construction and Building Materials 98 pp.570–582. Retrieved from: <[www.elsevier.com/locate/conbuildmat](http://www.elsevier.com/locate/conbuildmat)>.
- Jeronimidis, G.** (2004). Biodynamics. Emergence: Morphogenetic Design Strategies in Architectural Design, 74, pp. 90-96.
- Jodido P.** (2012). *Nouvel*. Taschen Press: Köln. (pp. 26-32).
- Kolarevic B, and Parlac V.** (2016). Architecture of Change Adaptive Building Skins. In Kanaani and Kopec (Eds). *Routledge Companion for Architectural Design and Practice* (pp. 223-238). Routledge Press. New York.
- Kotnik, T. & Weinstock, M.** (2012). Material, Form and Force, *Material Computation in Architectural Design*, 216, pp. 104-112.
- Kremsa, Nakagi, Santigo** (2009). Cited from Menges, Correa, Reichert (2014). Meteorosensitive architecture: biomimetic building skins based on materially embedded and hygroscopically enabled responsiveness.
- Larsen K. E. and Marstein N.,** (2000). Conservation of Historic Timber Structures: An Ecological Approach, Butterworth-Heinemann, Oxford. **Cited from: Holstov A., Bridgens B. & Farmer G.** (2015). *Hygroscopic Materials for Sustainable Responsive Architecture*. Construction and Building Materials 98 pp.570–582.
- Maragkoudaki, A.** (2013). No-Mech Kinetic Responsive Architecture, Kinetic Responsive Architecture with no mechanical parts. 9th International Conference on Intelligent Environments. (pp. 145-150).

- Meagher M.** (2015). Designing for change: The poetic potential of responsive architecture. *Frontiers of Architectural Research*, pp. 159-165.
- Menges, A.** (2008a). 'Inclusive Performance Efficiency Versus Effectiveness Towards a Morphoecological Approach' *Versatility and Vicissitude Performance in Morpho-Ecological Design*, in *Architectural Design*, vol. 78, p. 56.
- Menges, A.** (2008b). 'Responsive Surface Structures: Instrumentalising Moisture-Content Activated Dimensional Changes of Timber Components' *Versatility and Vicissitude Performance in Morpho-Ecological Design in Architectural Design*, 192. pp. 39-41.
- Menges, A.** (2008c). 'Integral Formation and Materialisation: Computational Form and Material Gestalt' in B. Kolorevic and K. Klinger (Eds) *Manufacturing Material Effects: Rethinking Design and Making in Architecture*, Taylor & Francis Books (New York), pp. 195-210).
- Menges, A.** (2012a). 'Material Computation Higher Integration in Morphogenetic Design' *Material Computation, Architectural*, 216. pp. 16-21.
- Menges A.** (2012b). Material Resourcefulness: Activating Material Information in Computational Design. *Material Computation, Architectural Design*, pp. 34-43.
- Menges A., Fleischmann M., Knippers J., Lienhard J. and Schleicher S.** (2012). Material Behavior. *Material Computation in Architectural Design*, 216, pp. 44-50.
- Menges A. & Reichert S.** (2012). Material Capacity: Embedded Responsiveness, *Material Computation, Architectural Design* pp.52–59.
- Menges A.** (2014). 'Hygroscope: Meteorosensitive Morphology'. In *Volo 6: Digital and Parametric Architecture (2014) edited by Aiello C.* pp. 51-52.
- Menges A., Reichert S. and Correa D.,** (2014). Meteorosensitive architecture: biomimetic building skins based on materially embedded and hygroscopically enabled responsiveness, *Computer Aided Design, Vol. 60*, pp. 50-69.  
Retrieved from:  
<http://www.sciencedirect.com/science/article/pii/S0010448514000438>
- Mindell D.A.** (2000). Cybernetics Knowledge Domains in Engineering Systems.
- Nordenson G.** (1995) "Three Engineers (Sitting around Talking)," In Cynthia Davidson. *ANY: Architecture New York* no. 10. **Cited from: Fox M. and Kemp M.** (2009). *Interactive Architecture*. Princeton Architectural Press. New York.
- Ou, Jifei.** (2014). *Material Transformation: Designing Shape Changing Interfaces*

*Enabled by Material Anisotropy* (M.Sc. Thesis), Massachusetts Institute of Technology (MIT), Master in Media Arts and Sciences, Massachusetts USA.

**Oxman, N.** (2012). Programming Matter, *Material Computation in Architectural Design*, 216, pp. 88-96.

**Oxman, N.** (2010). *Material-based Design Computation* (Phd Thesis), Massachusetts Institute of Technology (MIT), Doctor of Philosophy in Architecture: Design and Computation, Massachusetts USA.

**Reyssat E. and Mahadevan L.** (2009). Hygromorphs: from pinecones to biomimetic bilayers, *Journal of Society Interface* 6<sup>th</sup> University, Cambridge USA, pp. 951-957.

**Sample H.** (2012). *ABrise- Soleil Without a Building. Matter: Material Processes in Architectural Production*, ed. Gail Peter Borden and Michael Meredith. Oxon: Routledge, p. 332.

**Schröpfer T.** (2012). *Material Design Informing by Materiality*, Birkhauser, Basel, pp. 164-171.

**Sterk T. D.** (2004). Using Actuated Tensegrity Structures to Produce a Responsive Architecture, *ACADIA22, Connecting Crossroads of Digital Discourse*, pp. 85-95.

**Sung, D. K.** (2012). *TED Talk: Metal that breathes*. LastRetrieved in 27.01.2016 from: [http://www.ted.com/talks/doris\\_kim\\_sung\\_metal\\_that\\_breathes](http://www.ted.com/talks/doris_kim_sung_metal_that_breathes)

**Sung, D.K.** (2014). 'Digital Architecture at DOSU Studio', in *eVolo 6: Digital and Parametric Architecture (2014)* edited by Aiello C. pp. 110-114.

**Url-1:** <<http://openarchitectures.com/2011/10/27/an-interview-with-nicholas-negroponete/>>, date retrieved 20.04.2016.

**Url-2:** <<http://cyberneticzoo.com/robots-in-art/1969-70-seek-nicholas-negroponete-american/>>, date retrieved 20.04.2016.

**Url-3:** <<http://www.interactivearchitecture.org/fun-palace-cedric-price.htm>>, date retrieved 21.04.2016.

**Url-4:** <<http://www.archdaily.com/162101/ad-classics-institut-du-monde-arabe-jean-nouvel>>, date retrieved 21.04.2016.

**Url-5:** <<https://www.arduino.cc/>>, date retrieved 24.04.2016.

**Url-6:** <<https://www.arduino.cc/en/Main/ArduinoBoardUno>>, date retrieved 20.04.2016.

**Url-7:** <<https://www.tes.com/lessons/WWwCpNw9OdO1vQ/chapter-7-mems->



- technology*>, date retrieved 21.04.2016.
- Url-8:** <<http://www.techietonics.com/futuretech-tonics/mems-can-be-used-for-creating-seismic-network.html>>, date retrieved 21.04.2016.
- Url-9:** Al- Bahar responsive unit <<http://www.archdaily.com/270592/al-bahar-towers-responsive-facade-aedas>>.date retrieved 2.05.2016.
- Url-10:** smart material <<https://materia.nl/article/smart-materials-for-architecture/>>date retrieved 20.01.2017.
- Url-11:** smart material <<https://materia.nl/article/material-xperience-first-day-preview/>> date retrieved 20.01.2017.
- Url-12:** smart material <<http://www.carnorama.com/1225/automotive-smart-memory-materials/>>date retrieved 20.01.2017.
- Url-13:** optical fiber <<https://global.britannica.com/science/fiber-optics>>, date retrieved 20.08.2016.
- Url-14:** Reef installation <<http://www.reefseries.com/index.php?/media/project-information/>>, date retrieved 20.08.2016.
- Url-15:** Reef installation <<http://www.radical-craft.com>>, date retrieved 20.08.2016.
- Url-16:** Shape shift <<http://caad-eap.blogspot.com.tr>>, date retrieved 20.08.2016.
- Url-17:** Responsive Surface. Achim Menges. <http://icd.uni-stuttgart.de/?p=5655> , date retrieved 15.02.2016.
- Url-18:** Microstructural Manipulation. Jose Ahedo.  
<<http://www.achimmenges.net/?p=4852>>, date retrieved 20.01.2017
- Url-19:**HygroScope: Meteorosensitive Morphology. Menges Achim & Reichert Steffen. <<http://www.achimmenges.net/?p=5083>> ,date retrieved 26.01.2016.
- Url-20:** Bloom. Doris Kim Sung. <<http://www.designboom.com/architecture/doris-sung-bloom-at-materials-applications/>> , date retrieved 27.01.2016.
- Url-21:** Bloom. Doris Kim Sung. <<http://dosu-arch.com/bloom.html>>date retrieved 27.01.2016.
- Url-22:** Tracheolis. Doris Kim Sung. <<http://dosu-arch.com/tracheolis.html>>date retrieved 27.01.2016.
- Url-23:** Distortions of wood due to shrinkage and swelling.  
<<https://global.britannica.com/science/wood-plant-tissue/images-videos>>, date retrieved 20.02.2017.

- Url-24:** <<http://matsysdesign.com/studios/compositebodies/tag/mashrabiya/>>, date retrieved 12.09.2016.
- Url-25:** <<https://www.youtube.com/watch?v=AdYDsIhy2VU>>, date retrieved 28.10.2016.
- Url-26:** <<http://www.doogeveneers.com/specifying-veneer/veneer-cuts>>, date retrieved 20.09.2016.
- Url-27:** <<https://github.com/mostaphaRoudsari/Ladybug#licence>> date retrieved 20.10.2016.
- Url-28:** <<http://www.food4rhino.com/project/fabtools?etx>>, date retrieved 20.02.2016.
- Url-29:** <<http://sustainabilityworkshop.autodesk.com/buildings/psychrometric-charts>> date retrieved 24.06.2016.
- Velikov K. and Thün G.** (2012). Design and Construction of High Performance Homes: Building Envelopes, Renewable Energies and Integrated Practice. Chapter 1.3: Responsive Building Envelopes, Routledge Press: London, UK; pp. 75–92.
- Viray, E.** (2010). Why Material Design. *Material Design Informing by Materiality* edited by Thomas Shröpfer, Birkhauser, Basel, pp. 8-9.
- Weinstock, M.** (2008). ‘Metabolism and Morphology’, *Versatility and Vicissitude Performance in Morpho-Ecological Design, Architectural Design*, Profile No 192 Vol 78 No 2. pp. 26-33.
- Winandy J. E.** (1994). Wood Properties, Arntzen, Charles J., (Ed.) *Encyclopedia of Agricultural Science. Orlando, FL: Academic Press, Vol. 4*, pp. 549-561.
- Yiannoudes, S.** (2010). Kinetic Digitally- driven Architectural Structures as ‘Marginal’ Objects - a Conceptual Framework, *Footprint Delft Architectural Theory Journal, Issue 6*, (pp 41-53).

## **APPENDICES**

**APPENDIX A.1:** Shape transformation process of oak wood veneer.

**APPENDIX A.2:** Shape transformation process of teak and balsa wood veneer.

**APPENDIX B:** Arduino code to control the actuation period of the fan.

**APPENDIX C:** Calculation for the curvature change radius

**APPENDIX D.1:** Experiment 1 for testing polymer types

**APPENDIX D.2:** Experiment 1 for testing polymer types

**APPENDIX E.1:** Experiment 2 for testing wood types

**APPENDIX E.2:** Experiment 2 for testing wood types

**APPENDIX F:** Experiment 3 for testing grain direction

**APPENDIX G.1:** Experiment 4 for testing fibered polymer layers

**APPENDIX G.2:** Experiment 4 for testing fibered polymer layers

**APPENDIX H:** Bending (curving) simulation of the composite material

**APPENDIX I:** Ladybug definition of sunlight analysis

**APPENDIX J:** Form development according to attractor points

**APPENDIX K:** Grasshopper definition of puzzle joint method

**APPENDIX L:** Grasshopper definition of finger joint detail

**APPENDIX M:** Grasshopper definition of unfolding and labelling the units

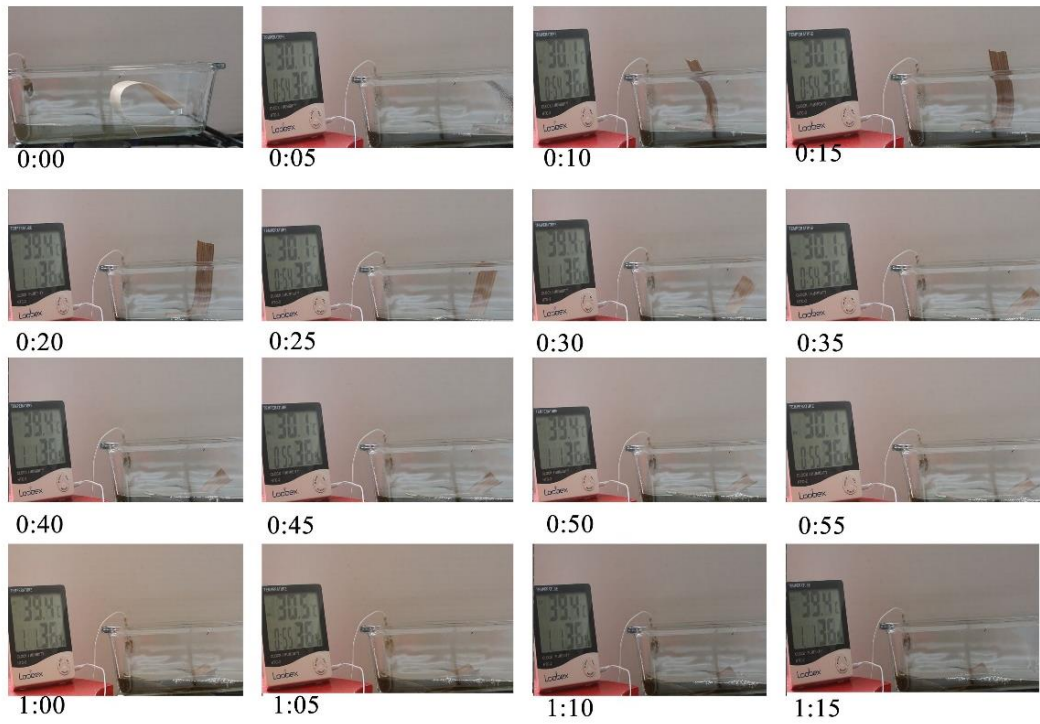
**APPENDIX A**

**EXPERIMENT-1: Oak wood tangential**

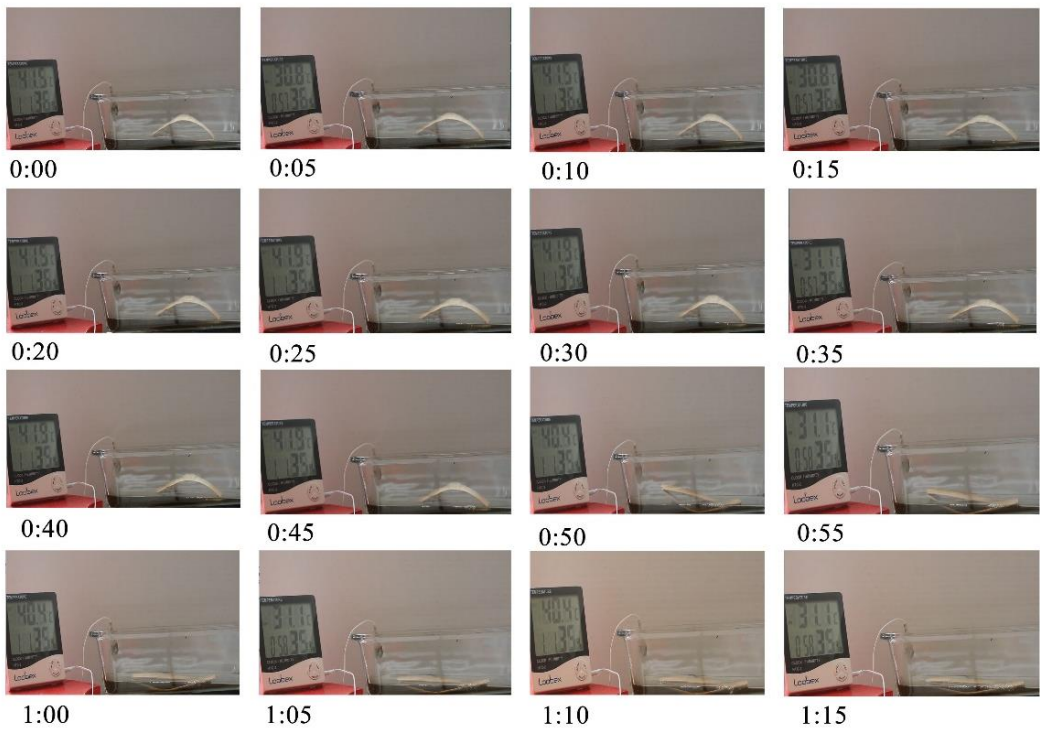


**Figure A.1:**Experiment to test shape transformation process of oak veneer sample.

Wood type: Teak wood (Hardwood) Grain direction: Radial



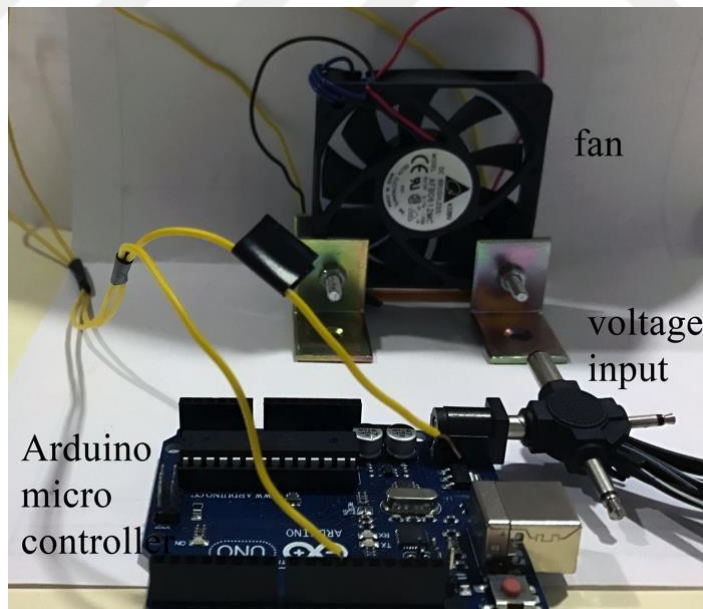
Wood type: Balsa wood (Hardwood) Grain direction: Longitudinal



**Figure A.2:** Experiment to test shape transformation process of oak veneer sample.

## APPENDIX B

```
int led=11; // location of the pin of the fan which we connect
void setup()//
{
pinMode(fan,OUTPUT);
}
void loop() //to start the loop
{
digitalWrite(fan, HIGH); //to activate the fan
delay(5000); //to activate the fan in 5000ms
digitalWrite(led, LOW); //to stop the fan
delay(30000); //to delay the activation of the fan in 3000s
}
//
```



**Figure B.1:** The fan connection with Arduino components.

## APPENDIX C 4.1

### Experiment 1: Testing different polymer types

$$m = \frac{t_p}{t_a} = \frac{\text{thickness passive l.}}{\text{thickness active l.}} ; \quad n = \frac{e_p}{e_a} = \frac{\text{elasticity coef. passive l.}}{\text{lasticity coef. active l.}} ;$$

$$f(m, n) = \frac{6(1 + m)^2}{3(1 + m^2) + (1 + m \cdot n) \left( m^2 + \frac{1}{m \cdot n} \right)}$$

$$\text{For } P_1 \text{ (Petg+beech)} \quad m_1 = \frac{0,8mm}{0,45mm} = 1,78 \text{ mm} \quad n_1 = \frac{2,9 \text{ Gpa}}{15 \text{ Gpa}} = 0,19 \text{ Gpa}$$

$$\text{For } P_1 \quad f(m, n) = \frac{6(1+1,78)^2}{3(1+1,78^2)+(1+1,78 \cdot 0,19) \left( 1,78^2 + \frac{1}{1,78 \cdot 0,19} \right)} = 1,48$$

$$\text{For } P_2 \text{ (Pvc+beech)} \quad m_2 = \frac{0,65mm}{0,45mm} = 1,44 \text{ mm} \quad n_2 = \frac{3,25 \text{ Gpa}}{15 \text{ Gpa}} = 0,22 \text{ Gpa}$$

$$\text{For } P_2 \quad f(m, n) = \frac{6(1+1,44)^2}{3(1+1,44^2)+(1+1,44 \cdot 0,22) \left( 1,44^2 + \frac{1}{1,44 \cdot 0,22} \right)} = 1,44$$

$$\text{For } P_3 \text{ (Pc+beech):} \quad m_3 = \frac{0,95mm}{0,45mm} = 2,11 \text{ mm} \quad n_3 = \frac{2,2 \text{ Gpa}}{15 \text{ Gpa}} = 0,15 \text{ Gpa}$$

$$\text{For } P_3 \quad f(m, n) = \frac{6(1+2,11)^2}{3(1+2,11^2)+(1+2,11 \cdot 0,15) \left( 2,11^2 + \frac{1}{2,11 \cdot 0,15} \right)} = 1,49$$

**The experiment result:  $P_3 < P_1 < P_2$**

### Experiment 2: Testing different wood types

$$m = \frac{t_p}{t_a} = \frac{\text{thickness passive l.}}{\text{thickness active l.}} ; \quad n = \frac{e_p}{e_a} = \frac{\text{elasticity coef. passive l.}}{\text{lasticity coef. active l.}} ;$$

$$f(m, n) = \frac{6(1 + m)^2}{3(1 + m^2) + (1 + m \cdot n) \left( m^2 + \frac{1}{m \cdot n} \right)}$$

$$\text{For } 1P_2 \text{ (maple+pvc)} \quad m_1 = \frac{0,15mm}{0,6mm} = 0,25 \text{ mm} \quad n_1 = \frac{3,25 \text{ Gpa}}{12 \text{ Gpa}} = 0,27 \text{ Gpa}$$

$$f(m, n) = \frac{6(1+0,25)^2}{3(1+0,25^2)+(1+0,25 \cdot 0,27) \left( 0,25^2 + \frac{1}{0,25 \cdot 0,27} \right)} = 0,457 \cong \mathbf{0,46}$$

$$\text{For } 2P_2 \text{ (ash+pvc)} m_2 = \frac{0,15\text{mm}}{0,6\text{mm}} = 0,25 n_2 = \frac{3,25 \text{ Gpa}}{12,2\text{Gpa}} = 0,271 \cong 0,27$$

$$f(m, n) = \frac{6(1+0,25)^2}{3(1+0,25^2) + (1+0,25 \cdot 0,27) \left(0,25^2 + \frac{1}{0,25 \cdot 0,27}\right)} = 0,451 \cong \mathbf{0,45}$$

$$\text{For } 3P_2 \text{ (beech+pvc)} m_3 = \frac{0,15\text{mm}}{0,45\text{mm}} = 0,33 n_3 = \frac{3,25 \text{ Gpa}}{15\text{Gpa}} = 0,217 \cong 0,22$$

$$f(m, n) = \frac{6(1+0,25)^2}{3(1+0,25^2) + (1+0,25 \cdot 0,22) \left(0,33^2 + \frac{1}{0,22 \cdot 0,22}\right)} = 0,525 \cong \mathbf{0,52}$$

$$\text{For } 4P_2 \text{ (oak+pvc)} m_4 = \frac{0,15\text{mm}}{0,6\text{mm}} = 0,25 n_4 = \frac{3,25 \text{ Gpa}}{11,9\text{Gpa}} = 0,273 \cong 0,27$$

$$f(m, n) = \frac{6(1+0,25)^2}{3(1+0,25^2) + (1+0,25 \cdot 0,27) \left(0,25^2 + \frac{1}{0,25 \cdot 0,27}\right)} = \mathbf{0,46}$$

**The experiment result:  $3P_2 > 1P_2 > 2P_2 > 4P_2$**

*The radius of curvature of the composite which has optimum material parameters;*

$$K = \frac{1}{R} = \frac{\Delta\alpha \cdot f(m, n) \cdot \Delta MC'}{t_{total}} + \frac{1}{R_0}$$

$$\alpha_{beech} = \%11.9 = 0.119 \Delta\alpha = \alpha_{beech} - \alpha_{pvc} = 0.119 - 0 = 0.119$$

$$\Delta MC = \%80 - \%40 = \%40 = 0,4 \quad R_0 = \infty \frac{1}{R_0} = \frac{1}{\infty} = 0$$

$$t_{beech} = 0.6 \text{ mm} \quad t_{pvc} = 0.15 \text{ mm} \quad t_{total} = 0.75 \text{ mm}$$

$$\text{For } 3P_2 \text{ (beech+pvc)} m_3 = \frac{0,15\text{mm}}{0,45\text{mm}} = 0,33 n_3 = \frac{3,25 \text{ Gpa}}{15\text{Gpa}} = 0,22$$

$$f(m, n) = \frac{6(1+0,33)^2}{3(1+0,33^2) + (1+0,33 \cdot 0,22) \left(0,33^2 + \frac{1}{0,33 \cdot 0,22}\right)} = 0,52$$

$$K = \frac{1}{R} = \frac{\Delta\alpha \cdot f(m, n) \cdot \Delta MC'}{t_{total}} + \frac{1}{R_0} = \frac{0,119 \cdot 0,52 \cdot 0,4}{0,60} + 0 = 0,041253$$

$$0,041253 = \frac{1}{R} \quad R = \frac{1}{0,041253} = 24,24066 \cong 24,2$$





APPENDIX D

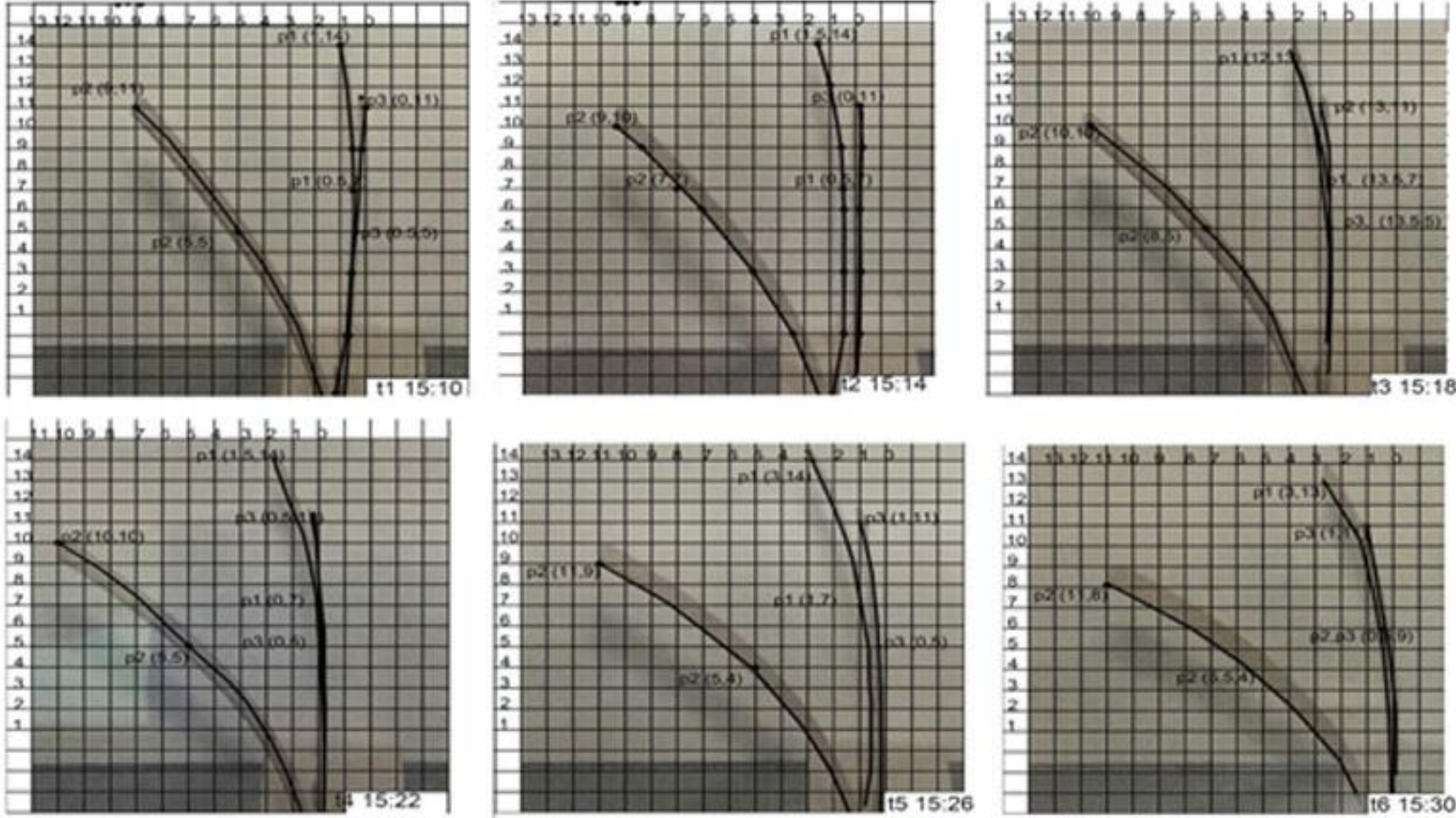
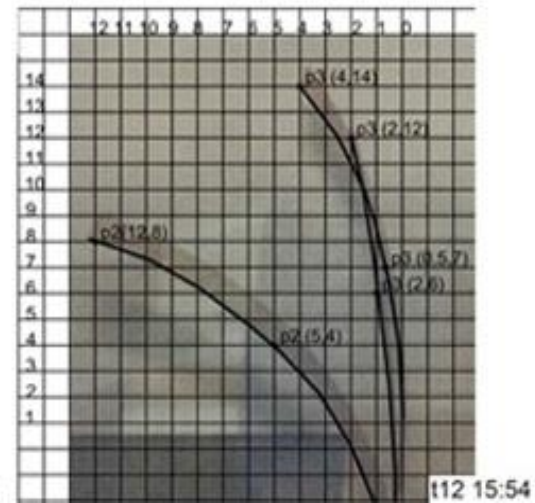
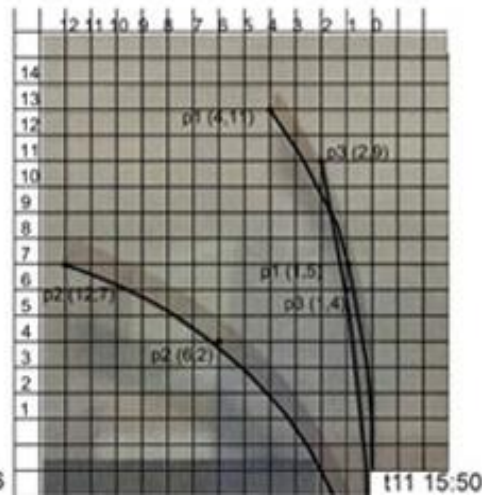
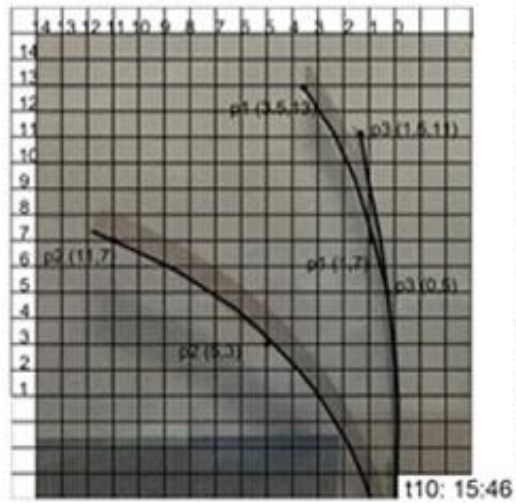
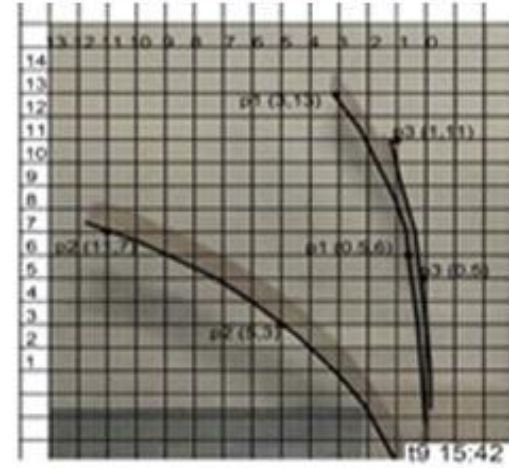
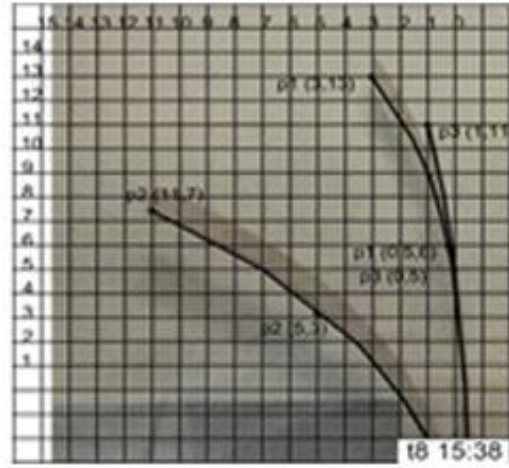
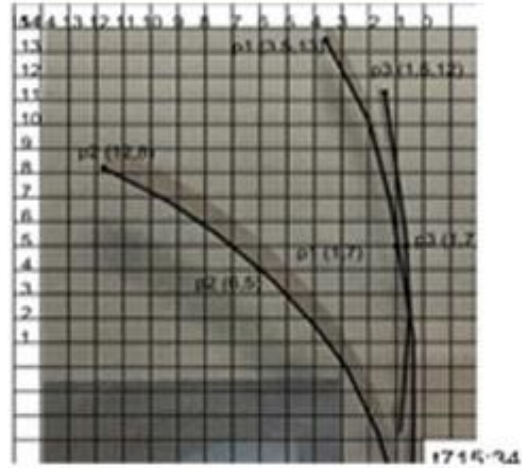
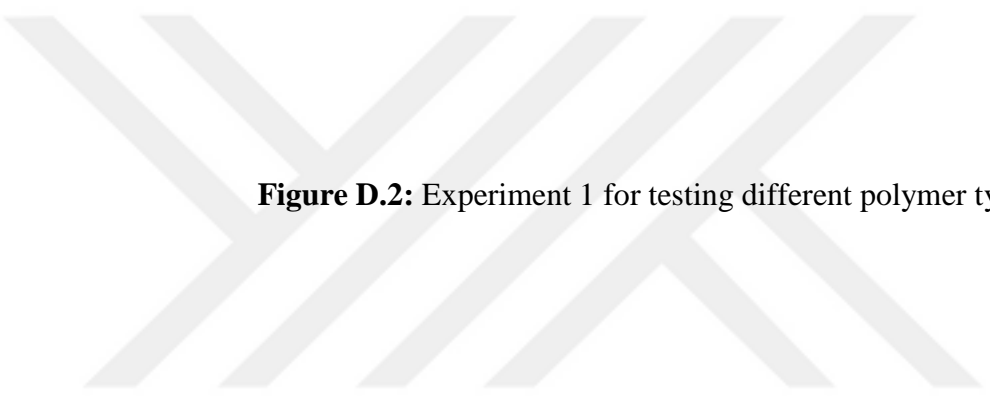
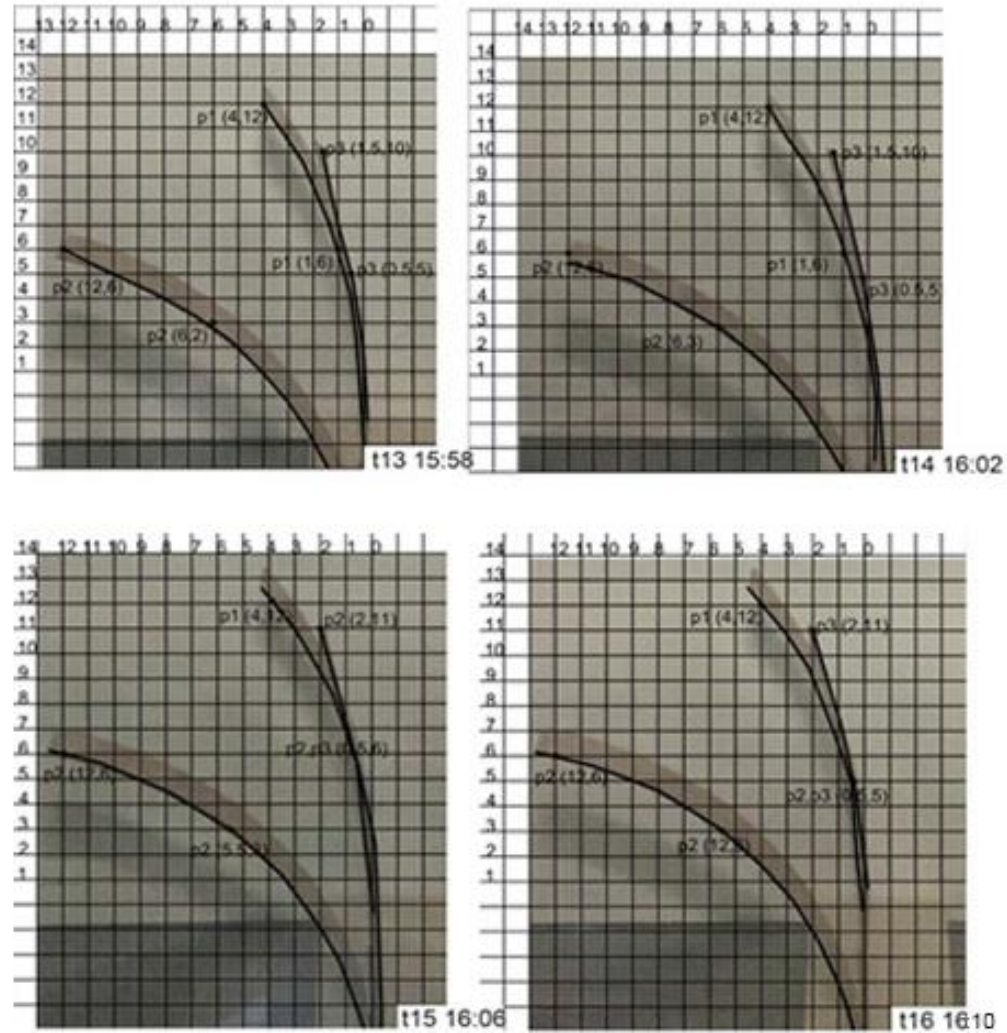


Figure D.1: Experiment 1 for testing different polymer types ( $P_2$ (PVC) $\succ$  $P_1$ (PETG) $\succ$  $P_3$ (PC)).





**Figure D.2:** Experiment 1 for testing different polymer types ( $P_2$  (PVC) $>P_1$ (PETG) $>P_3$ (PC)).



**Figure D.3:** Experiment 1 for testing different polymer types ( $P_2$  (PVC) $\gg P_1$  (PETG) $\gg P_3$  (PC)).



APPENDIX E.1

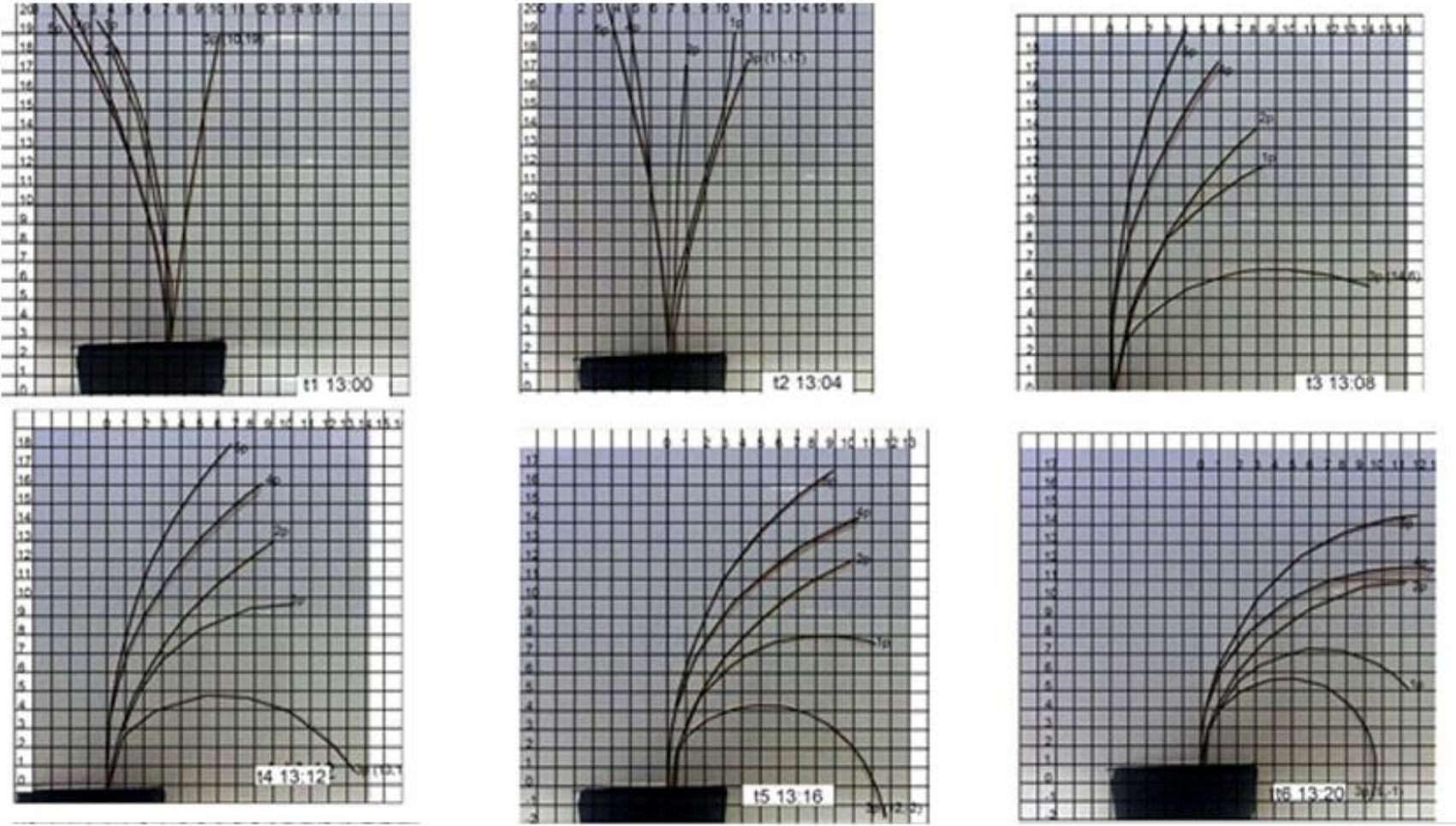
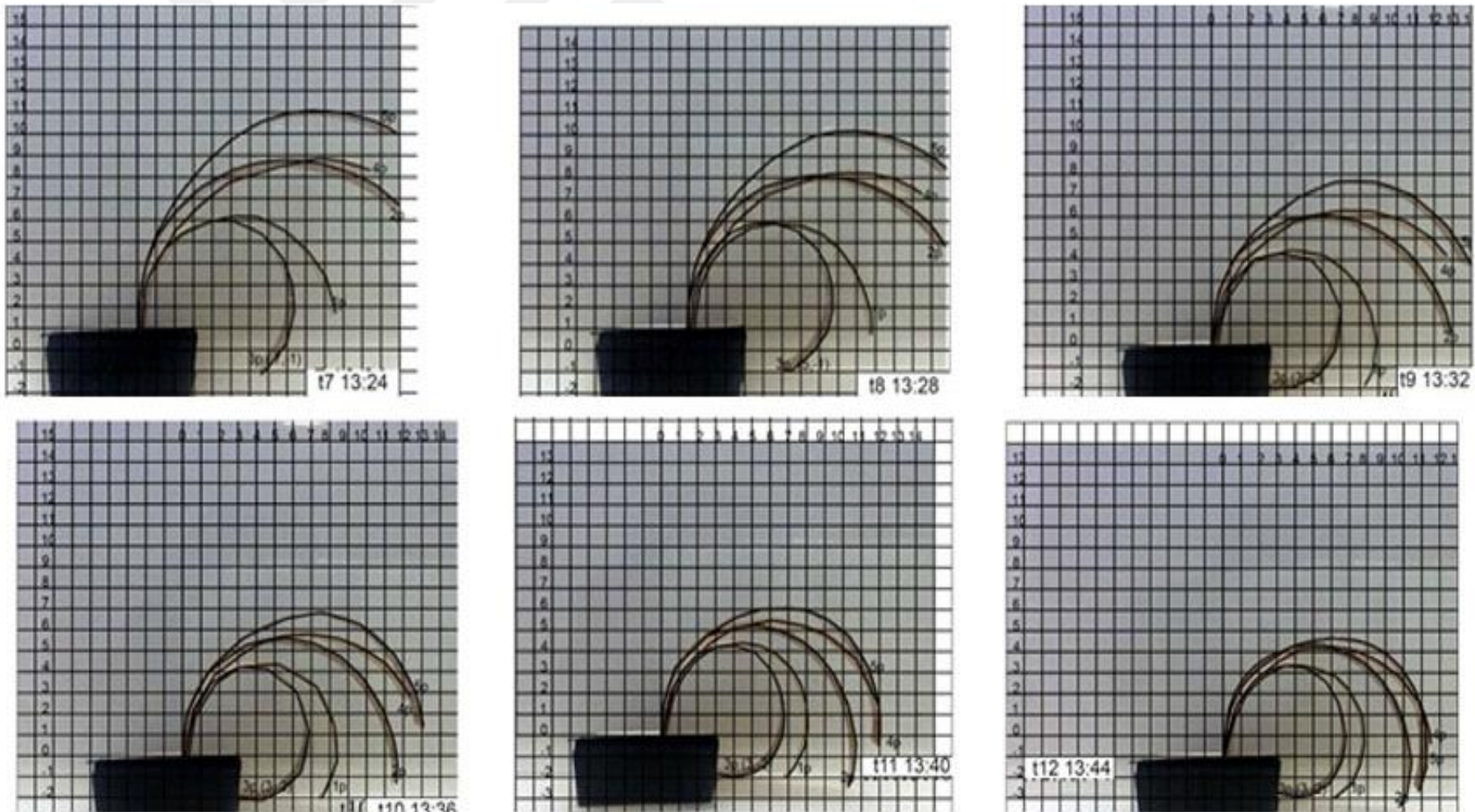
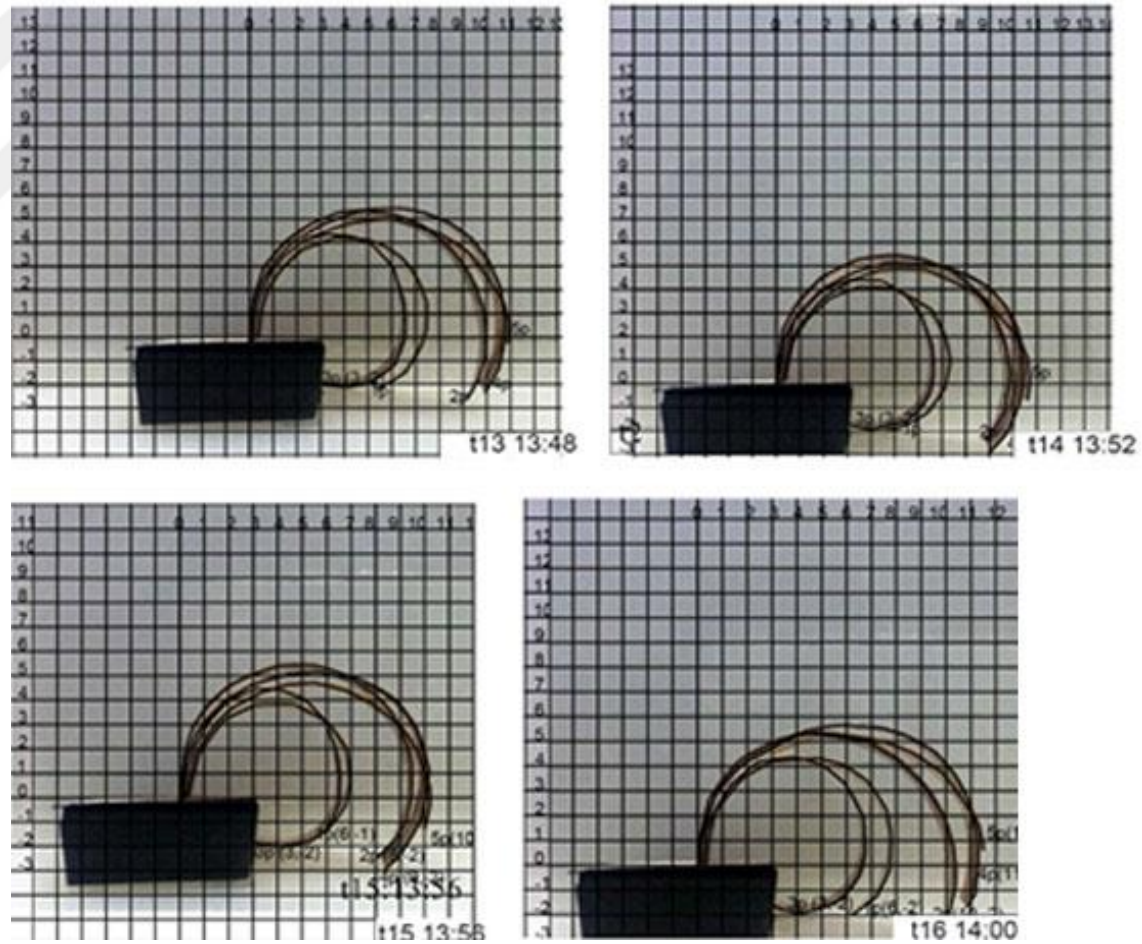


Figure E.1: Experiment 2 for testing different wood types (3P<sub>2</sub>(beech)>1P<sub>2</sub>(maple)>2P<sub>2</sub>(ash)>4P<sub>2</sub>(oak)).

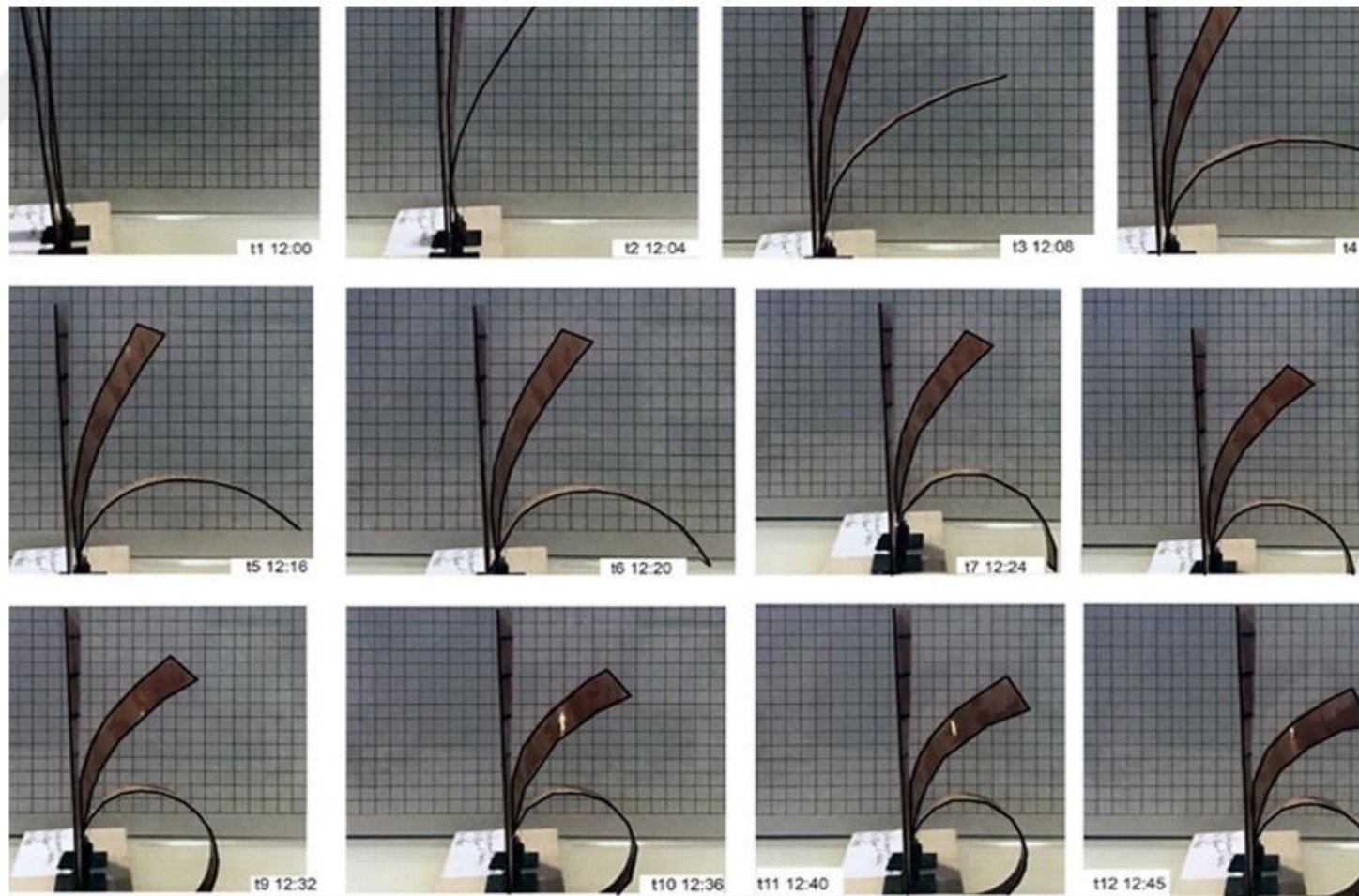


**Figure E.2:** Experiment 2 for testing different wood types (3P<sub>2</sub> (beech)>1P<sub>2</sub>(maple)>2P<sub>2</sub> (ash)> 4P<sub>2</sub>(oak)).



**Figure E.3:** Experiment 2 for testing different wood types (3P<sub>2</sub>(beech)>1P<sub>2</sub>(maple)>2P<sub>2</sub>(ash)>4P<sub>2</sub>(oak)).

## APPENDIX F



**Figure F.1:** Experiment 3 for testing polymer types ( $3D_2$  (perpendicular)  $>$   $3D_1$  (parallel)  $>$   $3D_3$  (diagonal)).





APPENDIX G

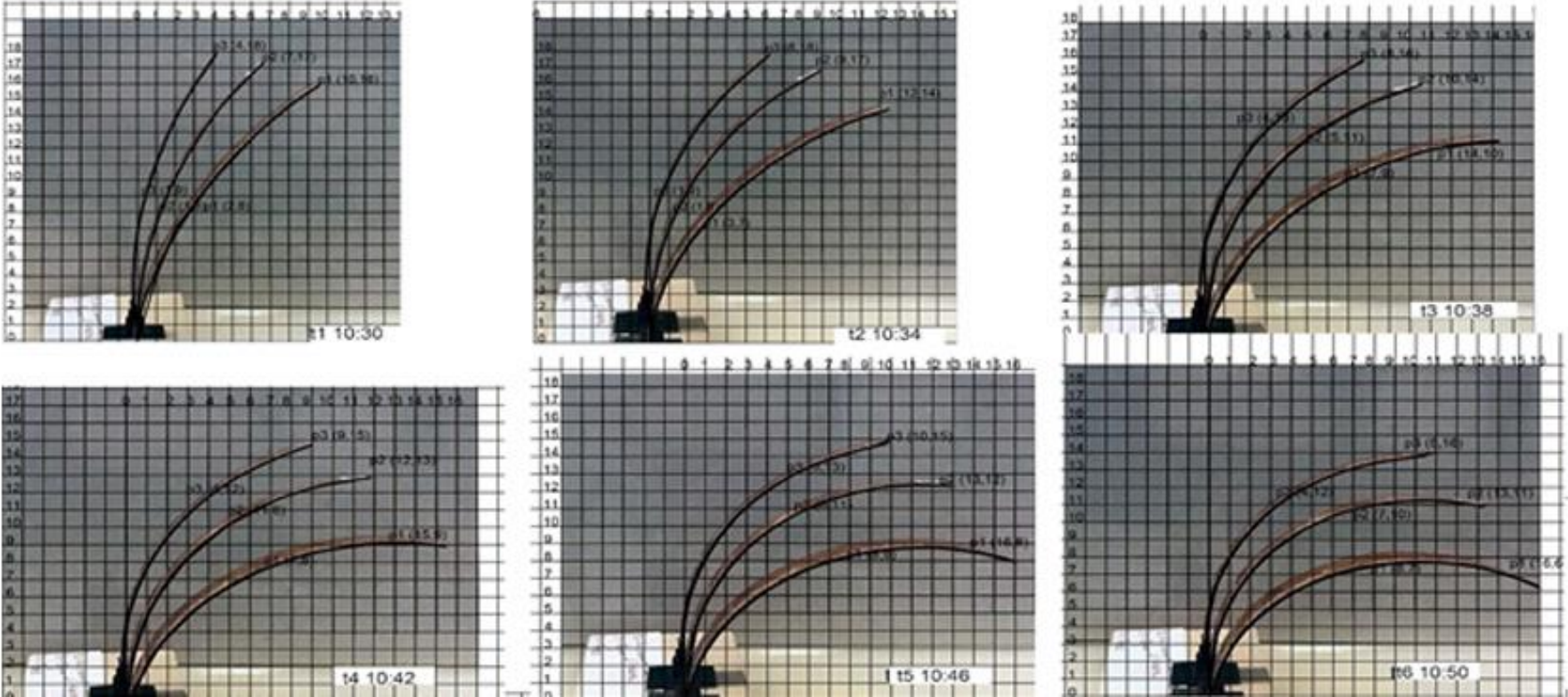
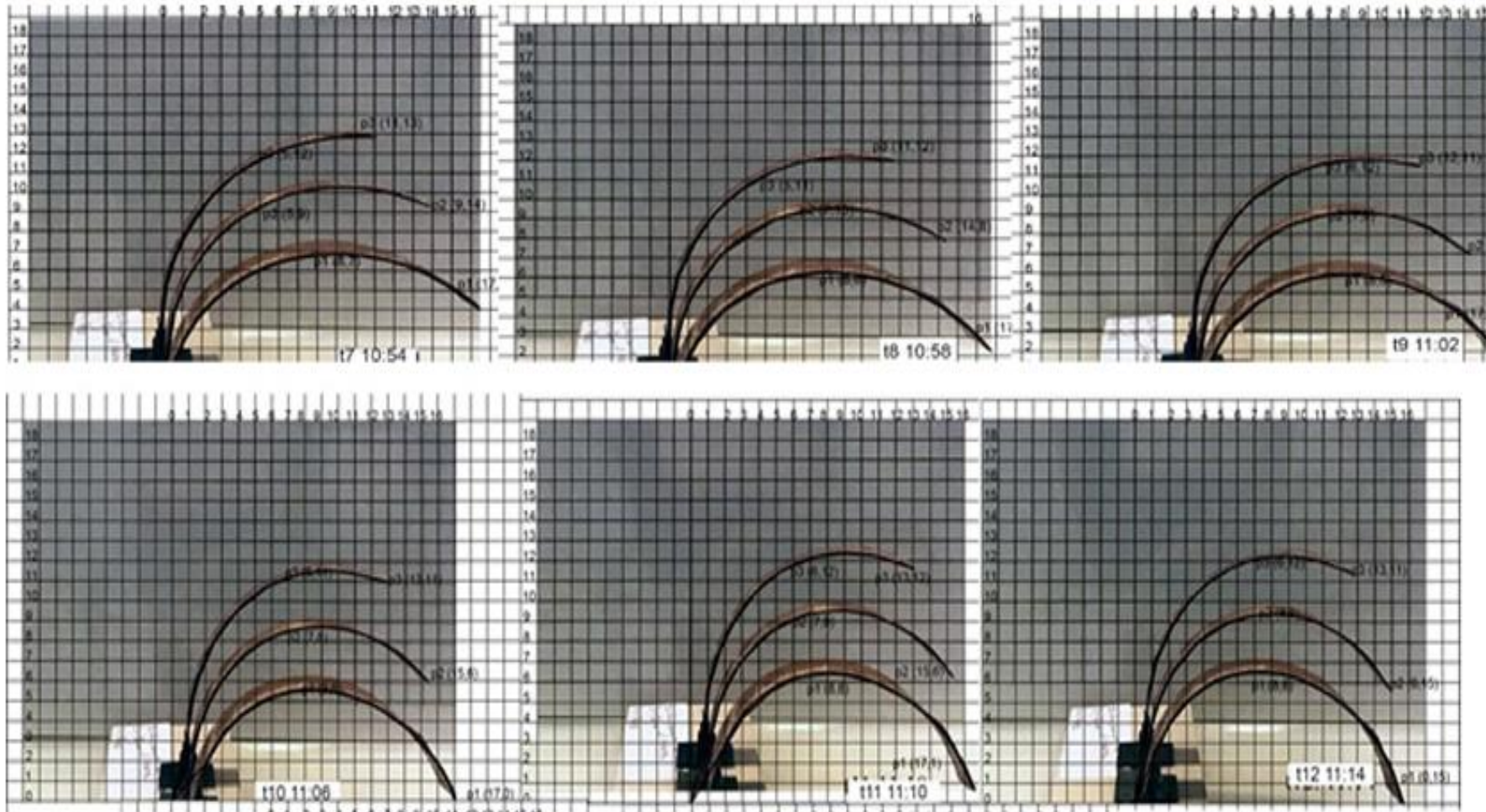
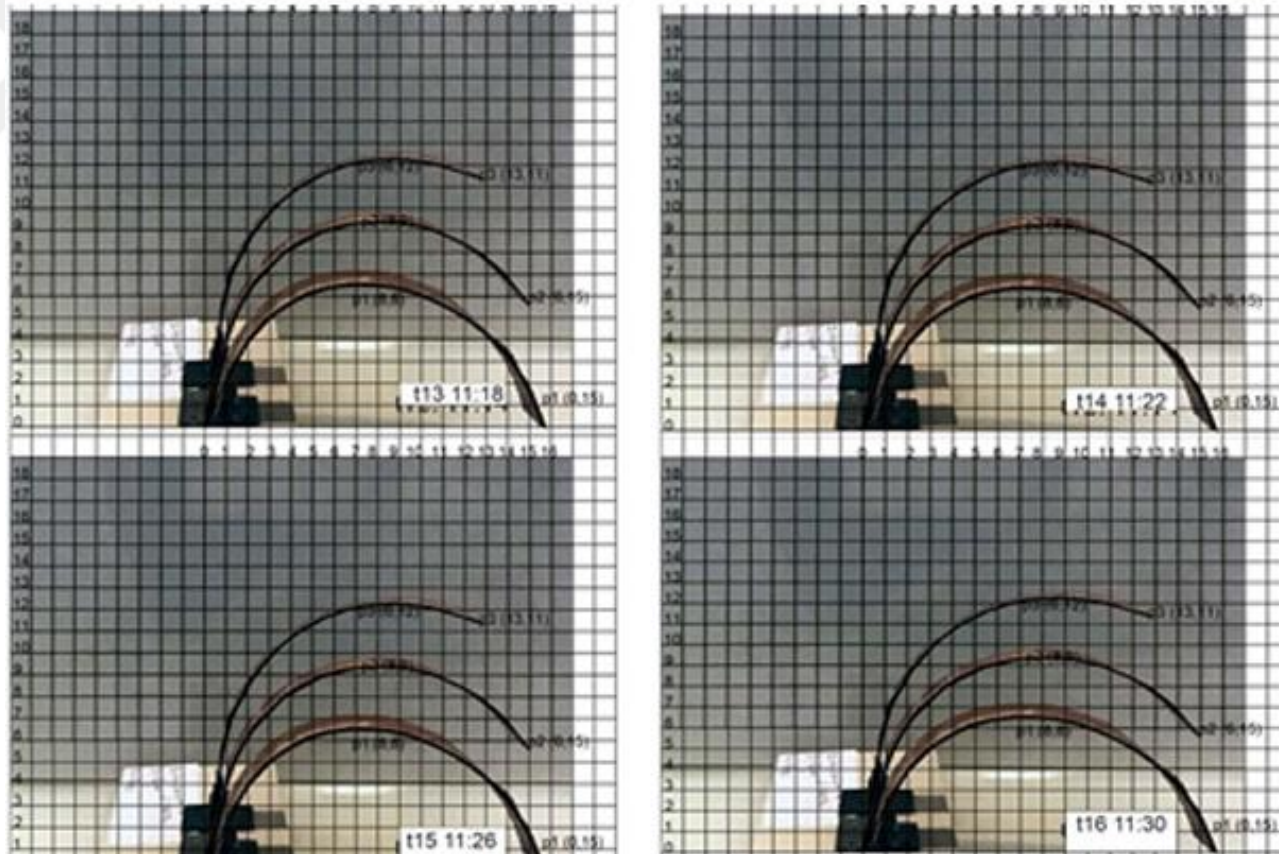


Figure G.1: Experiment 4 testing fibered polymer ( $3G_1$  (dist. 2.5mm) $>3G_2$  (dist. 5 mm) $>3G_3$ (dist. 10mm)).

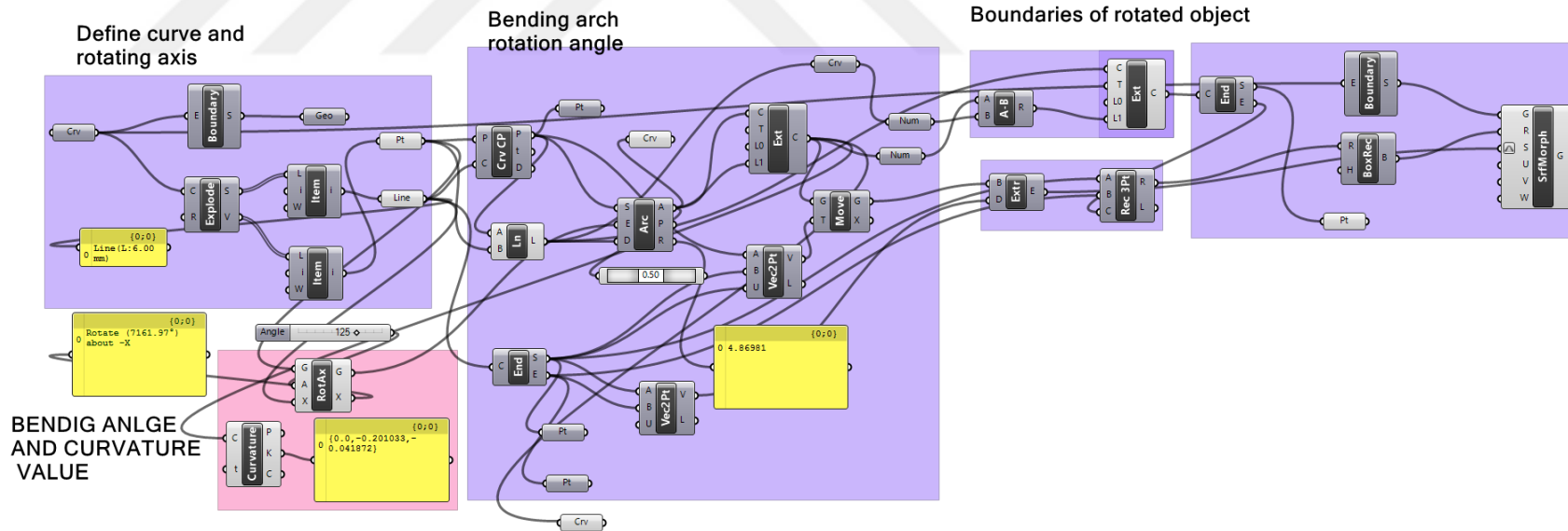


**Figure G.2:** Experiment 4 testing fibered polymer ( $3G_1$  (dist. 2.5mm) $>3G_2$  (dist. 5 mm) $>3G_3$ (dist. 10mm)).



**Figure G.3:** Experiment 4 testing fibered polymer ( $3G_1$  (dist. 2.5mm) $>3G_2$  (dist. 5 mm) $>3G_3$ (dist. 10mm)).

## APPENDIX H

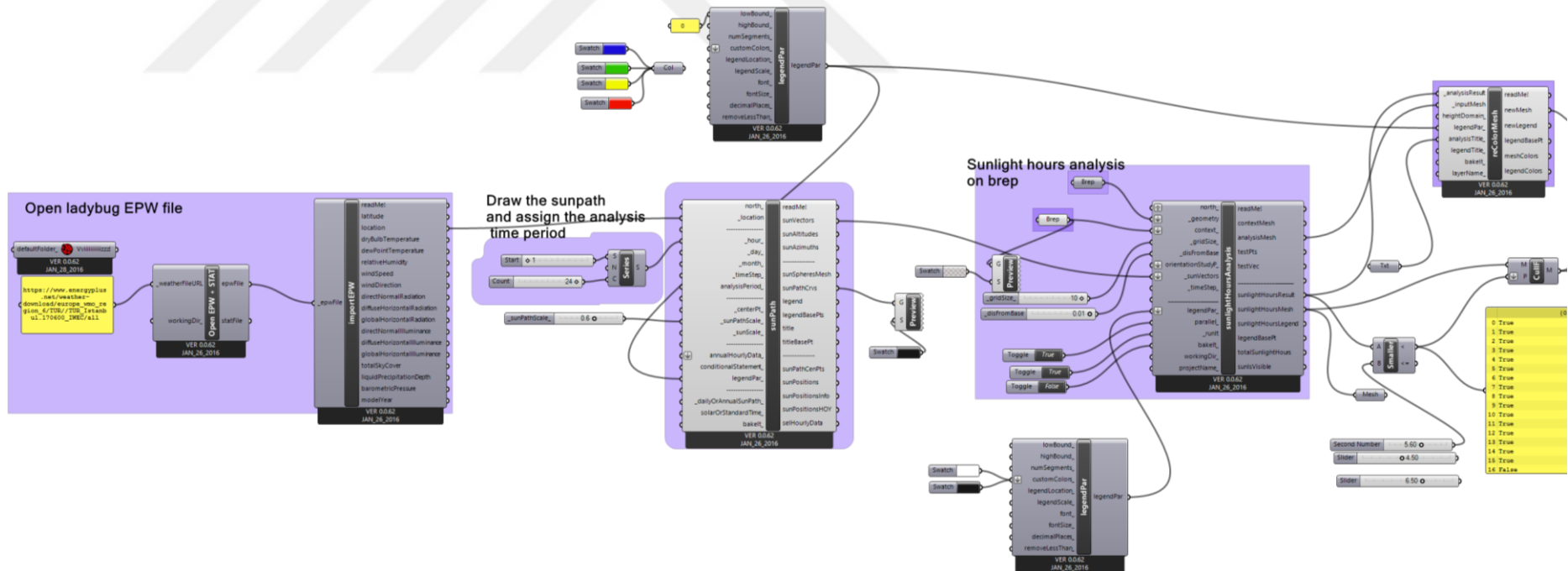


**Figure H.1:** Bending (curving) simulation of the composite material.

**The algorithmic process in Grasshopper:** Finding hinge line and top points of the curve/ Rotate curve on the line/ Draw an arch to define rotation axis/ Find the start and end points of the curve/ Draw rectangle box to identify the rotating borders/ morph the surface in these borders. The maximum curvature (K) is obtained by bending approximately 125° through component analysis component<sup>7</sup>.

<sup>7</sup>Reference for Grasshopper code: <http://www.designcoding.net/bend/>

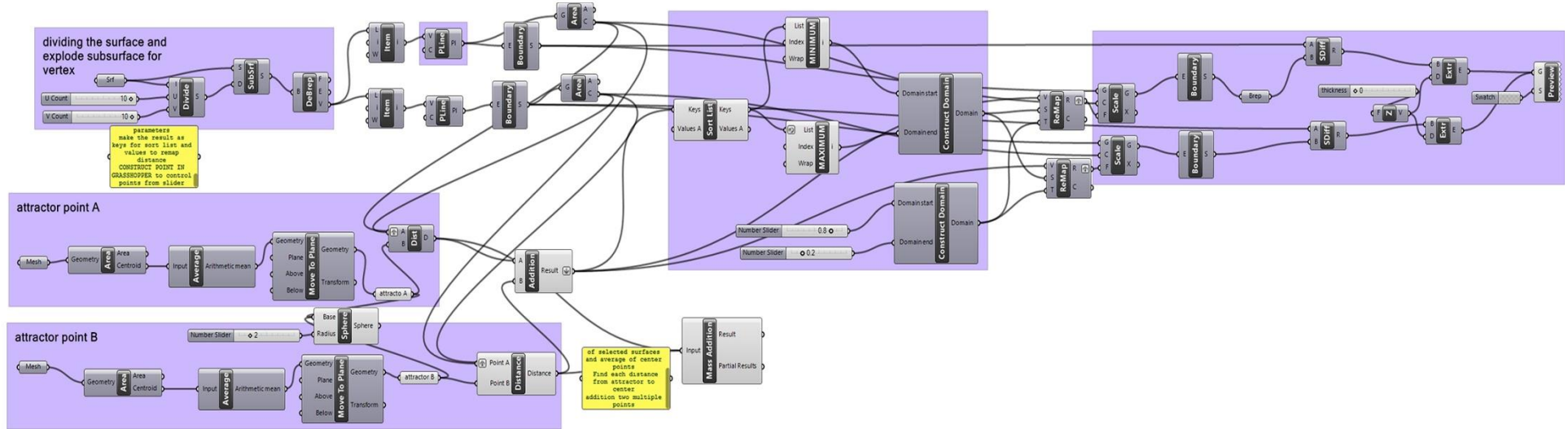
## APPENDIX I



**Figure I.1:** Ladybug definition for the Sunlight Analysis.

**The algorithmic process in Grasshopper:** Import EPW Files (Energy Plus Weather) for climate data of desired context (Istanbul)/ Draw the Sunpath of Istanbul/ Arrange the hours (24 hours)/ Draw Sunlight hours analysis/ Link the Sun vector data with sunlight hours analysis/ Define the Brep (the designed geometry) by linking the geometry parameter/ Define the context (surrounding buildings) by linking the context parameter/ Make legend and recolor the analysis according to sunlight hour.

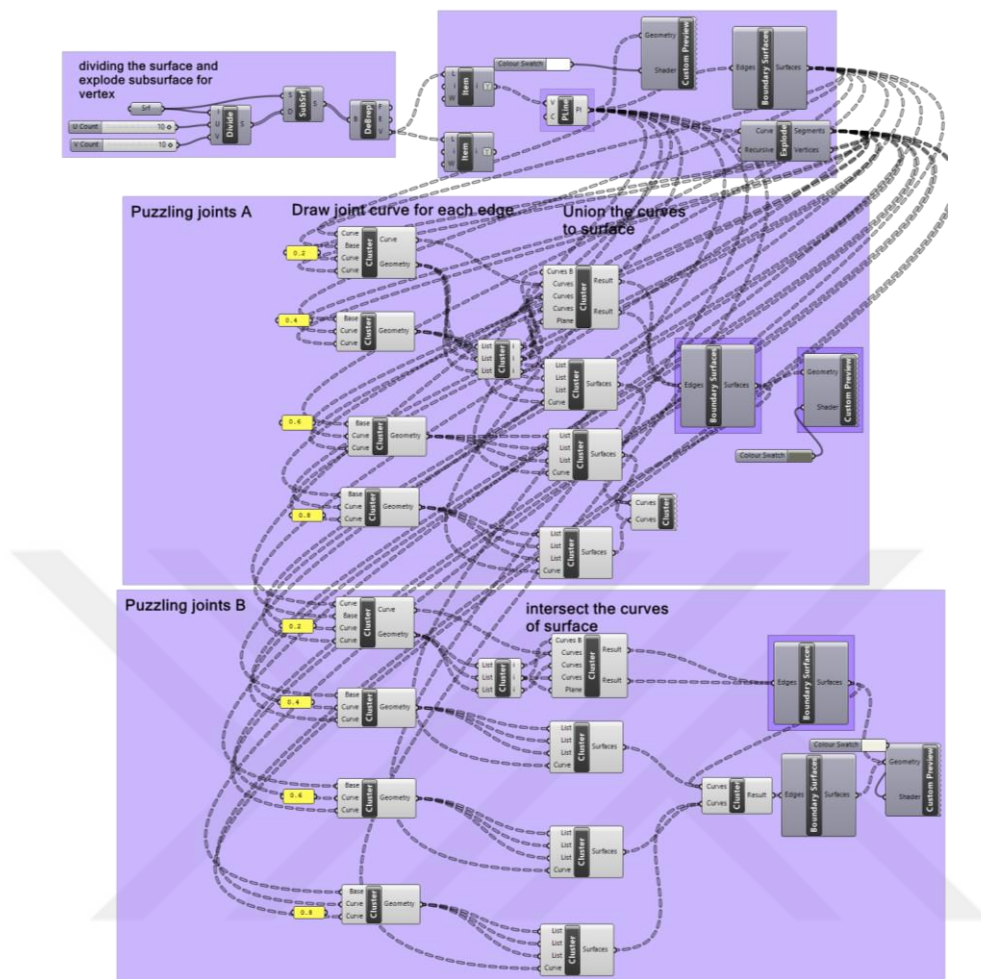
## APPENDIX J



**Figure J.1:** Form development according to attractor points through Grasshopper definition.

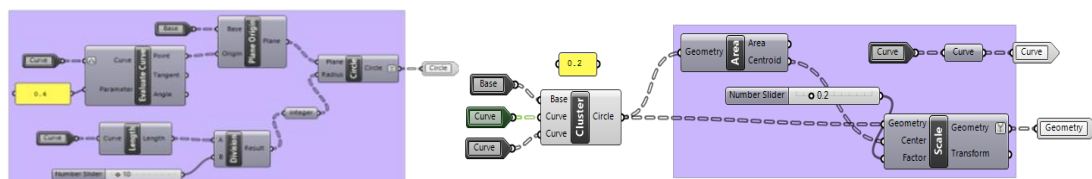
**The algorithmic process in Grasshopper: 1-Determine the location of attractor points:** Extract the areas, which gets sunlight more than 7 hours from the sunlight analysis simulation/ Define the extracted areas as surface/ Find the center of the extracted areas/ Calculate the average of the centers/ Determine these points as attractor points (Attractor point A and B). **2-Modify the modules in the effect of attractor points:** Subdivide the surface into modules/ Find the center of the modules/ Find the distance between the center of the modules and attractor point A and B/ Make a sort list of the distance value /From the list find the maximum and minimum distance with list item/ Construct domain with the minimum and maximum distance value/ Construct another domain for the scaling factor/ Remap the scaling factor with distance value/ Scale the units according to the results that come from remapping the scaling factor and distance value.

## APPENDIX K

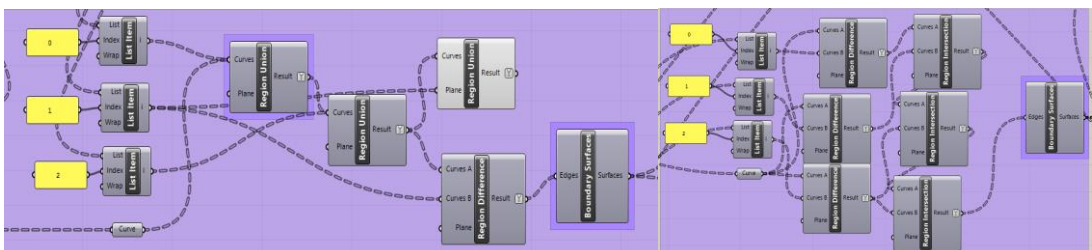


**Figure K.1:**Grasshopper definition of puzzle joint detail<sup>8</sup>.

**Cluster 1:** Draw a circle and scale for each edge.

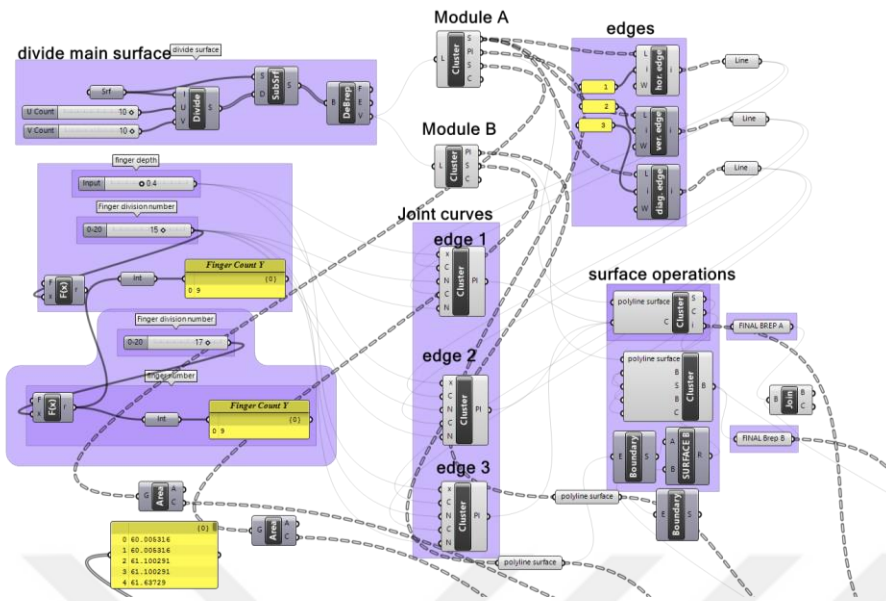


**Cluster 2:** Surface operations adding and subtracting the curves to surface.



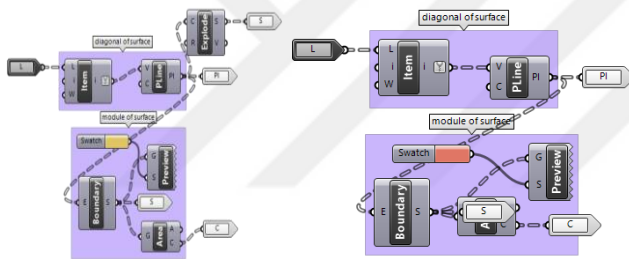
<sup>8</sup>Reference for Grasshopper code: <http://www.designcoding.net/puzzling/>

# APPENDIX L

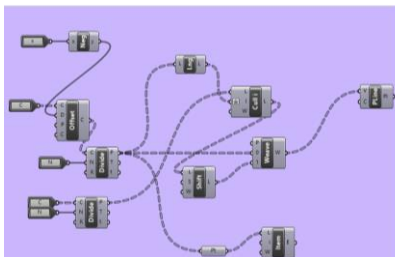


**Figure L.1:** Grasshopper definition of finger joint detail.

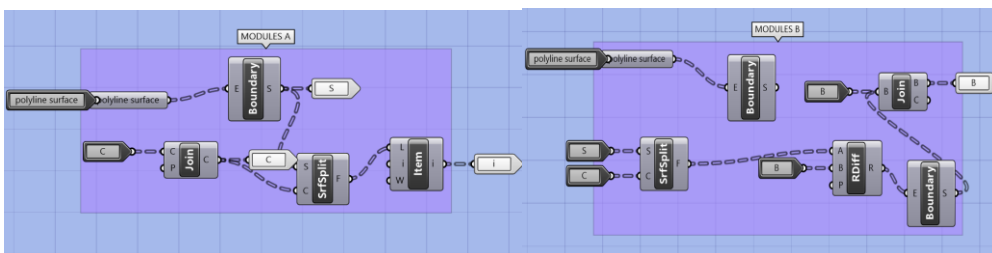
**Cluster 1:** Dividing the surfaces into the modules (Module A and Module B)



**Cluster 2:** Finger Joint Curves (for edge 1-2-3).

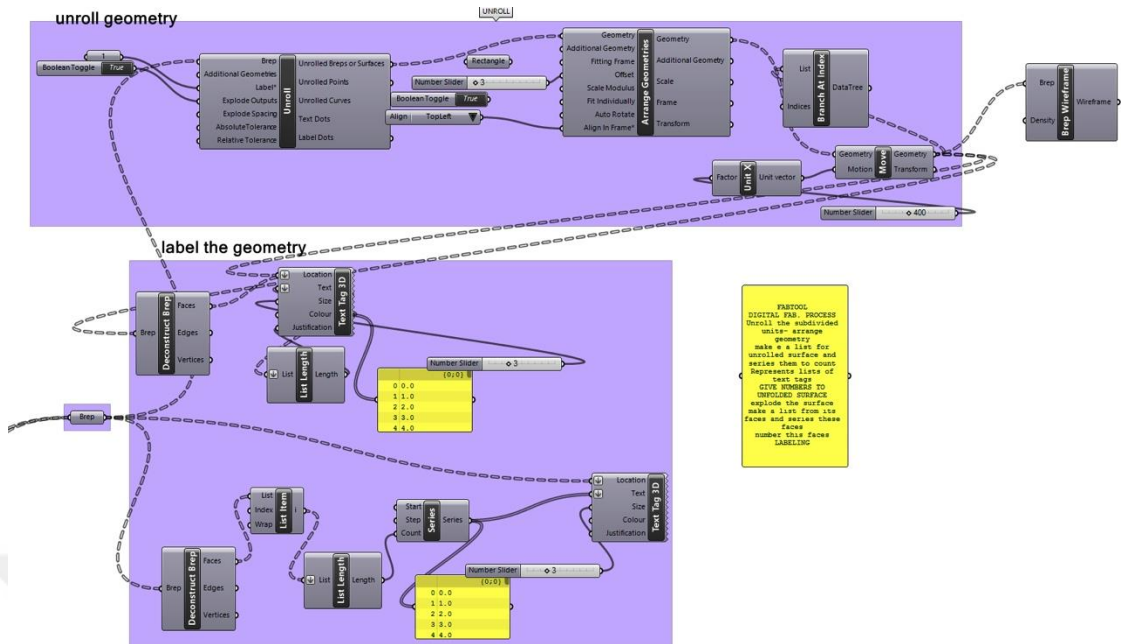


**Cluster 2:** Surface operations (joining and adding the curves for joint).





## APPENDIX M



**Figure M.1:** Unrolling and labeling the geometry.

**The algorithmic process in Grasshopper:** Unroll the subdivided units /Arrange geometry/ Make a list for unrolled surface and series them to count/ Explode the surface make a list and series from these faces/Number this faces with list length/ Represents lists of text tags.

## CURRICULUM VITAE



**Name Surname** :Gülce Kırdar  
**Place and Date of Birth** : Istanbul- 22/10/1990  
**E-Mail** : gulcekirdar@gmail.com

### EDUCATION

- **B.Sc.** :2013, Bahçeşehir University, Architecture.

### PROFESSIONAL EXPERIENCE AND REWARDS:

- Istanbul Kemerburgaz University, Research Assistant (2015-.....)
- Atılım Architecture, Architect (2014-2015)

### PUBLICATIONS, PRESENTATIONS ON THE THESIS:

- **Kırdar G., Çolakoğlu B.**, Tepkimeli Mimari Sistem Tasarımlarında Malzemenin Kullanımı ve Enerji Tüketimine Etkisi. *X. Mimarlıkta Sayısal Tasarım Ulusal Sempozyumu*, June 27-28 2016, Istanbul Bilgi University, Istanbul, Turkey.
- **Kırdar G., Çolakoğlu B.**, Hygro\_Responsive Structure. *eCAADe Educational and Research in Computer Aided Architectural Design in Europe*, 20-22 September 2017, Sapienza University of Rome, Rome, Italy.

### OTHER PUBLICATIONS:

- **Kırdar G.**,ExperiencetheKineticTextileModules: A Research on Interactive Design Process. *DCA European Conference 2016*, May 11-14 2016, Istanbul Özyeğin University, İstanbul, Turkey.